International
Progress Report

IPR-01-34

Äspö Hard Rock Laboratory

Compilation of laboratory data for buffer and backfill materials in the Prototype Repository

Lennart Börgesson

Clay Technology AB

August 2001

Svensk Kärnbränslehantering AB
Swedish Nuclear Fuel
and Waste Management Co
Box 5864
SE-102 40 Stockholm Sweden
Tel +46 8 459 84 00
Fax +46 8 661 57 19

Äspö Hard Rock
Laboratory

Report no.
IPR-01-34

No.
F63K

Author
L Börgesson

Date

Checked by

Date

Approved
Christer Svemar

Date
01-11-07

Äspö Hard Rock Laboratory

Compilation of laboratory data for buffer and backfill materials in the Prototype Repository

Lennart Börgesson

Clay Technology AB

August 2001

Keywords: Prototype Repository, buffer, backfill, THM, laboratory datarelative humidity, water uptake, uniaxiall compression, triaxial test

Abstract

The present report is a compilation of reports and results concerning THM laboratory tests on the buffer and backfill material that will be used in the Prototype Repository. The purpose is to supply the modelling groups of the project with the available results for creating material models that can be used for THM modelling of the behaviour of the Prototype Repository.

The report contains results of thermal, hydraulic and mechanical (THM) tests in the laboratory, partly as references to useful reports and partly as descriptions of tests and results. Description of tests and results has only been done if the results have not been reported or if the tests have only been reported in internal reports.

The following tests on water unsaturated buffer material (MX-80 bentonite) are reported: Shrinkage tests, relative humidity tests, water uptake tests, temperature gradient tests, one-dimensional compression tests and triaxial tests. In addition tests on bentonite canister interaction and tests on the interaction between bentonite blocks and different slot fillings are reported.

The following tests on different backfill materials (mixtures of crushed rock and MX-80 bentonite are reported: Compaction tests, compression tests and shear tests.

Sammanfattning

Föreliggande rapport utgör en sammanställning av rapporter och resultat rörande laboratorietester av THM-processer i buffert-och återfyllningsmaterial, vilka ska användas i Prototypförvaret. Syftet är att förse projektets modelleringsgrupper med tillgängliga data i deras arbete med materialmodeller, vilka kan användas för THM-modellering av förhållandena i Prototypförvaret.

Rapporten innehåller valda delar av rapporter, som ej har status som refererbara rapporter liksom resultat som ej tidigare överhuvudtaget publicerats.

Contents

1 Introduction

The present report is a compilation of reports and results concerning THM laboratory tests on the buffer and backfill material that will be used in the Prototype Repository. The purpose is to supply the modelling groups of the project with the available results for creating material models that can be used for THM modelling of the behaviour of the Prototype Repository.

The report contains results of thermal, hydraulic and mechanical (THM) tests in the laboratory, partly as references to useful reports and partly as descriptions of tests and results. Description of tests and results has only been done if the results have not been reported or if the tests have only been reported in internal reports.

The following Technical Reports contain useful information and are recommended:

Börgesson L., and Hernelind J., 1999. Coupled thermo-hydro-mechanical calculations of the water saturation phase of a KBS-3 deposition hole. Influence of hydraulic rock properties on the water saturation phase. SKB Technical Report TR 99-41.

Börgesson L., Johannesson L.-E., Sandén T. and Hernelind J., 1995. Modelling of the physical behaviour of water saturated clay barriers. Laboratory tests, material models and finite element application. SKB Technical Report TR 95-20.

Börgesson L., Fredriksson A. and Johannesson L.-E. 1994. Heat conductivity of buffer materials. SKB Technical Report TR 94-29.

The following International Progress Report contains results from laboratory tests on backfill materials:

Johannesson L.-E., Börgesson L. and Sandén T., 1998. Backfill material based on crushed rock. Geotechnical properties determined in the laboratory (part 2). SKB ÄHRL IPR 99-23.

The information in these reports is supplemented with information from the following project work and laboratory tests that have not been published or only published in internal reports:

<u>Buffer material</u>

- Thermo-Hydro-Mechanical laboratory tests on water unsaturated buffer materials (chapter 2).
- Laboratory simulation of bentonite/canister THM interaction before water saturation (chapter 3).
- Additional water uptake tests (chapter 4)

- Water uptake tests with different slot filling materials (chapter 5)

Backfill material

- Compaction tests, compression tests and shear tests on backfill materials based on crushed rock (chapter 6)

2 THM laboratory tests on water unsaturated buffer materials

This chapter is based on work conducted in 1995.

2.1 General

Seven different types of laboratory tests, most of them rather simple ones, have been made on unsaturated samples of MX-80 Na-bentonite. The aim of these tests has been to get a general understanding of the behaviour, to evaluate parameters of some sub-models, and to check the validity of some sub-models.

2.2 Reference tests of one dimensional compaction

2.2.1 General

Earlier evaluated compaction tests have shown that it is very difficult to compact bentonite to homogenous samples if the height/diameter relation is large due to friction between the sample and the form. In Fig 2-1 results from compaction tests on samples with diameters of 50 mm and heights varying between 5 mm to 100 mm are plotted. The compaction was made in a cylindrical form with a fixed bottom. The samples were compacted from the top under a pressure of 100 MPa. The water ratio of the material was $w \approx 10\%$. The figure shows that it is not possible to get a reasonably homogeneous sample if the height/diameter ratio is larger than 0.4 if the compaction is made in a cylinder with fixed bottom. However, most laboratory tests require larger height. In order to minimise the effects of the friction a special device was built and a number of tests made.

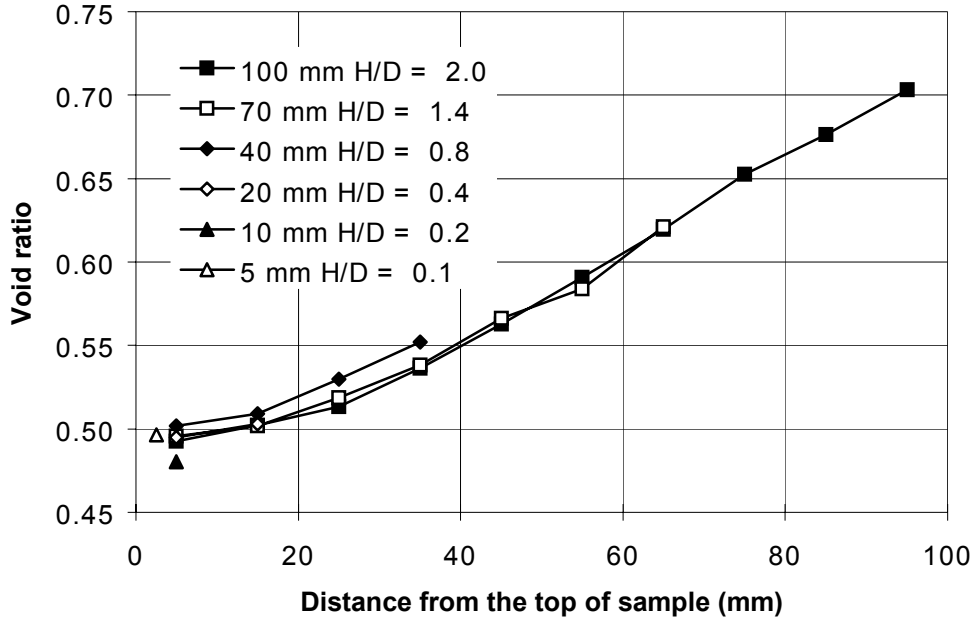

Figure 2-1. *Void ratio plotted as a function of the distance from the top surface of the sample for different sample heights. $w \approx 10\%$.*

2.2.2 Compaction technique

The tests described in this chapter need to be made on samples with specified, uniform void ratios and degrees of saturation. The samples usually have a diameter of 50 mm and a height of 50 mm. For this purpose a compaction device was constructed in order to minimise the friction. A schematic drawing of the device is shown in Fig 2-2. It consists of three cylinders and two pistons. The upper and lower cylinders are attached to the centre cylinder. The following procedure was used for preparing the samples:

The bentonite was mixed with water. A specified amount of material was poured into the cylinders and the two pistons were placed in the upper and lower cylinder, respectively. Then, the device was placed in the press. During compaction both pistons were pushed. The sample was compacted until the central cylinder was completely filled. After compaction the upper and lower cylinders were dismantled from the central cylinder and the sample pushed out of the device. The sample was then cut in 5 slices. Water ratio and density were measured on each slice and the degree of saturation and void ratio calculated.

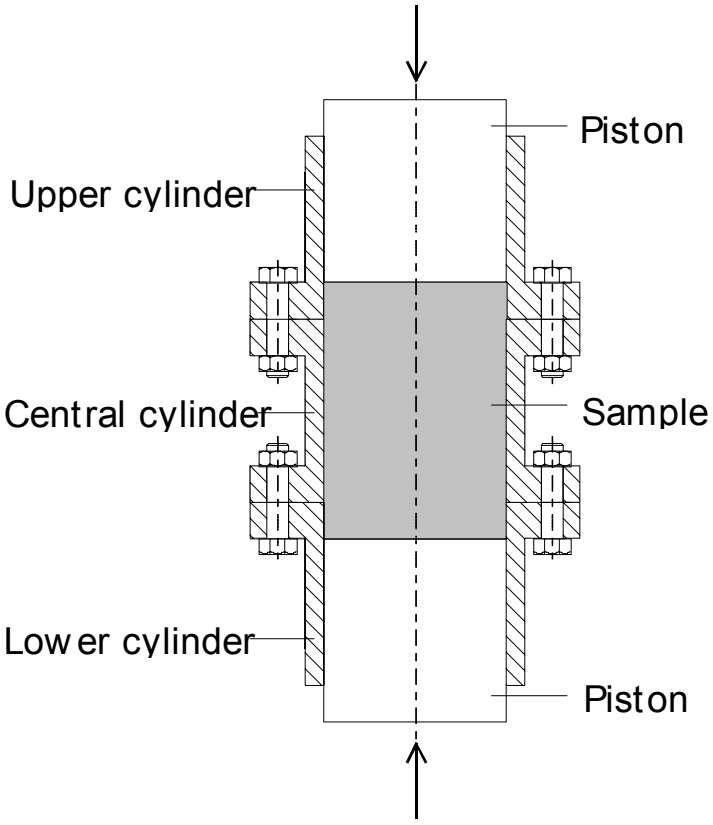

Figure 2-2. *Schematic drawing of the compaction device.*

2.2.3 Results

A number of tests were made in order to study the homogeneity of the samples. The tests were made on samples with the target void ratios 0.70 and 1.00. For each void ratio samples with 50%, 70% and 90% degree of saturation were compacted. After compaction the change in density and water ratio along the axis of the samples were measured. Four or five identical samples were compacted for checking the variation.

- The results from these tests are shown in Fig 2-3 and Fig 2-4. The following preliminary conclusions can be drawn:

- As expected the void ratio was largest in the centre of the sample in all tests.

- For each void ratio and degree of saturation the scatter of the void ratio within the sample was found to be of the same range with one exception (Test 2 at e=0.7 and S_r=50%).

- The samples with a high degree of saturation were more homogeneous than those with a low degree of saturation.

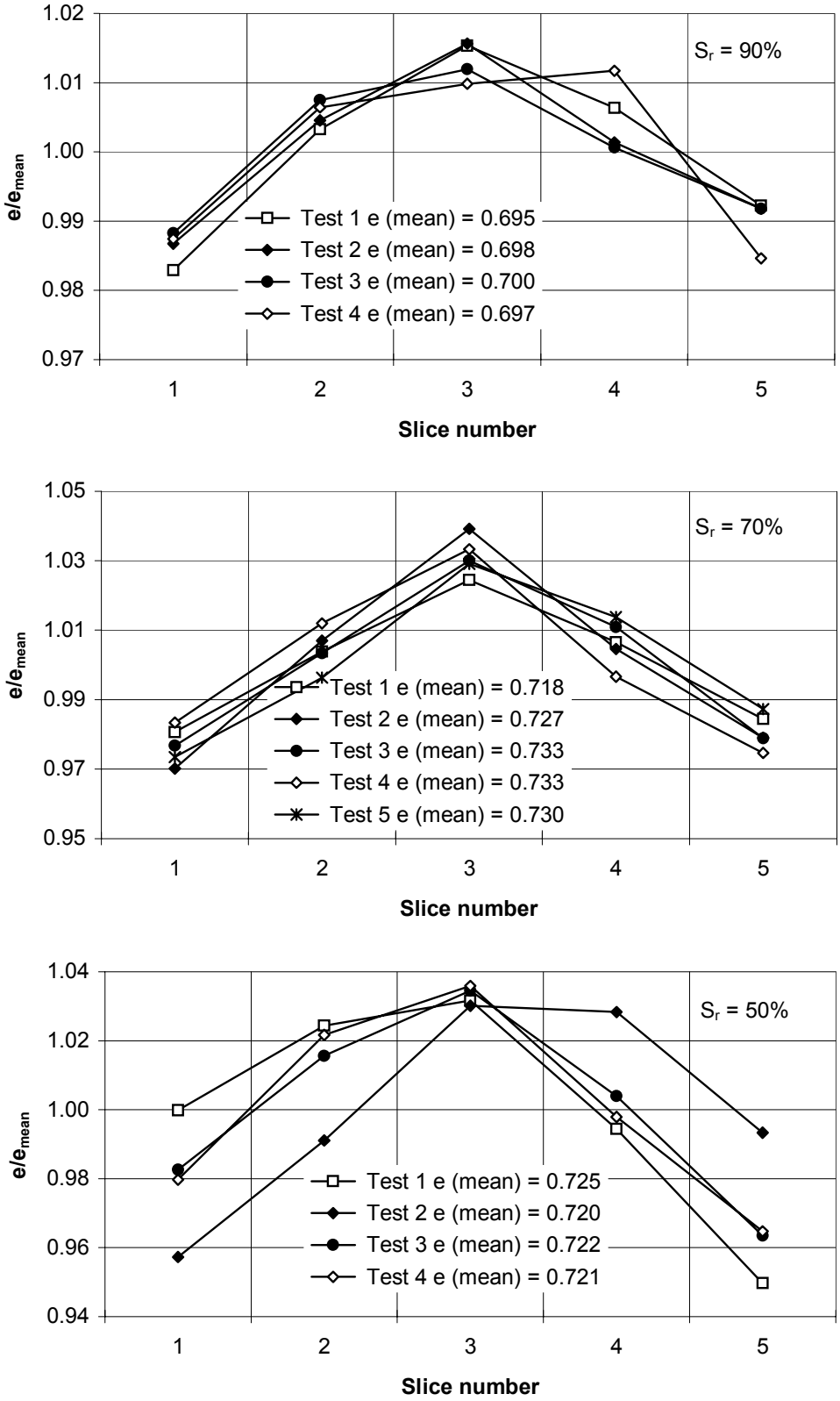

Figure 2-3. *Measured void ratio divided by the mean void ratio for different degrees of saturation (S_r) at the target void ratio e=0.70.*

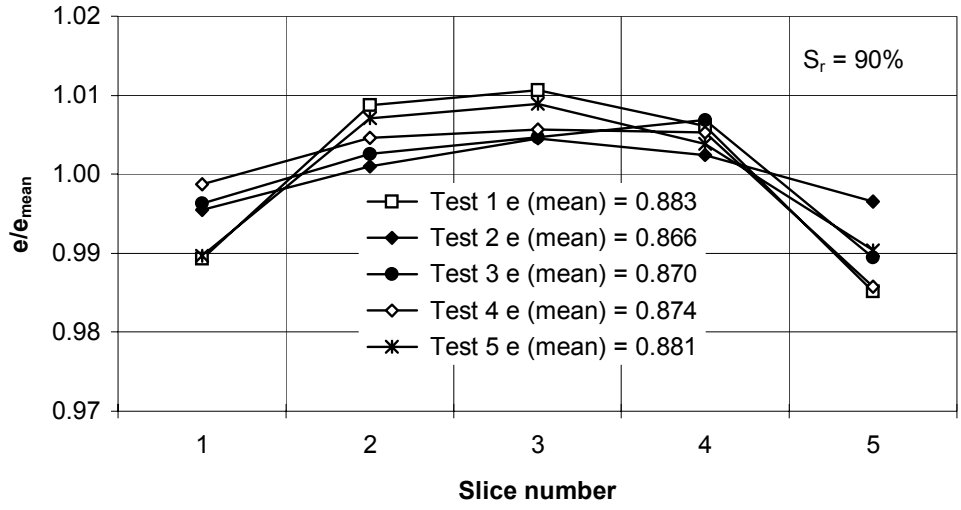

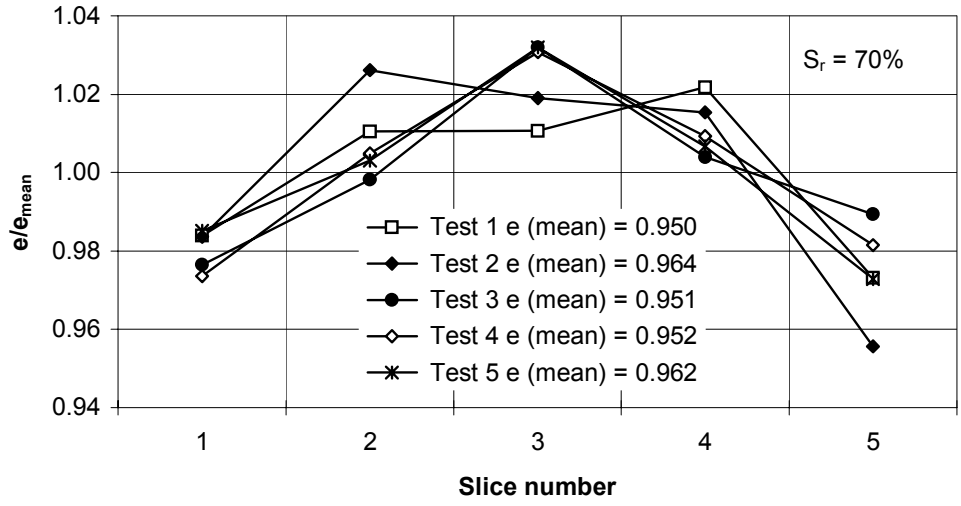

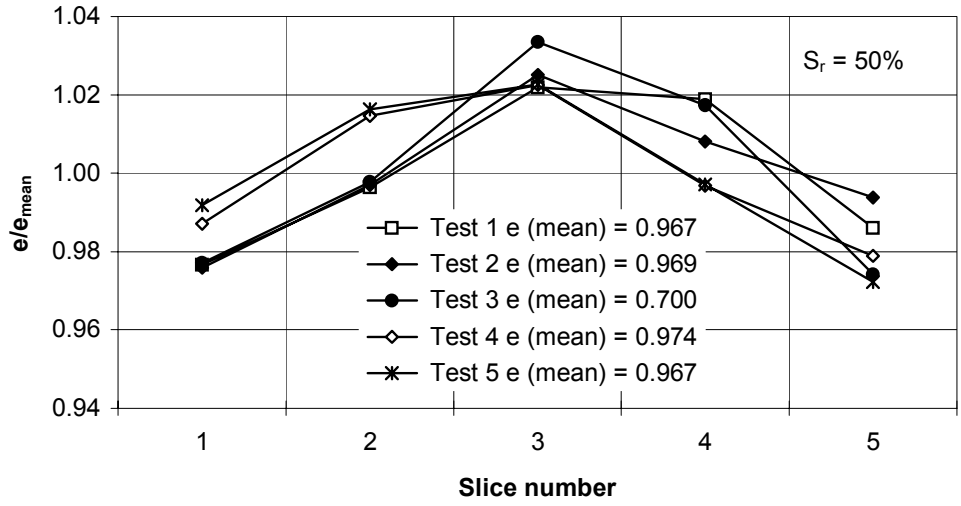

Figure 2-4. *Measured void ratio divided by the mean void ratio for different degrees of saturation (S_r) at the target void ratio e=1.00.*

2.3 Shrinkage test

In this test series the change in void ratio due to drying was measured. Six samples were compacted to a target void ratio of 0.8 and a water ratio of 27%. The samples had a diameter of 50 mm and a height of 20 mm. Immediately after compaction the density and water ratio were measured on Sample 1 and the void ratio calculated. Sample 2 was dried in an oven at a temperature of 105 °C for 24 hours. Samples 3-6 were air-dried at room temperature for different time periods and left to homogenise in closed plastic bags. Then the density and water ratio were measured. The results from the tests are shown in Fig 2-5. The measured void ratio and the void ratio at $S_r = 100\%$ are plotted as a function of the water ratio. The results indicate that there is a volume change during the entire drying process but also that the volume change is less than the volume of the decreased amount of water.

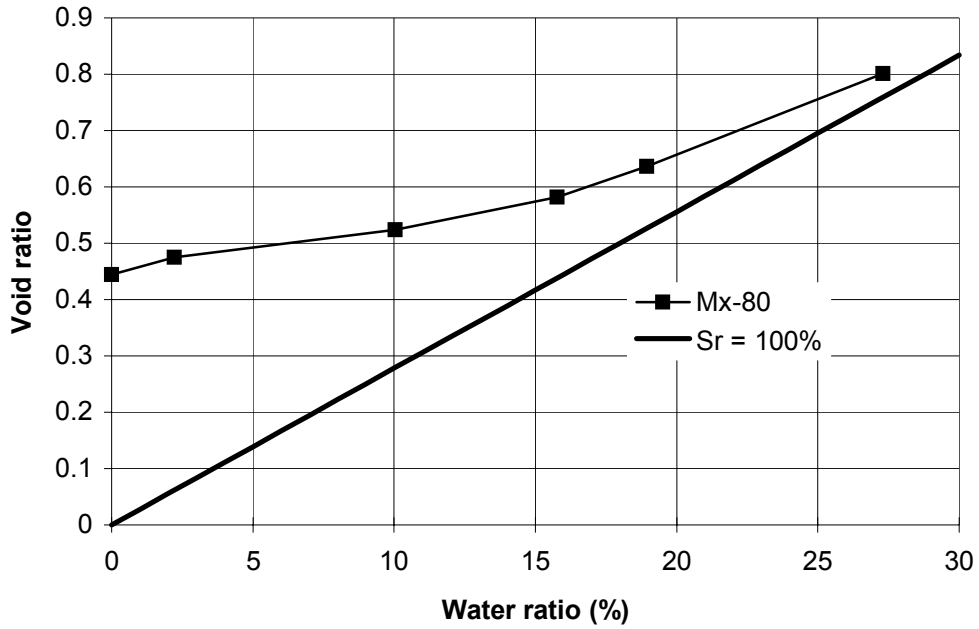

Figure 2-5. *The shrinkage curve of Mx-80 for the initial state e = 0.8 and w = 27%.*

2.4 Relative humidity tests

2.4.1 General

At a certain relative humidity (RH) in air the bentonite is in equilibrium, i.e. the water ratio (w) of a sample reaches a water ratio, which seems to be fairly independent of void ratio and density. If the sample has a lower water ratio than the water ratio in equilibrium, the sample will take up water from the air and if it has a higher water ratio the sample will dehydrate. The bentonite absorbs water with a potential and in a fashion that corresponds to a negative pore pressure, suction. The porewater tension is close to the swelling pressure of a fully saturated sample. The influence of the void ratio and degree of saturation and the difference between drying and wetting for the equilibrium between RH and w are important for the understanding and modelling of these processes.

2.4.2 Sample preparation and test technique

Samples were compacted in a cylinder with 50 mm diameter to 50 mm height with the technique and equipment described in chapter 2.2. Samples with nine different densities and water ratios were compacted. Three samples of each combination were compacted. One of these was used for measuring the density and water ratio immediately after compaction. The second sample was placed in a desiccator with RH = 41% and the third sample was placed in a climate chamber with RH = 80%. The weight, height and diameter were measured once a week. When there was no further change in weight, the samples were considered to have reached equilibrium, after which the density and water ratio were measured.

2.4.3 Results

The results from the desiccator tests with RH=41% are shown in Fig 2-6. The samples in all the tests had dried to w ≈ 8.5%. The volume of all test samples had decreased.

The results from the tests in the climate chamber with RH = 80% are shown in Fig 2-7. Seven of the samples had dried. One sample (e=0.7 S_r=50%) had taken up water and one sample had not changed its water ratio and void ratio at all. All dried samples had approximately the same water ratio (w ≈ 19-21 %) after the test. The two other samples had somewhat lower water ratio after the test (w ≈ 16-17 %), indicating a small hysteresis effect.

The results from the two tests are combined in Fig 2-8. The relation from Fig 2-5 is also plotted. The results in Fig 2-8 indicate that the shrinkage curves are almost parallel and have the same inclination as the curve S_r=100% until a water ratio of $w \approx$ 20% is reached, independently of the initial void ratio and water ratio.

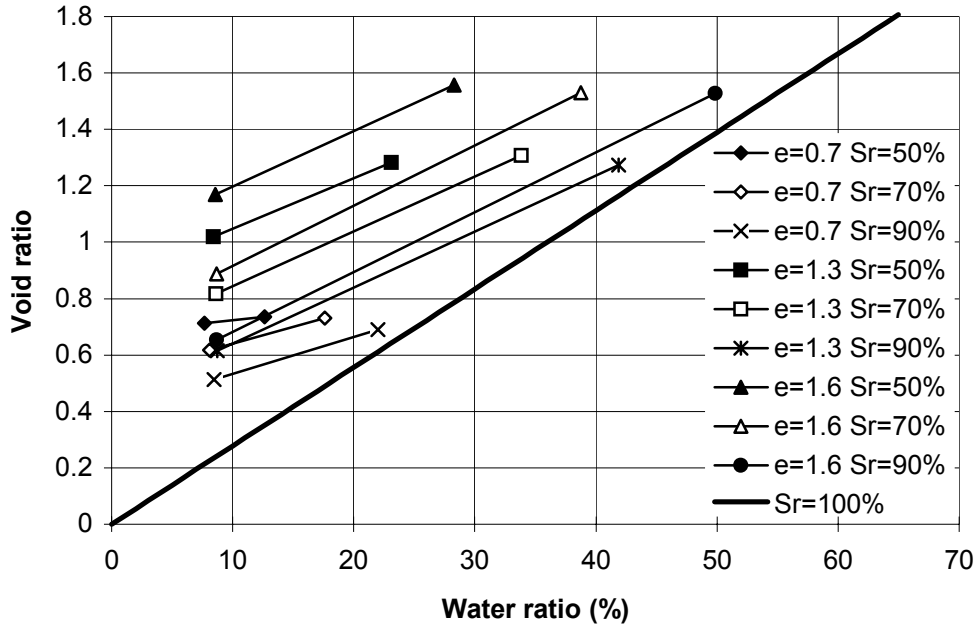

Figure 2-6. *Results from the tests with RH=41%. The legend shows the initial conditions.*

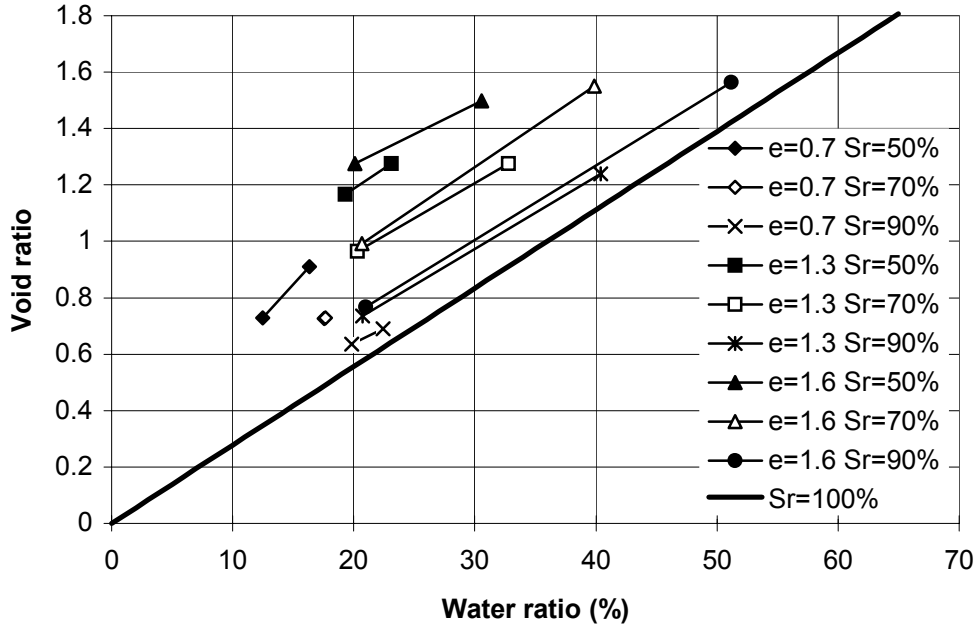

Figure 2-7. *Results from the tests with RH=80%. The legend shows the initial conditions.*

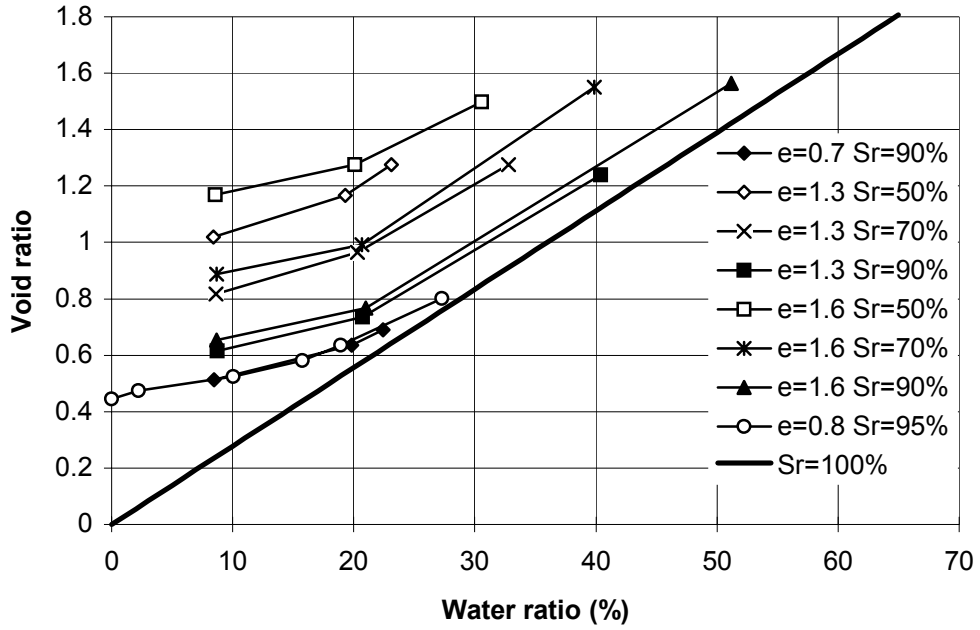

Figure 2-8. *Shrinkage curves of MX-80 with different initial void ratio and water ratio. The legend shows the initial conditions.*

2.5 Water uptake tests

2.5.1 General

The wetting rate of unsaturated bentonite depends on the original void ratio and degree of saturation. During this process the void ratio can also vary within the sample, i.e. some part may swell and some part may shrink. In order to study these processes a number of tests, described in this chapter, were carried out.

2.5.2 Sample preparation and test technique

For each test a sample was compacted to a diameter of 50 mm and a height of 50 mm with the technique and equipment described in Chapter 3.2. After compaction, the central cylinder containing the sample was attached to one end plate without filter and to one with filter, connected to a water source. The sample could thus take up water through the filter without changing volume. Samples with six combinations of initial void ratios (e = 0.7 and e=1.0) and degrees of saturation (S_r=50%, S_r=70% and S_r=90%) were made. Three identical samples were prepared for each combination. They were connected to burettes with water for 1, 2 and 4 weeks, respectively. After the tests, the samples were cut in seven slices and the water ratio and density of each slice measured.

2.5.3 Results

The results from the tests are shown in Figs 2-9 to 2-14. Water ratio, degree of saturation, and void ratio are plotted as functions of the distance from the water inlet. The following conclusions can be drawn from these results:

None of the samples had reached 100% degree of saturation after 4 weeks not even close to the water inlet. One reason for this is probably the elastic swelling at stress release, another may be the thickness of the slices.

All samples showed, after 1 week, no change in the degree of saturation at the dry end.

The ubiquitous initial inhomogeneity of the samples caused by the compaction technique can only be seen in the samples with $e = 0.7$.

The water uptake rate is very slow in the samples with a high initial degree of saturation ($S_r = 90\%$).

The swelling at the top of the samples close to the water inlet is remarkably large. This is not caused solely by void ratio redistribution. Most of this swelling is probably an effect of that the samples have not completely filled the probes axially.

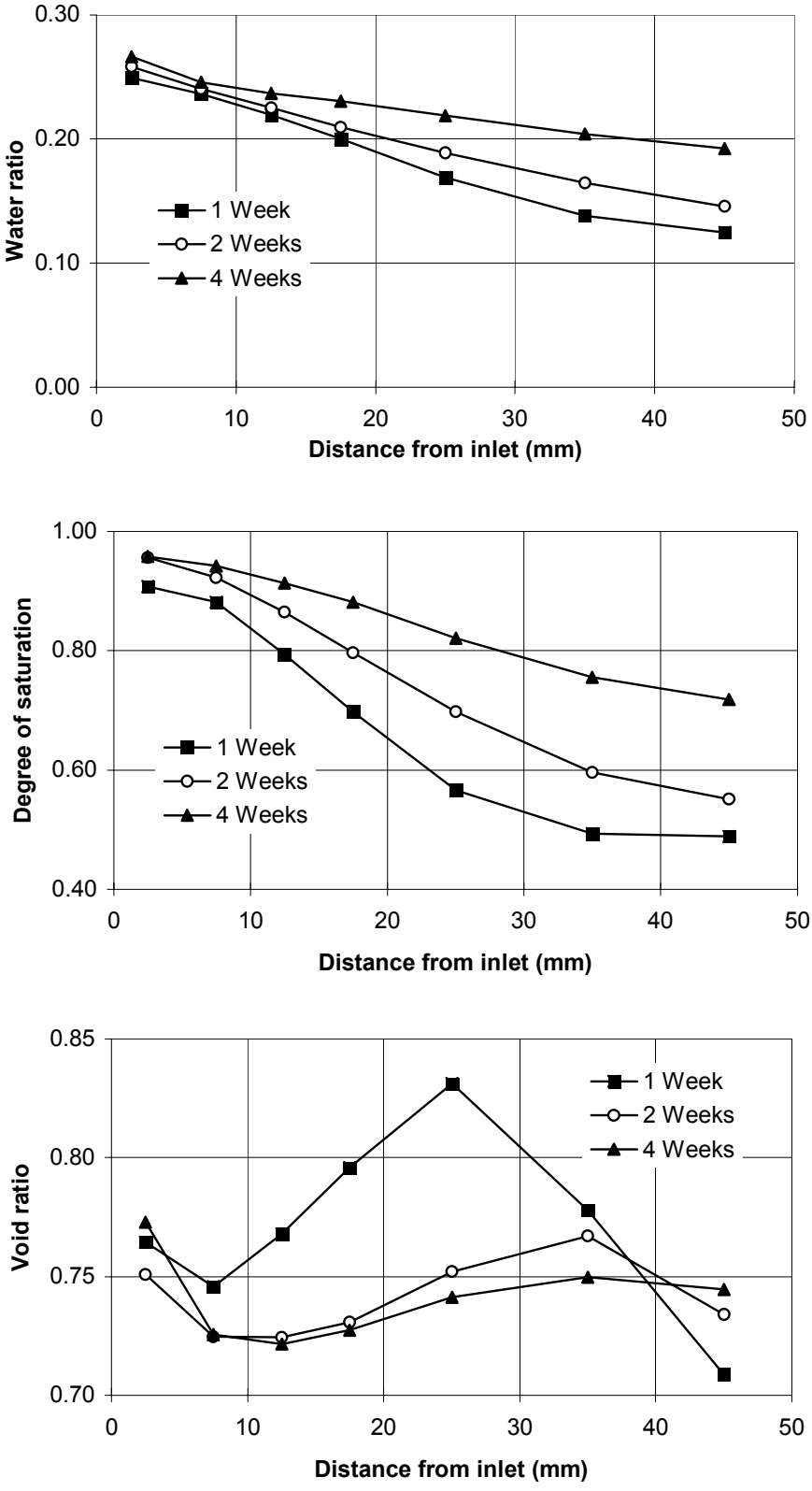

Figure 2-9. *Results from water uptake tests on samples with the initial target void ratio w = 0.7 and initial target degree of saturation S_r = 50% after 1 week, 2 weeks and 4 weeks.*

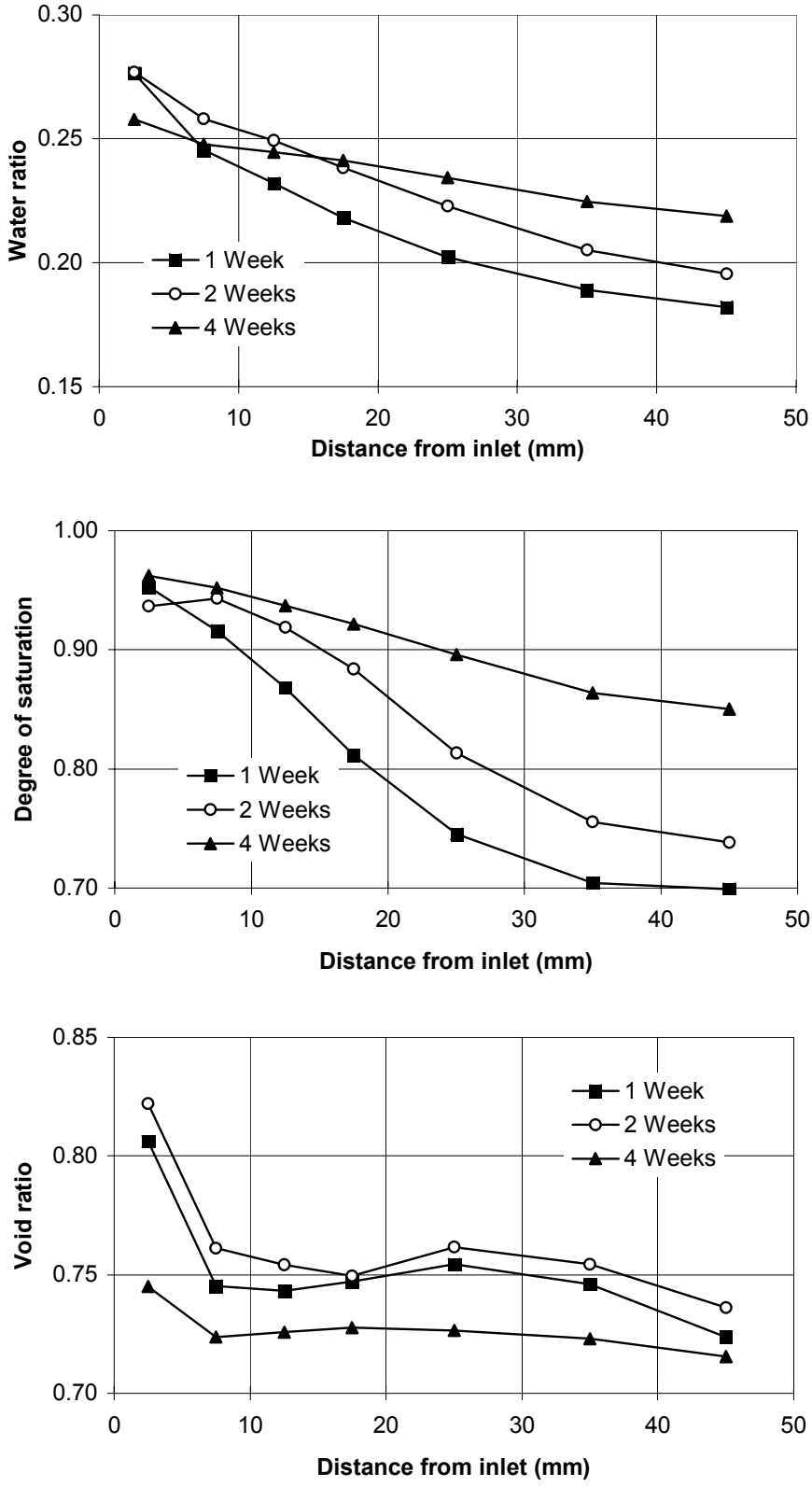

Figure 2-10. *Results from water uptake tests on samples with the initial target void ratio w = 0.7 and initial target degree of saturation S_r = 70% after 1 week, 2 weeks and 4 weeks.*

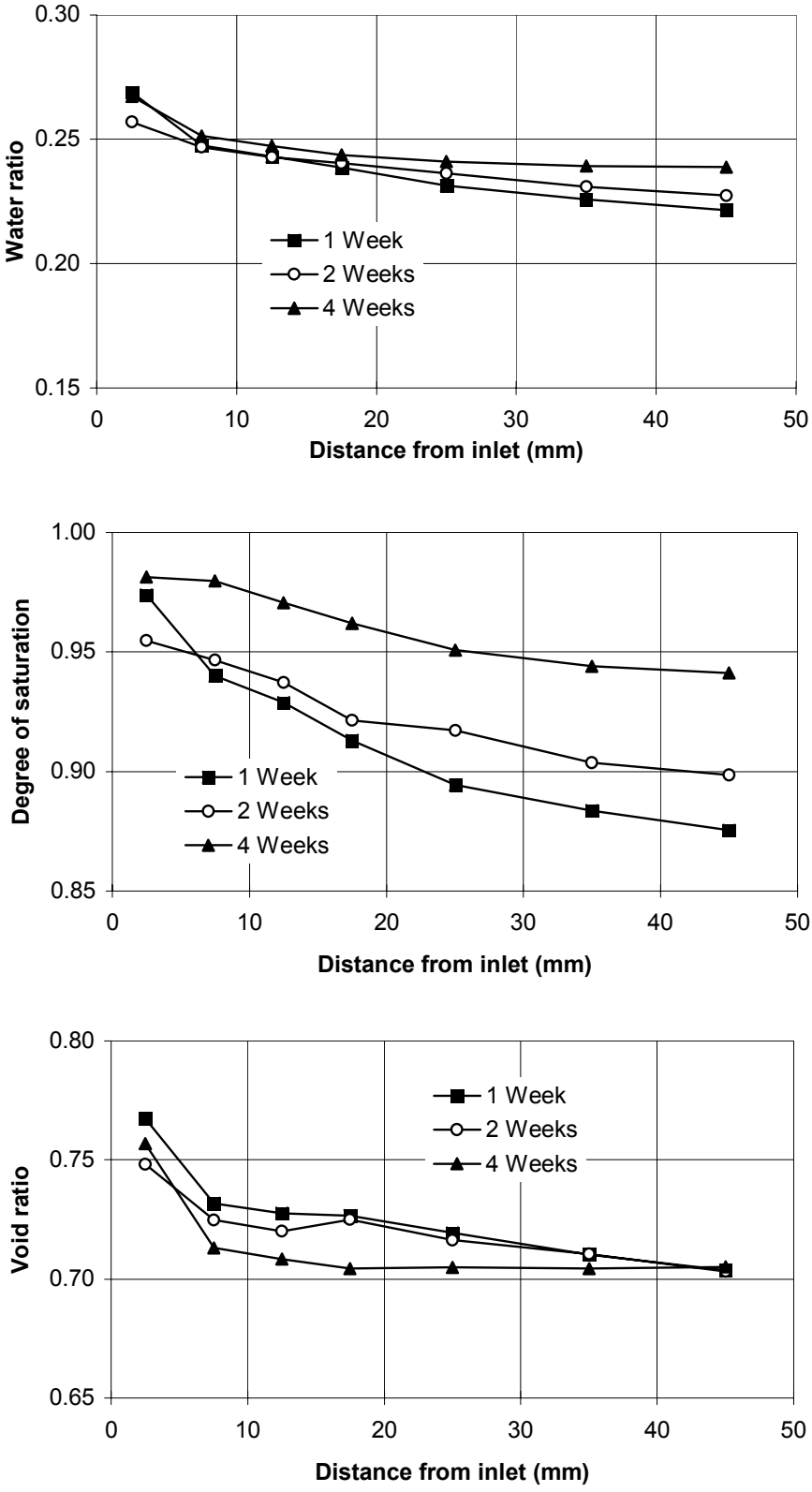

Figure 2-11. *Results from water uptake tests on samples with the initial target void ratio w = 0.7 and initial target degree of saturation S_r = 90% after 1 week, 2 weeks and 4 weeks.*

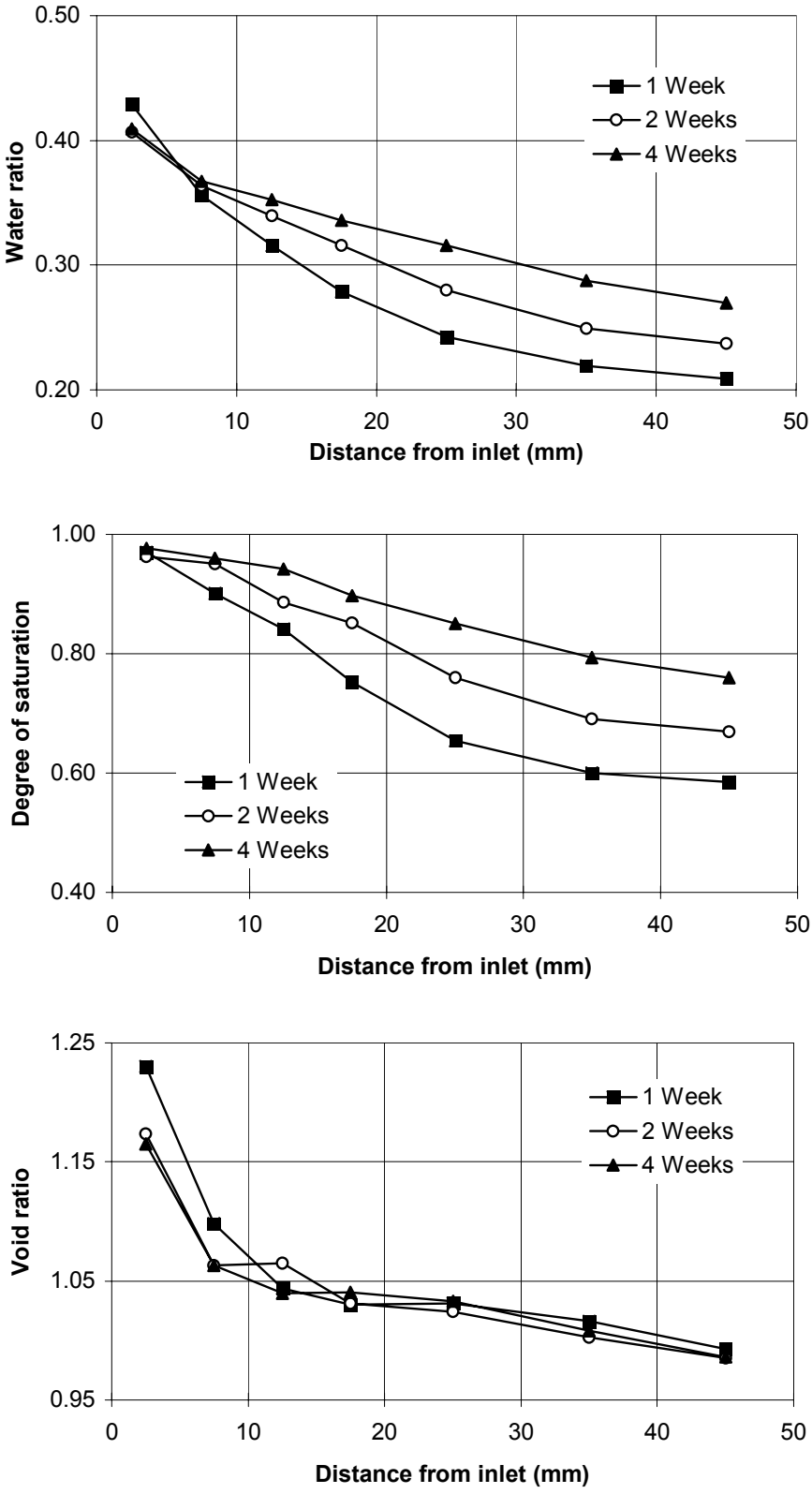

Figure 2-12. *Results from water uptake tests on samples with the initial target void ratio w = 1.0 and initial target degree of saturation S_r = 50% after 1 week, 2 weeks and 4 weeks.*

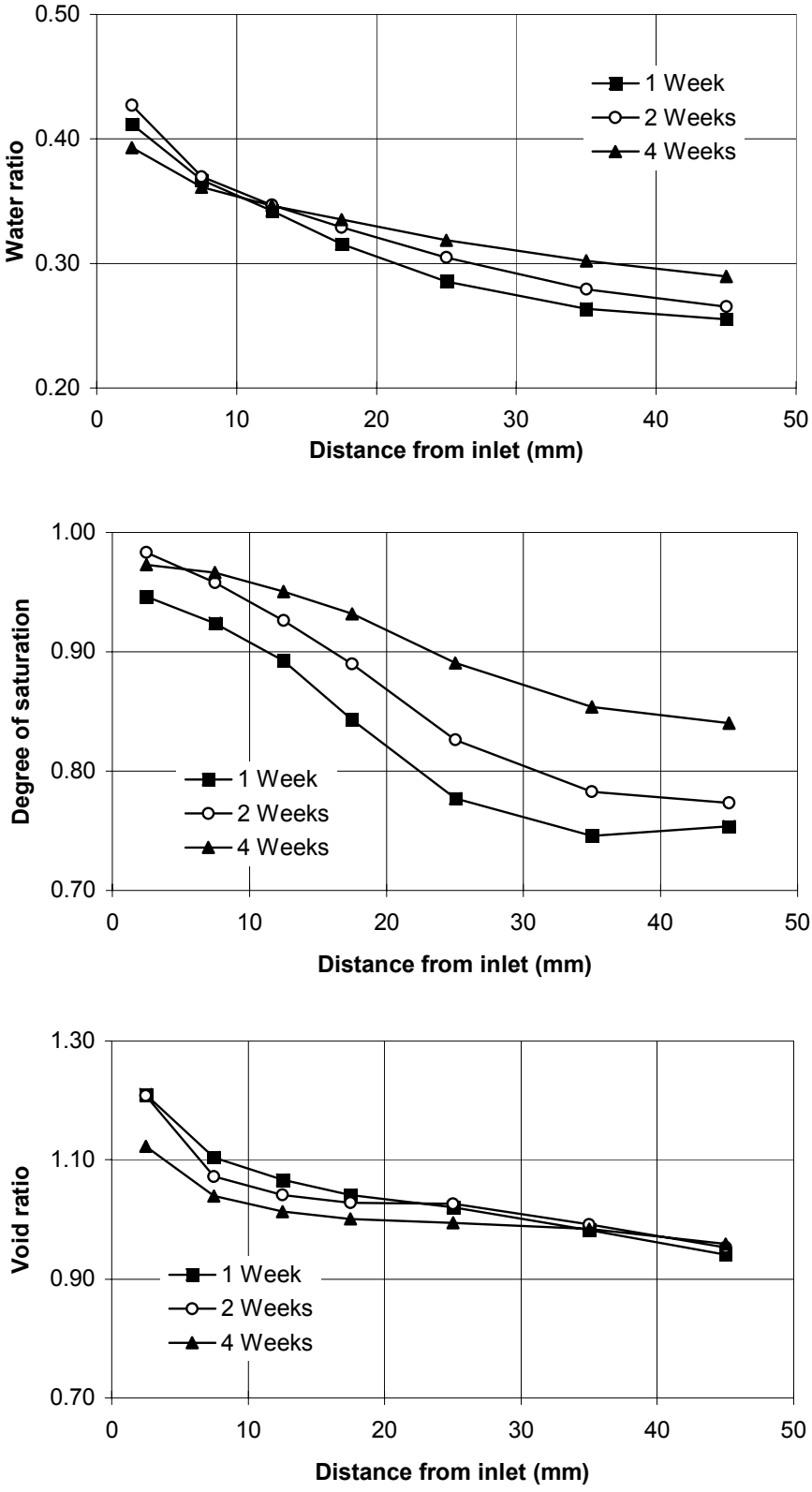

Figure 2-13. *Results from water uptake tests on samples with the initial target void ratio w = 1.0 and initial target degree of saturation S_r = 70% after 1 week, 2 weeks and 4 weeks.*

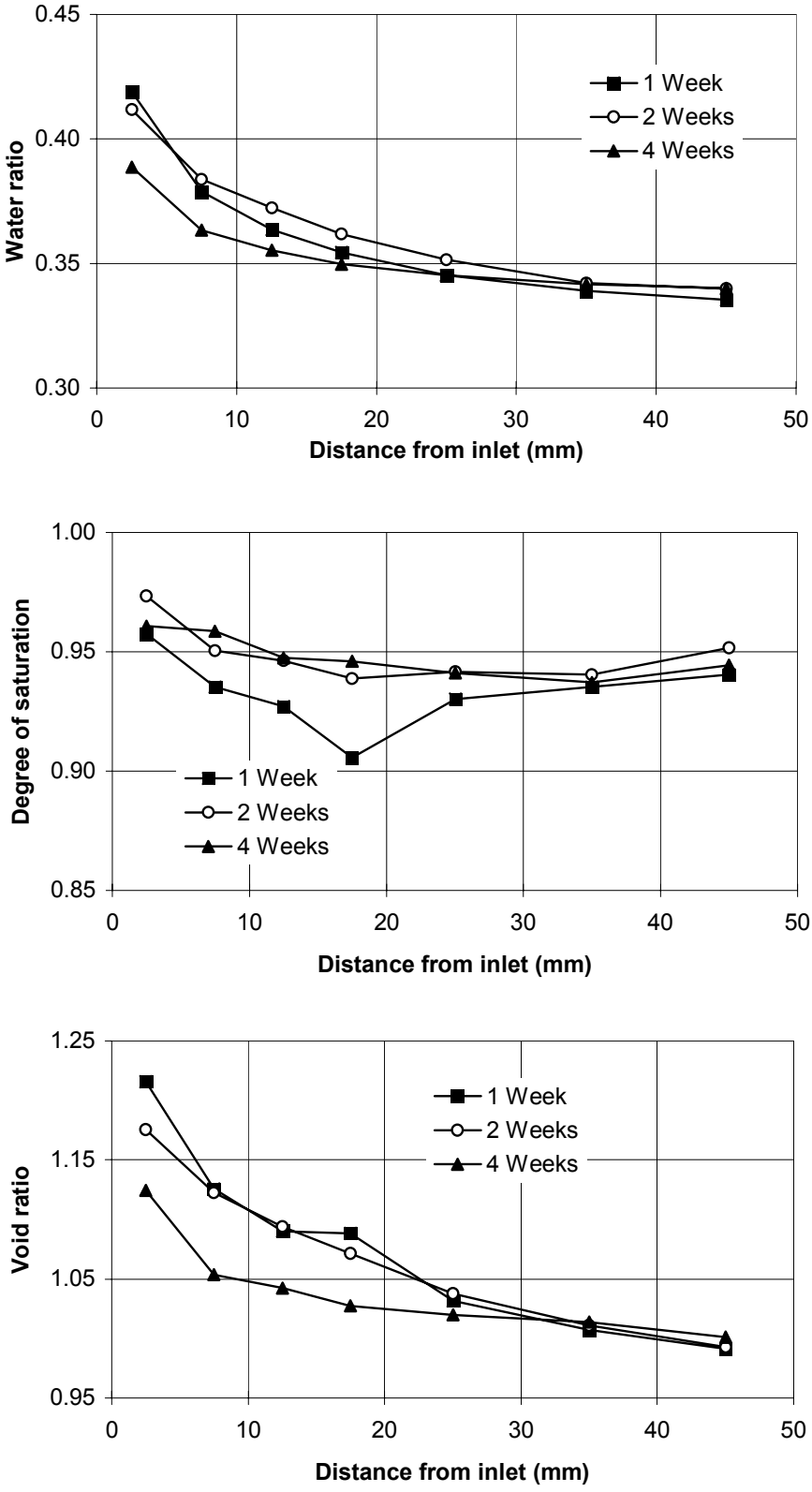

Figure 2-14. *Results from water uptake tests on samples with the initial target void ratio w = 1.0 and initial target degree of saturation S_r = 90% after 1 week, 2 weeks and 4 weeks.*

2.6 Tests of water redistribution at temperature gradients

2.6.1 General

If an unsaturated bentonite, that is confined in order to maintain its volume, is exposed to temperature gradient, the pore water will be redistributed within the sample. Thus, water will be transferred from the warm part to the cold part of the sample and the void ratio distribution within the sample may also be changed. In order to study these processes a number of tests were carried out.

2.6.2 Sample preparation and test technique

In each test, a sample was compacted in a cylinder to a diameter of 50 mm and a height of 50 mm using the same technique and equipment that was described in chapter 3.2. After compaction, one end of the cylinder was fixed to a plate with cooling flanges and the other to a solid steel cylinder surrounded by heat cables. The equipment is shown in Fig 2-15 from which it is seen that the temperature was measured at both ends of the sample. The power of the heat wires was controlled to yield a constant temperature at the hot end. The temperature at the other side was controlled by using a fan to cool the flanges. With this technique a fairly constant temperature gradient could be maintained over the sample. Samples with e = 1.0 and S_r = 50%, 70% and 90% were compacted. Two temperature gradients were applied, viz. 1 °C/cm and 10 °C/cm. The tests were run for 6 hours, 1 day, 4 days and 16 days. In total, 20 tests were performed. After testing, the samples were cut into seven slices and the water ratio and density of each slice were measured.

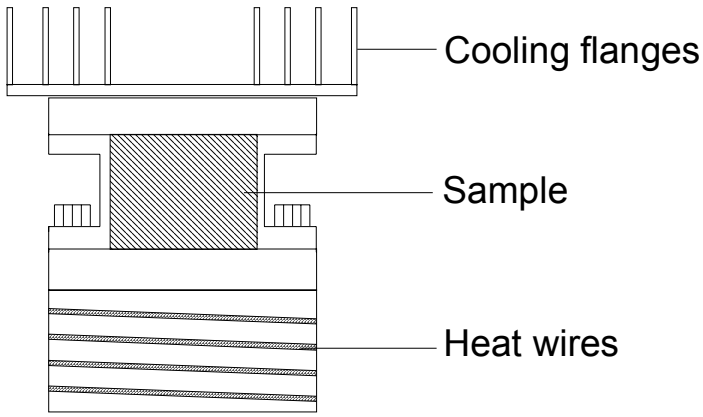

Figure 2-15. *Schematic drawing of the device used for the temperature gradient tests.*

2.6.3 Results

The results of the tests are shown in Figs 2-16 to 2-21. The figures show water ratio, degree of saturation and void ratio plotted as functions of the distance from the cold end. The following conclusions can be drawn from the test results:

All samples with the temperature gradient 10 °C/cm had the same water ratio and degree of saturation at the cold side after 4 days, while it varied with the initial degree of saturation at the hot side.

All samples with an initial degree of saturation of 50% and a temperature gradient of 10 °C/cm had a water ratio and a void ratio that were equal to the initial water ratio and void ratio at a distance of 1.7, 2.3 and 3.1 cm from the cold side, independent of test time.

Very little redistribution of water and void ratio within the samples were observed for the tests with the low temperature gradient 1 °C/cm.

The effect of the temperature gradient 1°C/cm is small in view of the natural inhomogeneity of the sample. However, the effect of the temperature gradient 10°C/cm was very obvious and these tests could be used for model calibration.

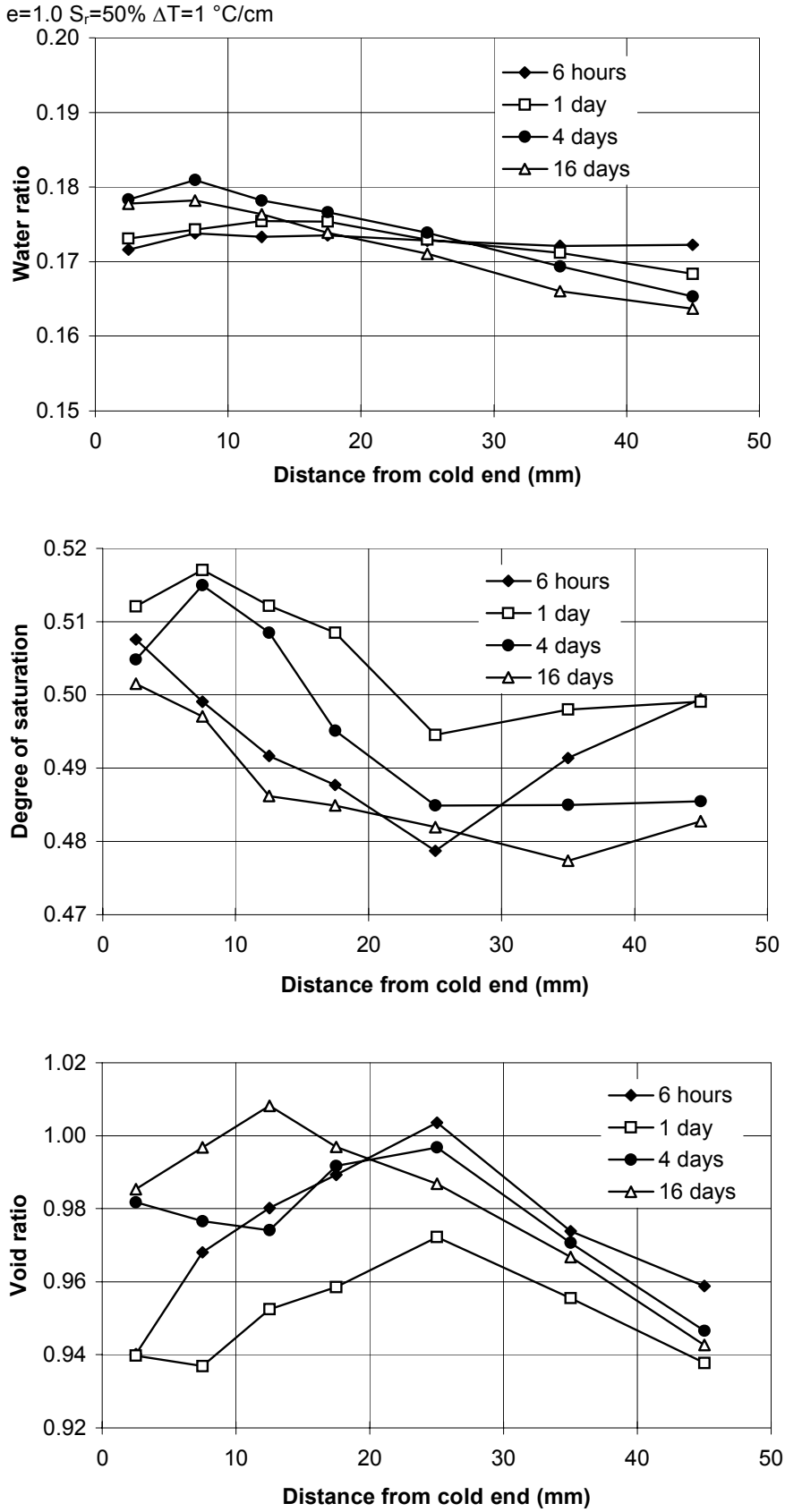

Figure 2-16. *Results from temperature gradient tests on samples with the initial target void ratio e= 1.0 and initial target degree of saturation S_r = 50% with a temperature gradient of 1 °C/cm.*

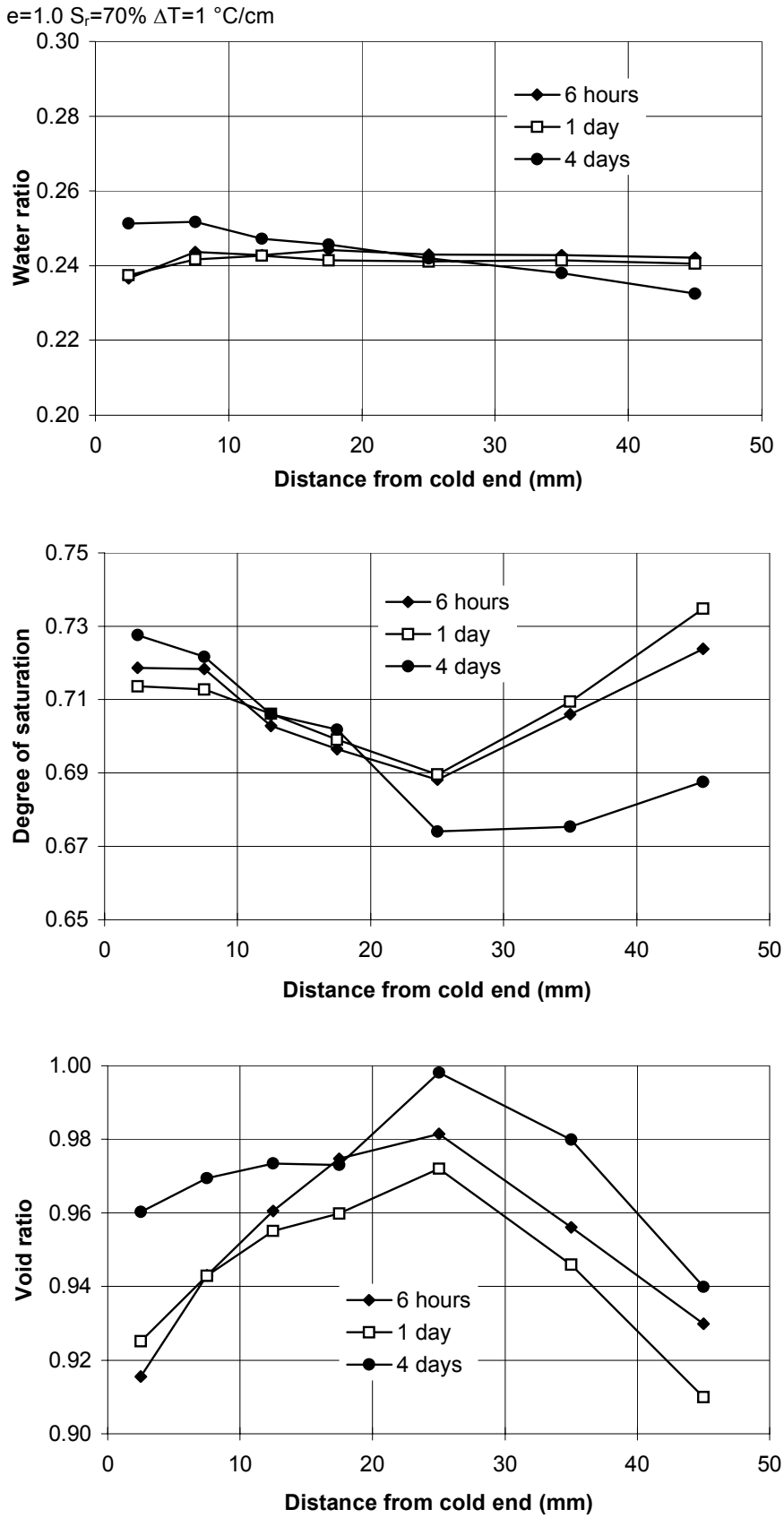

Figure 2-17. *Results from temperature gradient tests on samples with the initial target void ratio e = 1.0 and initial target degree of saturation S_r = 70% with a temperature gradient of 1 °C/cm.*

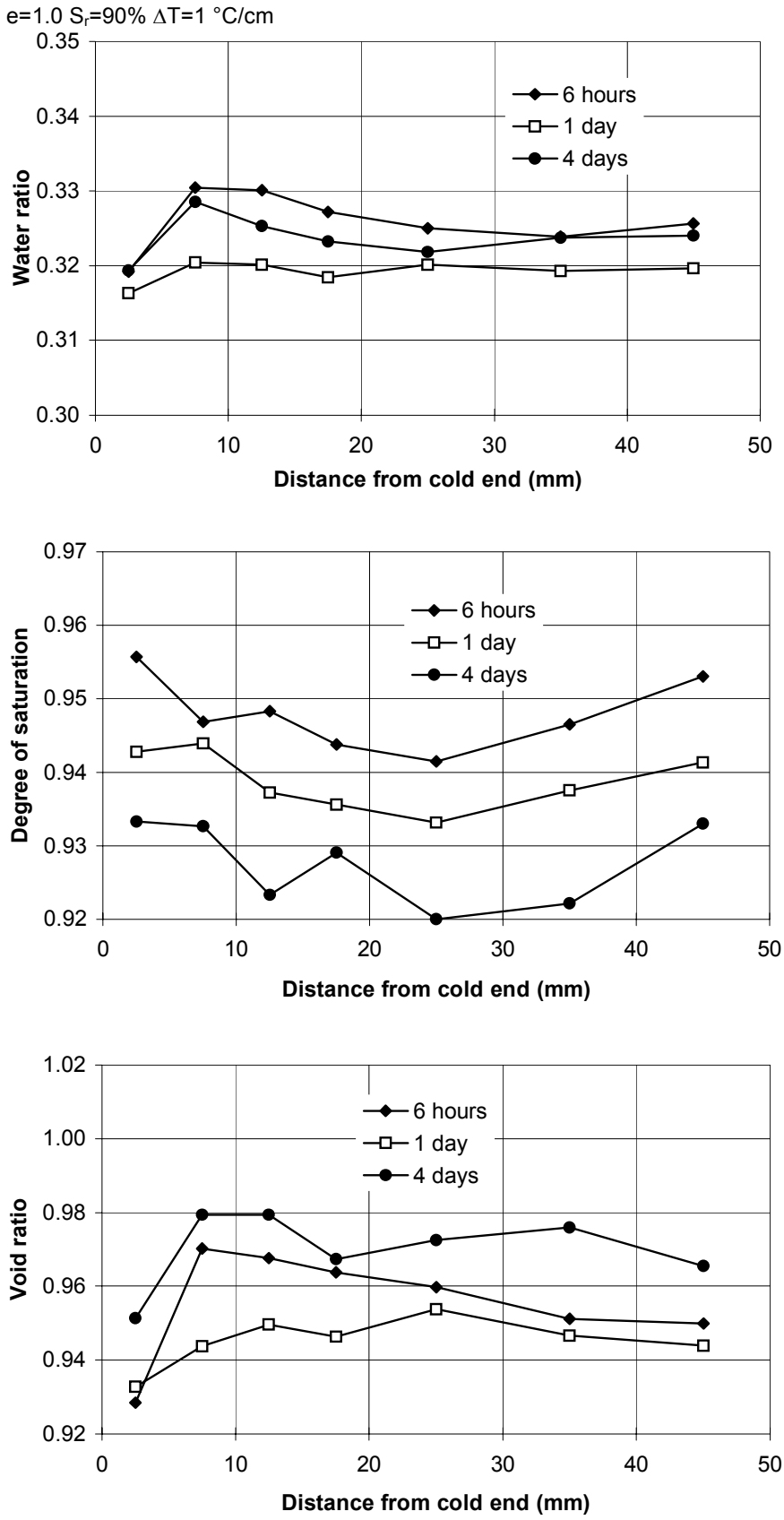

Figure 2-18. *Results from temperature gradient tests on samples with the initial target void ratio e = 1.0 and initial target degree of saturation S_r =90% with a temperature gradient of 1 °C/cm.*

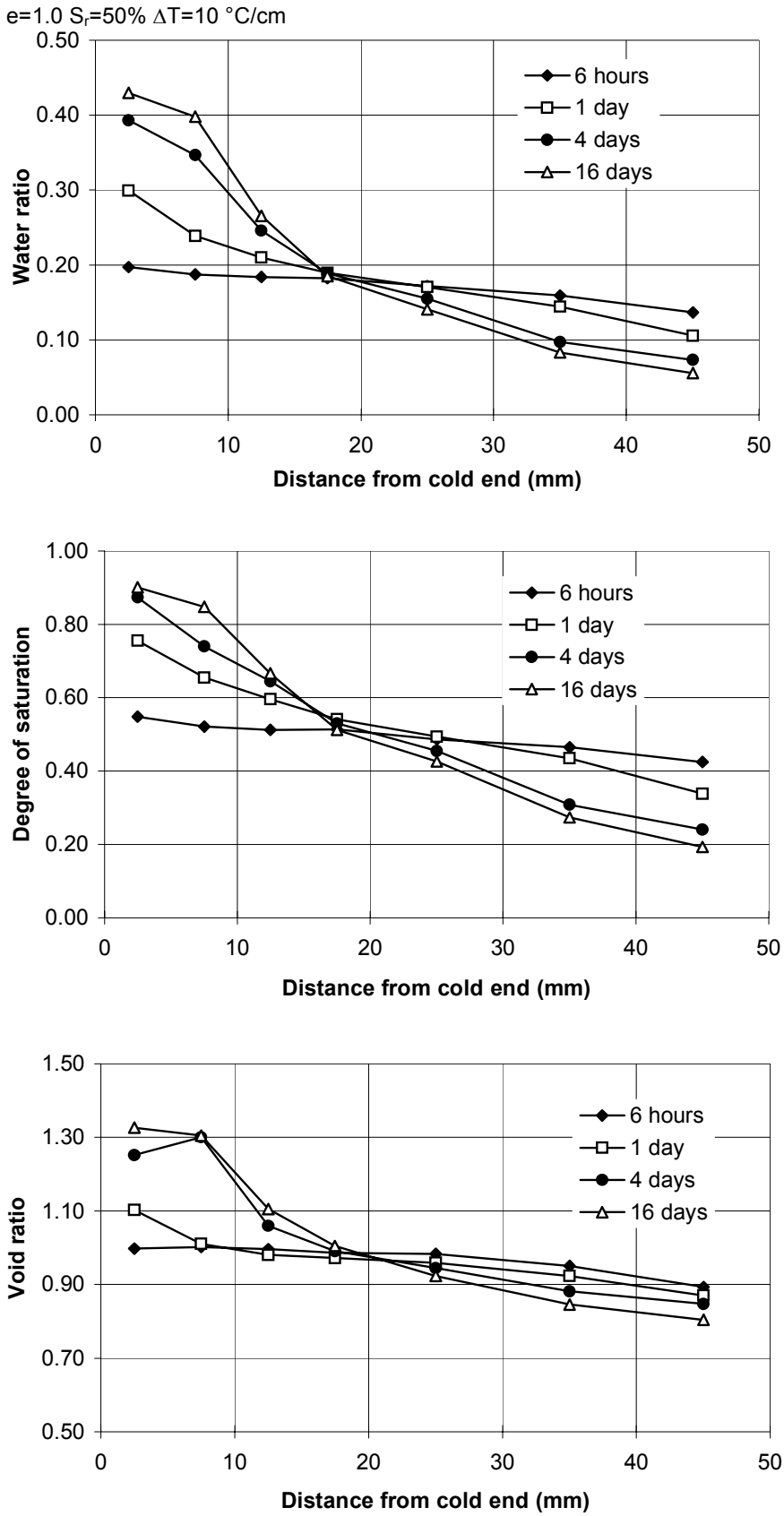

Figure 2-19. *Results from temperature gradient tests on samples with the initial target void ratio e = 1.0 and initial target degree of saturation S_r = 50% with a temperature gradient of 10 °C/cm.*

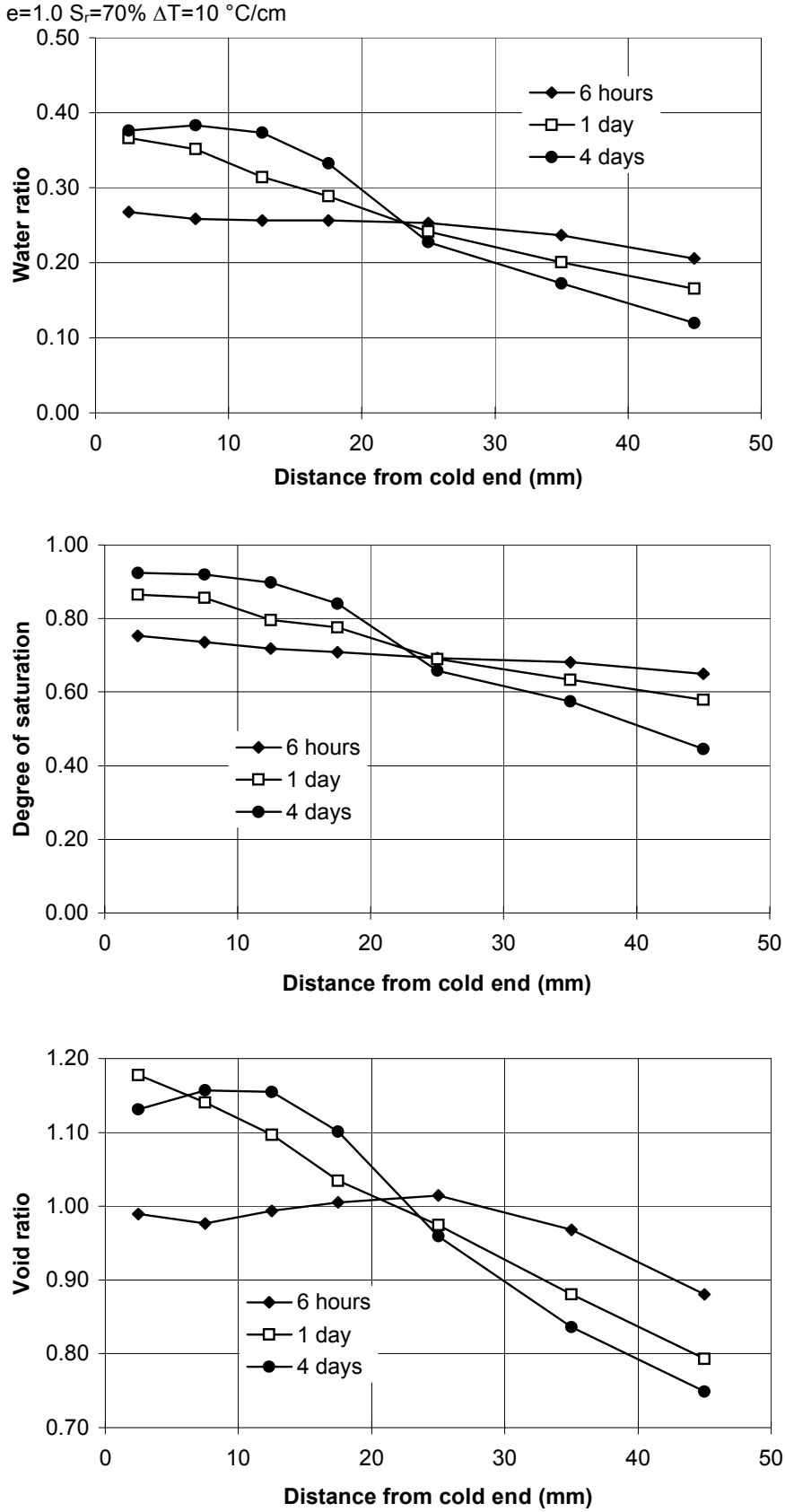

Figure 2-20. *Results from temperature gradient tests on samples with the initial target void ratio e = 1.0 and initial target degree of saturation S_r = 70% with a temperature gradient of 10 °C/cm.*

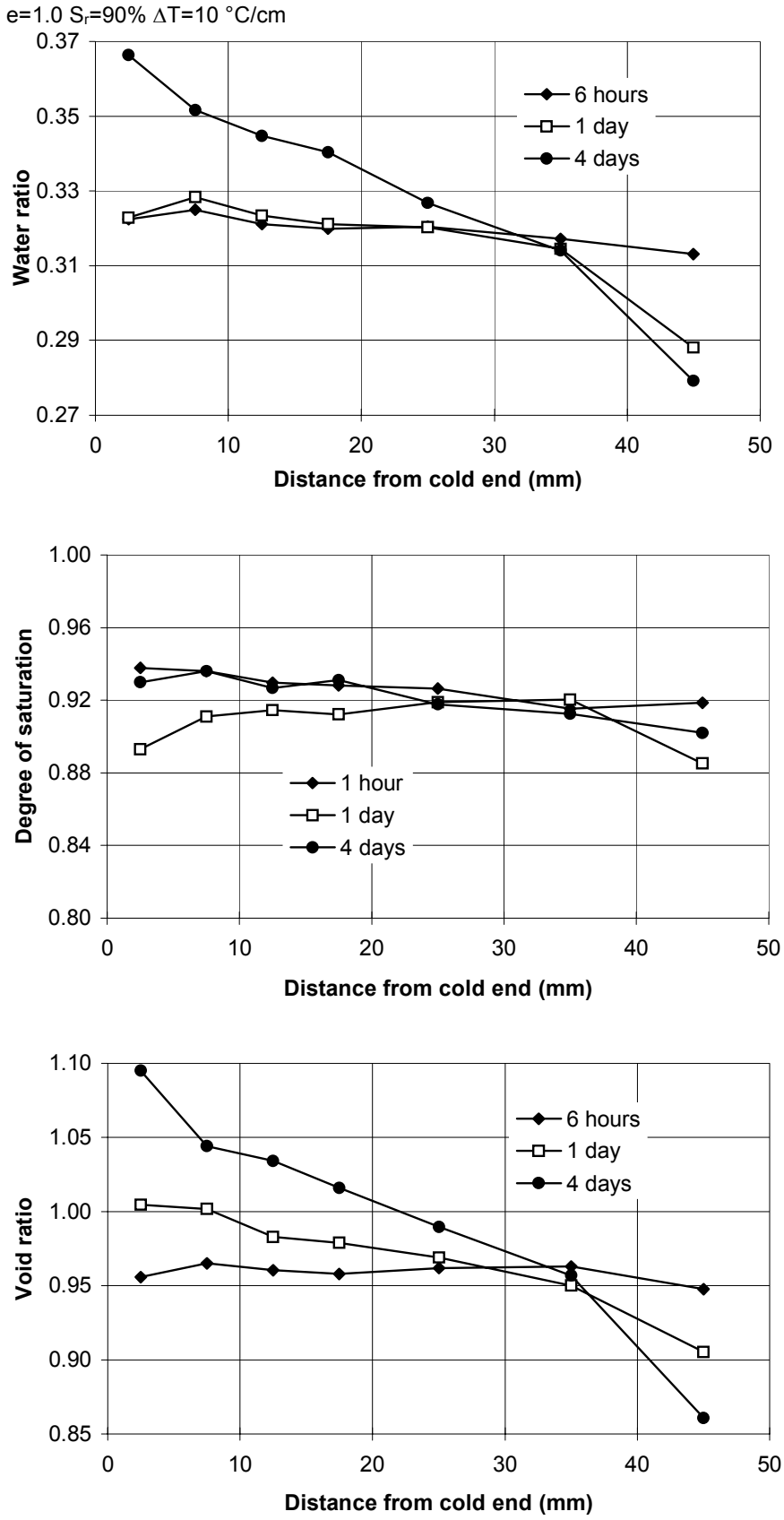

Figure 2-21. *Results from temperature gradient tests on samples with the initial target void ratio e = 1.0 and initial target degree of saturation S_r = 90% with a temperature gradient of 10 °C/cm.*

2.7 One-dimensional compression tests

2.7.1 General

The mechanical properties were investigated by use of three different test procedures, viz. one-dimensional compression tests, unconfined compression tests and triaxial tests. The two latter test types were used mainly for investigating the strength properties while the one-dimensional compression tests, which are described in the present chapter, were used for studying the compressibility.

2.7.2 Sample preparation and test technique

Bentonite and water were mixed and placed in an oedometer ring with a diameter of 5 cm and then compacted to a height of 2 cm. During compaction, the stress and deformation were measured continuously. The compaction was performed at a rate of 10 mm/min so that air could leave the sample. After compaction the sample was unloaded. The tests were performed one day after compaction. The tests were made at constant rate of strain (CRS-test) with the load and the deformation continuously measured. The deformation rate was 0.0005 mm/min.

2.7.3 Results

Nine CRS tests were made. The results measured during compaction, unloading and compression are exemplified by test CRS5 (Figs 2-22 to 2-24). Fig 2-22 shows that the deformation rate during compaction was constant and that the maximum compaction stress was 3000 kPa. The total swelling of the sample after unloading was 0.5 mm (see Fig 2-23). In Fig 2-24 the CRS test is plotted, indicating that one can identify three parts (A-B, B-C and C-D). The figure also shows a schematic visualization of the test. From the curve, the inclination (modulus) of the three pats of the test can be calculated and a ”precompression” stress can be evaluated. All nine tests have been evaluated in this way, the results being shown in Table 2-1. Fig 2-25 shows the precompression stress and compression modules as functions of the compaction stress.

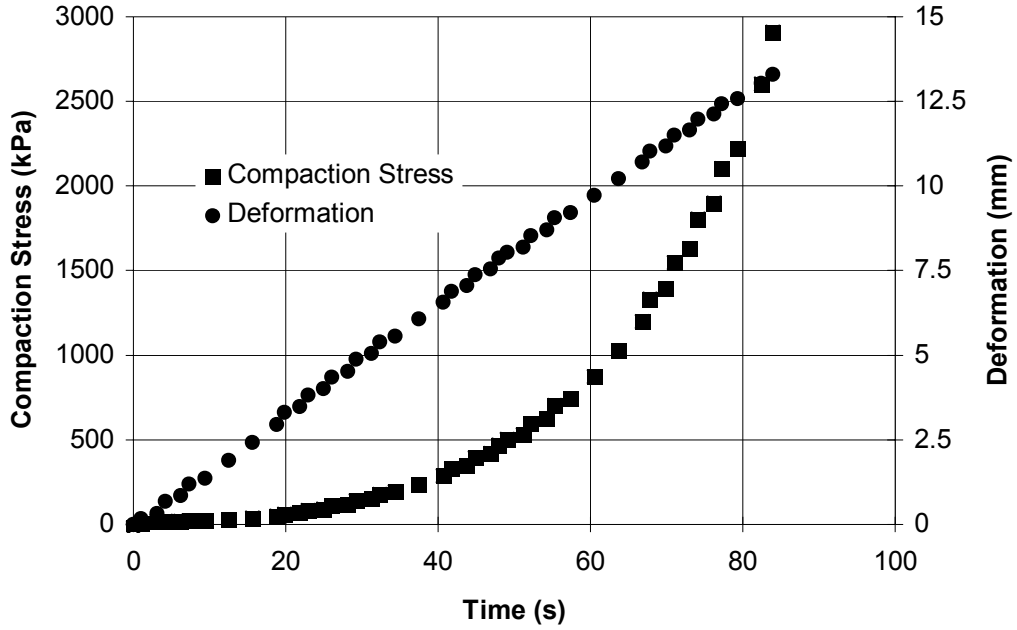

Figure 2-22. *Compaction of sample CRS5*

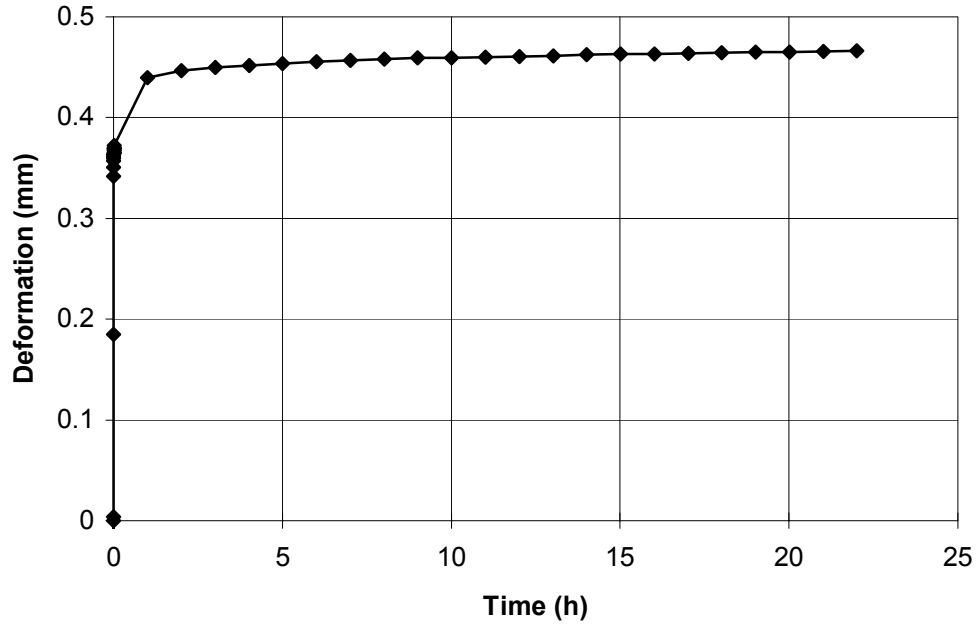

Figure 2-23. *Swelling of sample CRS5 after compaction and unloading*

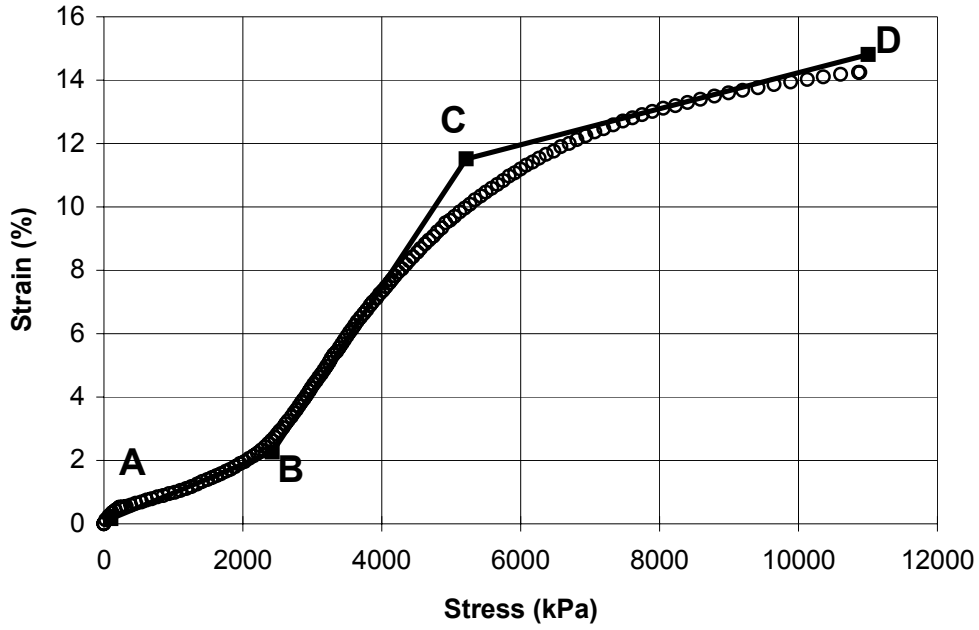

Figure 2-24. *The one-dimensional compression test CRS5.*

Table 2-1. Evaluated parameters from the compression tests.

No	e	S_r. (%)	Compac-tion stress (kPa)	B*) (kPa)	A-B**) (kPa)	B-C**) (kPa)	S_r at C (%)	C-D**) (kPa)
CRS5	1	70	2900	2420	110500	30270	0.88	176200
CRS6	1	50	5600	5800	168400	81040		
CRS3	1.3	90	1020	600	33000	16500	0.99	170000
CRS1	1.3	70	1130	890	42600	10000	0.93	215200
CRS7	1.3	50	1530	1130	56500	14700		
CRS4	1.4	65	900	620	23000	6650	0.92	203300
CRS2	1.6	90	410	240	11850	3650	1.01	39660
CRS8	1.6	70	440	250	20800	3820	0.95	92470
CRS9	1.6	50	670	590	25900	4910		

*) Measured stress at B (evaluated precompression stress)
**) Compression modulus evaluated between A-B, B-C and C-D respectively.

Although the tests are few Table 2-1 and Figure 2-25 indicate the following:

The precompression stress at B is slightly lower than the compaction stress.
The compaction modulus A-B is a function of the compaction stress.
The compaction modulus B-C is a function of the compaction stress.

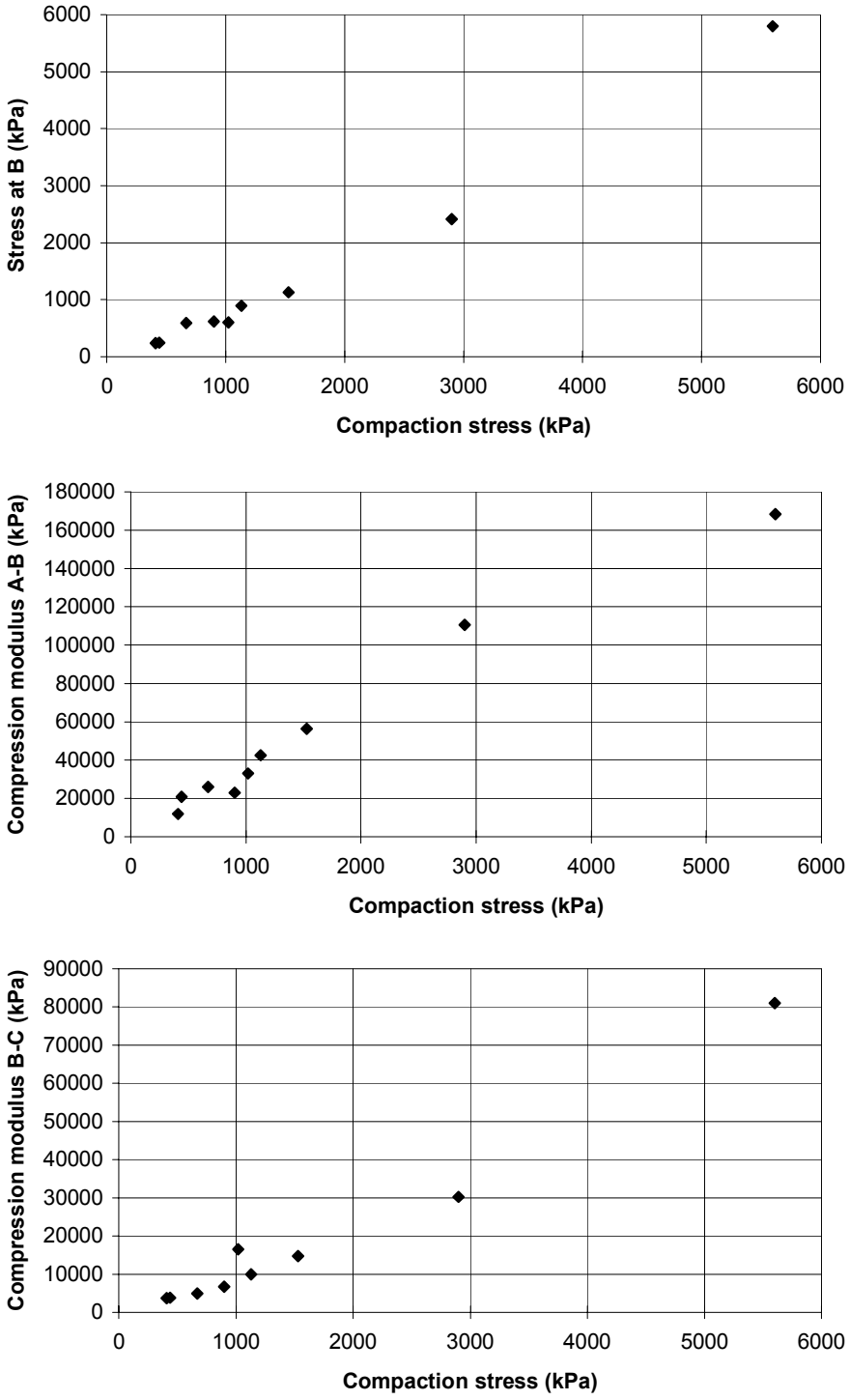

Figure 2-25. *Precompression stress and compression modulus plotted as function of the compaction stress*

2.8 Unconfined uniaxial compression tests

2.8.1 General

In an unconfined unaxial compression test a sample with no radial confinement or radial external stress is unaxially compressed at a constant strain until failure is reached. The test is normally run so fast that the failure is reached under undrained conditions, which means that no volume change of the sample occurs if the sample is water saturated. With these assumptions the strain and deviator stress can be calculated by use of Eqn. 2-1 and Eqn. 3-2.

$$\varepsilon = \frac{\Delta L}{L} \tag{2-1}$$

$$q = \frac{1}{A_0} F(1 - \varepsilon) \tag{2-2}$$

where

ε = Vertical strain
L = Length of the sample
ΔL = Deformation of the sample
A_0 = Cross section area
F = Vertical load
q = Deviator stress

If the samples are unsaturated, failure will not be reached at zero volume change. Still, these tests are evaluated according to Eqn. 3-1 and Eqn. 3-2 since the strain at failure is rather small and thus also the volume change at failure.

2.8.2 Sample preparation and test technique

For each test, three samples were compacted in a cylinder with a diameter of 50 mm and 50 mm height with the technique and equipment described in chapter 2.2. After compaction, the water ratio and density were measured on one of the samples. The other two samples were put together to form one sample and mounted in a press. The sample was compressed at a constant rate of strain (0.16 %/min), the applied force and deformation being recorded continuously. Tests with four different target void ratios were performed (e=0.7, e=1.0 , e=1.3 and e=1.6). For each void ratio three tests with different target degrees of saturation were performed. The water ratio and density of the samples were measured after each test.

2.8.3 Results

Figs 2-26 to 2-29 show the results of the tests. The deviator stresses are plotted as a function of the strain.

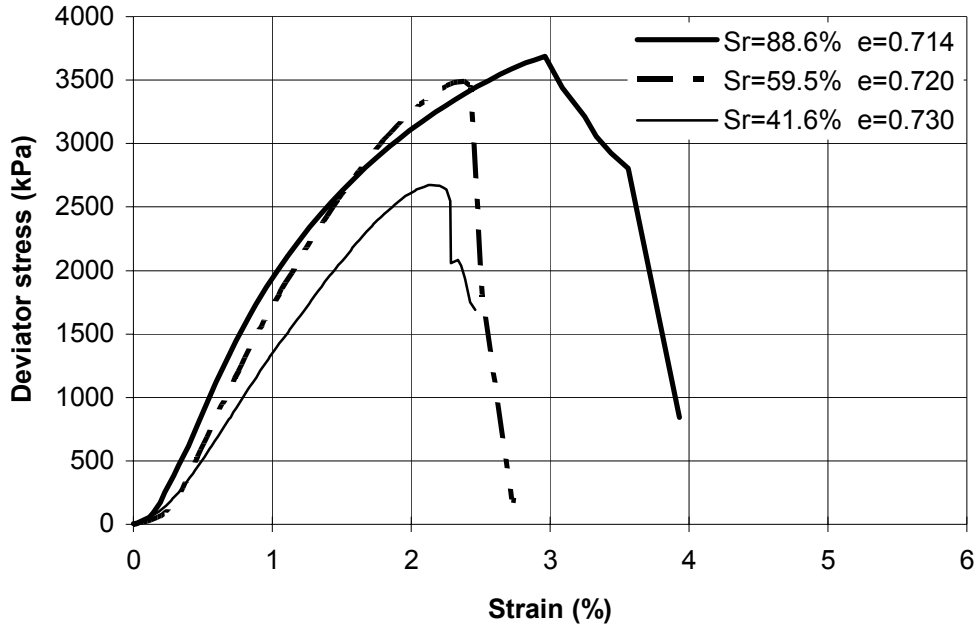

Figure 2-26. *Results from unconfined uniaxial compression tests on MX-80 with the target void ratio e=0.7.*

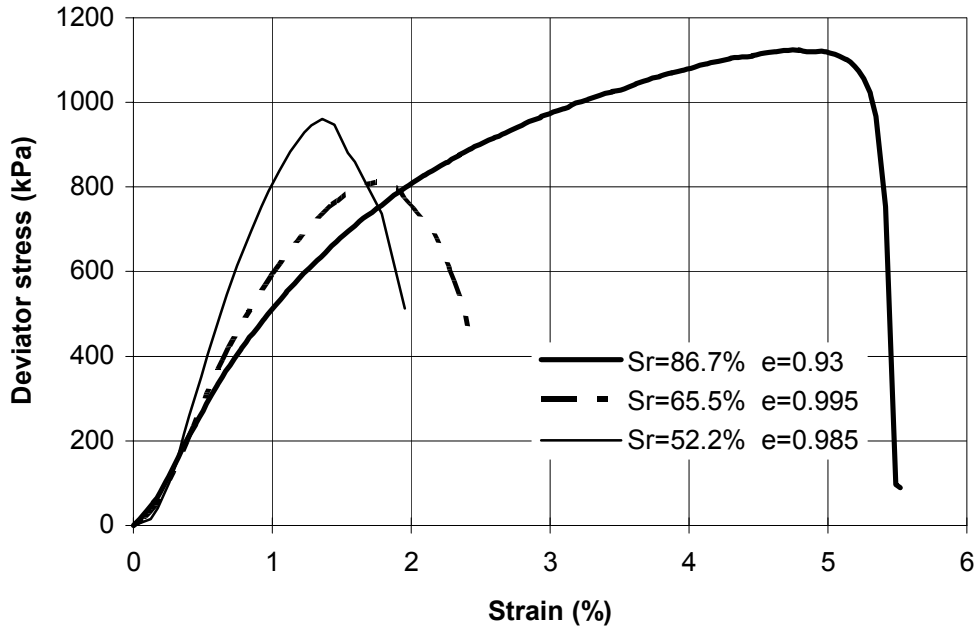

Figure 2-27. *Results from unconfined uniaxial compression tests on MX-80 with the target void ratio e=1.0.*

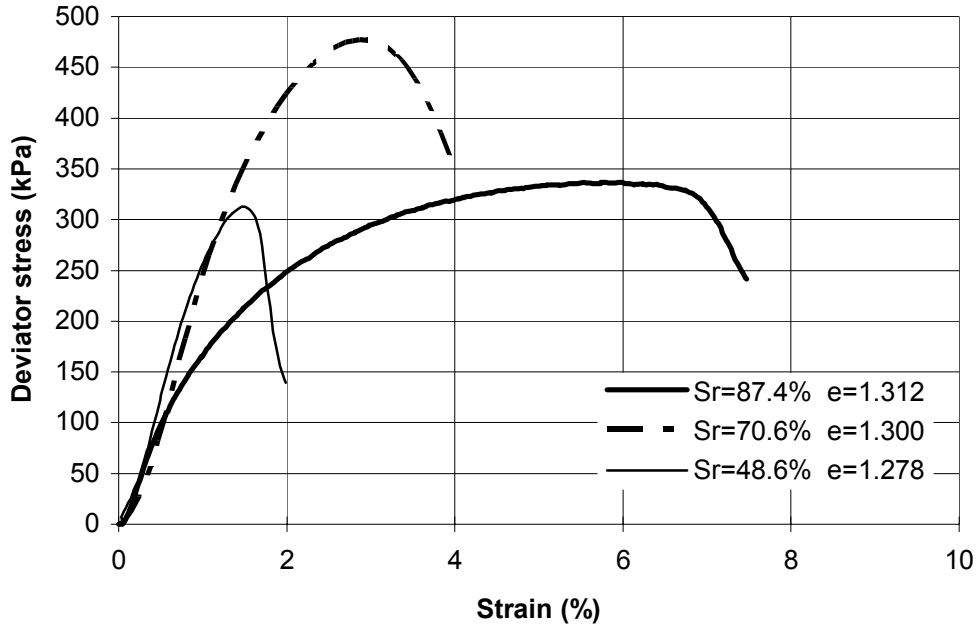

Figure 2-28. *Results from unconfined uniaxial compression tests on MX-80 with the target void ratio e=1.3.*

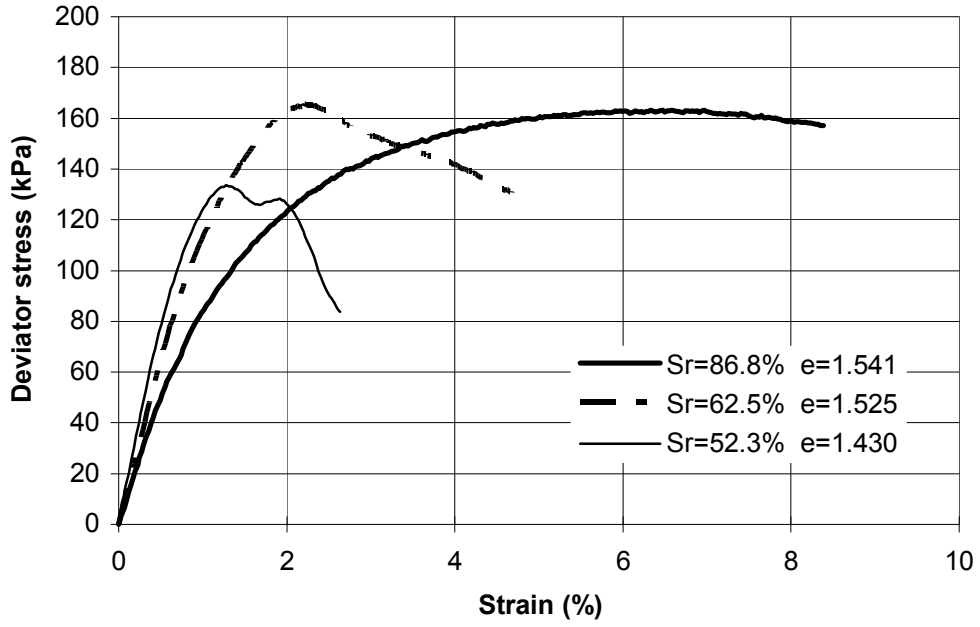

Figure 2-29 *Results from unconfined uniaxial compression tests on MX-80 with the target void ratio e=1.6.*

2.9 Triaxial tests

2.9.1 General

The stress-strain-strength properties of soils are preferably evaluated from triaxial tests. Fig 2-31 shows a schematic drawing of a triaxial test cell. Only two such tests have been carried out on unsaturated bentonite samples, the main purpose being to see if the equipment was suitable and if the technique for evaluating the response of an unsaturated sample was acceptable.

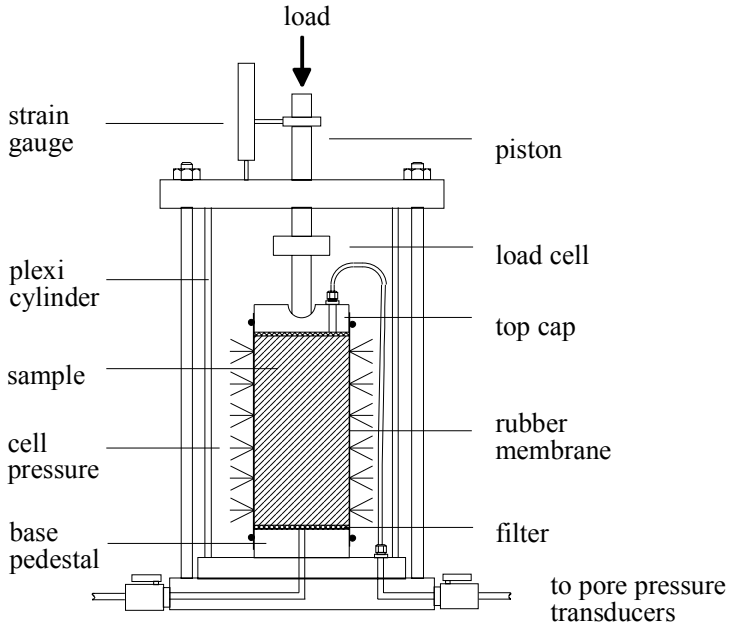

Figure 2-31. *Schematic drawing of the triaxial cell.*

2.9.2 Sample preparation and test technique

The samples were prepared in the same way as those for the unconfined compression tests. For each test three samples were compacted in a cylinder with a diameter of 50 mm to a height of 50 mm, with the technique and equipment described in chapter 2.2. After compaction, the water ratio and density of one of the samples were measured. The two other samples were put together to form one sample. After mounting the sample in a triaxial cell, a cell pressure was applied with a GDS[1] digital controller and equilibrium condition in the sample was allowed to be established. It was not possible to use the

[1] Microprocessor controlled hydraulic actuator for regulation and measurement of liquid pressure and liquid volume change (from GDS Instruments Ltd)

same technique for measuring the volume change during the tests as normally used for saturated samples, for which the amount of water entering and leaving the sample is measured. Instead, the volume change of the water in the cell was measured by the GDS. It is equal to the volume change of the sample, corrected for the penetration of the piston, provided that there is no leakage from the cell.

The volume change of the sample was measured directly after applying the cell pressure. After equilibrium, the cell was placed in a press and compression at a constant rate of strain applied. The force, the volume change, and the deformation were continuously measured during the test. After the test, the weight of each sample was measured and the sample cut in five slices. The density and water ratio of the slices were determined.

2.9.3 Results

Data from the two samples, determined before and after testing, are shown in Table 2-2. The first test (Triax1) was performed on a sample with the bulk density 1.61 g/cm^3 and water ratio 31.4% at a cell pressure of 500 kPa. After the test the density and water ratio of the sample had changed to 1.80 g/cm^3 and 30.9%, respectively. Table 2-2 shows that there was a small loss in weight but a large decrease in volume. The volume change measured by the GDS was 3.78 cm^3 at equilibrium after application of cell pressure and 20.70 cm^3 during the test, yielding a total volume change of 24.48 cm^3. This is similar to the direct measurement on the sample which yielded a volume change of 25.92 cm^3. The results from the tests are shown in Fig 2-32.

In the second test (Triax2), the sample was compacted to a density of 1.62 g/cm^3 and a water ratio of 50.6% and performed at a cell pressure of 200 kPa. After the test, the density was 1.70 g/cm^3 and the water ratio 48.9%. The volume change calculated from the difference in weight for this sample was 10.55 cm^3. The volume change measured by the GDS was 3.52 cm^3 after equilibrium and 8.28 cm^3 during the test, yielding a total volume change of 11.80 cm^3. The results from the test are shown in Fig 2-33.

The two tests indicate that it is feasible to measure the volume change of the sample by measuring the volume change of the cell water.

Table 2-2. Determined parameters of the triaxial samples.

	Weight (g)	Volume (cm^3)	ρ (g/cm^3)	w (%)	e	Sr (%)
Triax1 before the test	312.7	199.47	1.62	31.4	1.26	69.5
Triax1 after the test	312.3	173.55	1.80	30.9	1.02	84.0
Triax2 before the test	318.1	197.52	1.62	50.6	1.59	88.8
Triax2 after the test	318.7	186.97	1.70	48.9	1.43	95.2

The volume of air leaving the samples was also measured during the tests. This volume was in accordance with the volume change of Triax 1 until 12% strain corresponding to

S_r = 79%. Beyond this strain there was no agreement at all between the measured volume of air leaving the sample and measured volume change, as was also the case for the entire test Triax 2. The results indicate that the continuity of the air phase ceases at about S_r =80%, which agrees very well with measurements on other sorts of soils.

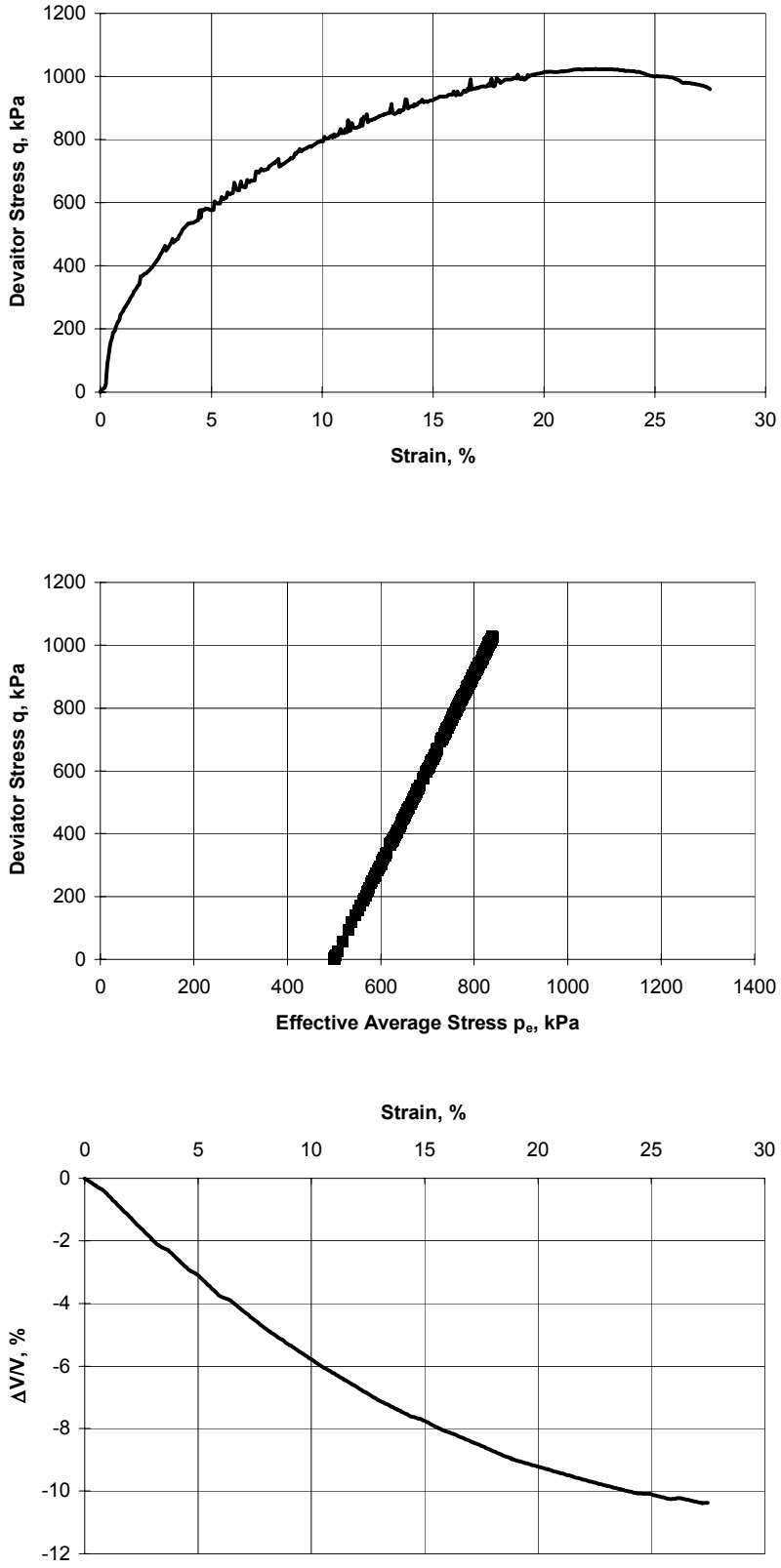

Figure 2-32. *Results from the test Triax1.*

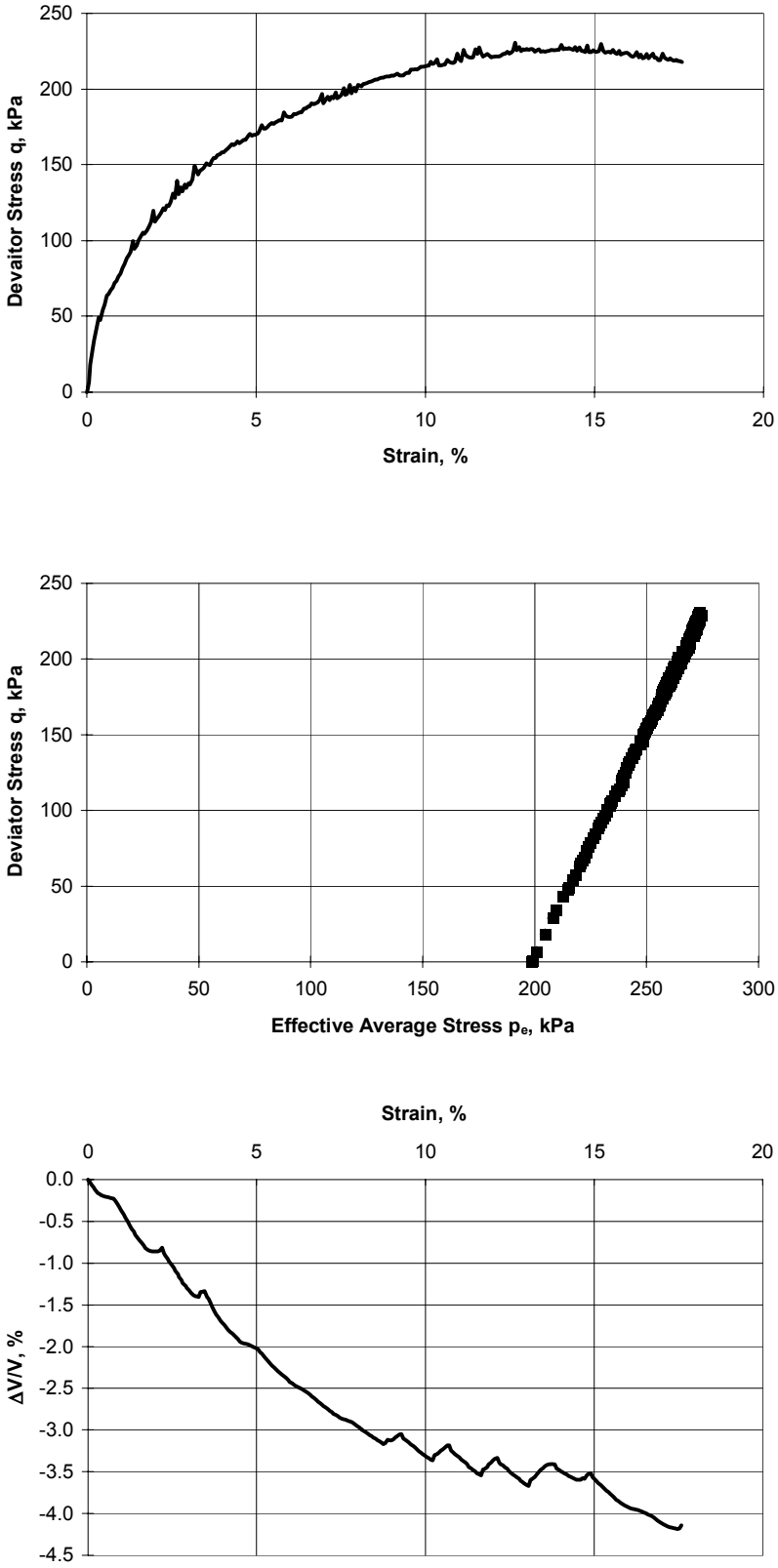

Figure 2-33. *Results from the test Triax2.*

3 Laboratory simulation of bentonite/canister THM interaction before saturation

This chapter is based on work done in 1993.

3.1 Test arrangements

3.1.1 General

Equipment, which simulates a horizontal cut through a canister with bentonite buffer and surrounding rock, was built. The diameter of the bentonite sample holder that simulates the rock is 116 mm and the diameter of the simulated canister is 20 mm. A precompacted bentonite sample with an outer diameter of 104 mm and a central hole of 24 mm was placed in the sample holder. The density of the bentonite block was the same as the intended one in a deposition hole. After having filled the outer and inner slots with water, the sample holder was closed, i.e. no further water was added during testing. This simulates a dry rock. A constant temperature of 90°C was applied on the copper. The test time lasted for about 6 weeks. During this time the temperature was measured in 5 radial positions on two levels. The swelling pressure in radial direction was also measured. Two tests with MX-80 bentonite with the following initial properties were performed:

One test sample (Test 1) had an initial water ratio of 10% and a density of 2.09 g/cm³ and the other (Test 2) had an initial water ratio of 16% and a density of 2.09 g/cm³.

The samples originate from bigger blocks (d=280mm), compacted with 100 MPa. The test samples were drilled from these blocks with a core drill. A central hole was then drilled for the copper tube.

Before test start the slots were filled up with water. During testing the samples had no access to further water.

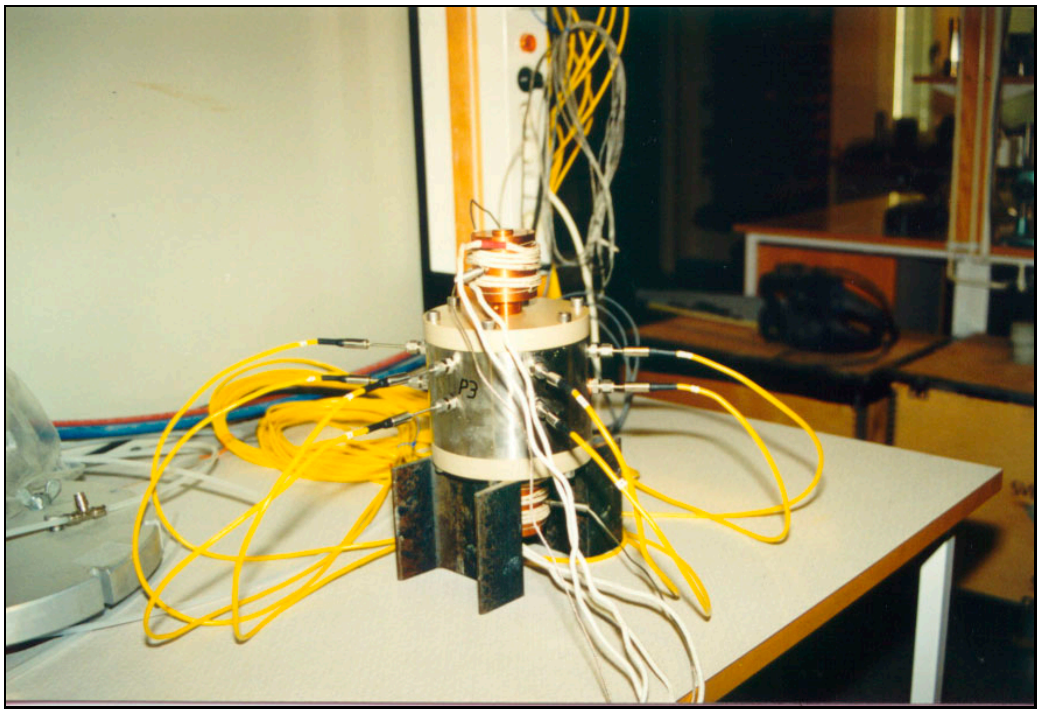

Figure 3-1. *Photo showing the test equipment.*

3.1.2 Techniques

The simulated canister consists of a solid copper rod. The rod passes through the lids of the sample holder. The lids are made of PEEK (polyetheretherketon). This material was chosen because of its high strength in combination with its thermal properties. In order to avoid edge effects it is important to have a material with low heat conductivity (0.25 W/m°C for PEEK compared to 16-24 W/m°C for stainless steel). The cylindrical sample holder is made of stainless steel (Fig 3-1).

Ten thermocouples are placed on two levels in the clay sample (Figs 3-2 and 3-3). They are placed in different radial positions in order to provide information on the temperature distribution in the sample. Thermocouples are also placed in the steel cylinder, in one of the PEEK lids and in the copper tube where it enters the sample.

A radial piston is placed centrally on the sample holder, in order to measure the swelling pressure.

The heat is applied by heat wires wound around the ends of the copper tube. The effect of the heat wires is trigged to give a constant temperature of 90°C at the ends of the copper tube.

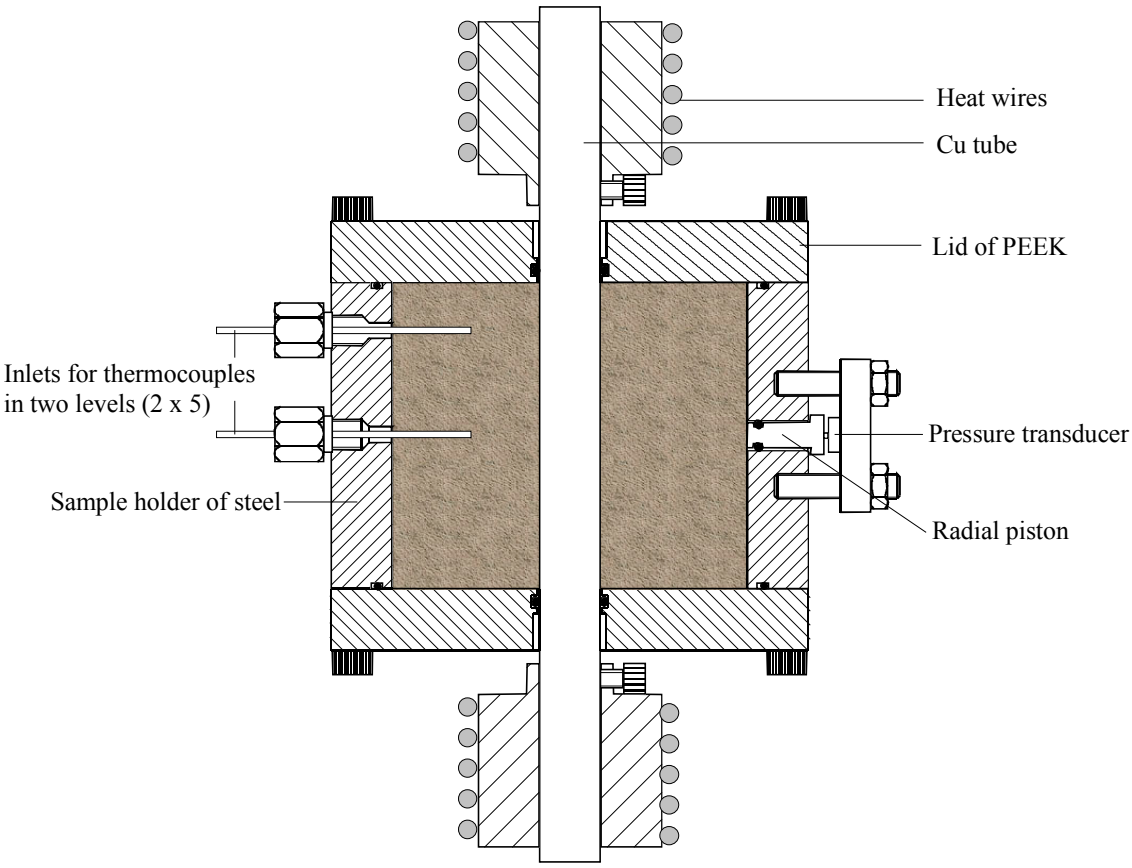

Figure 3-2. *Schematic drawing of the test equipment.*

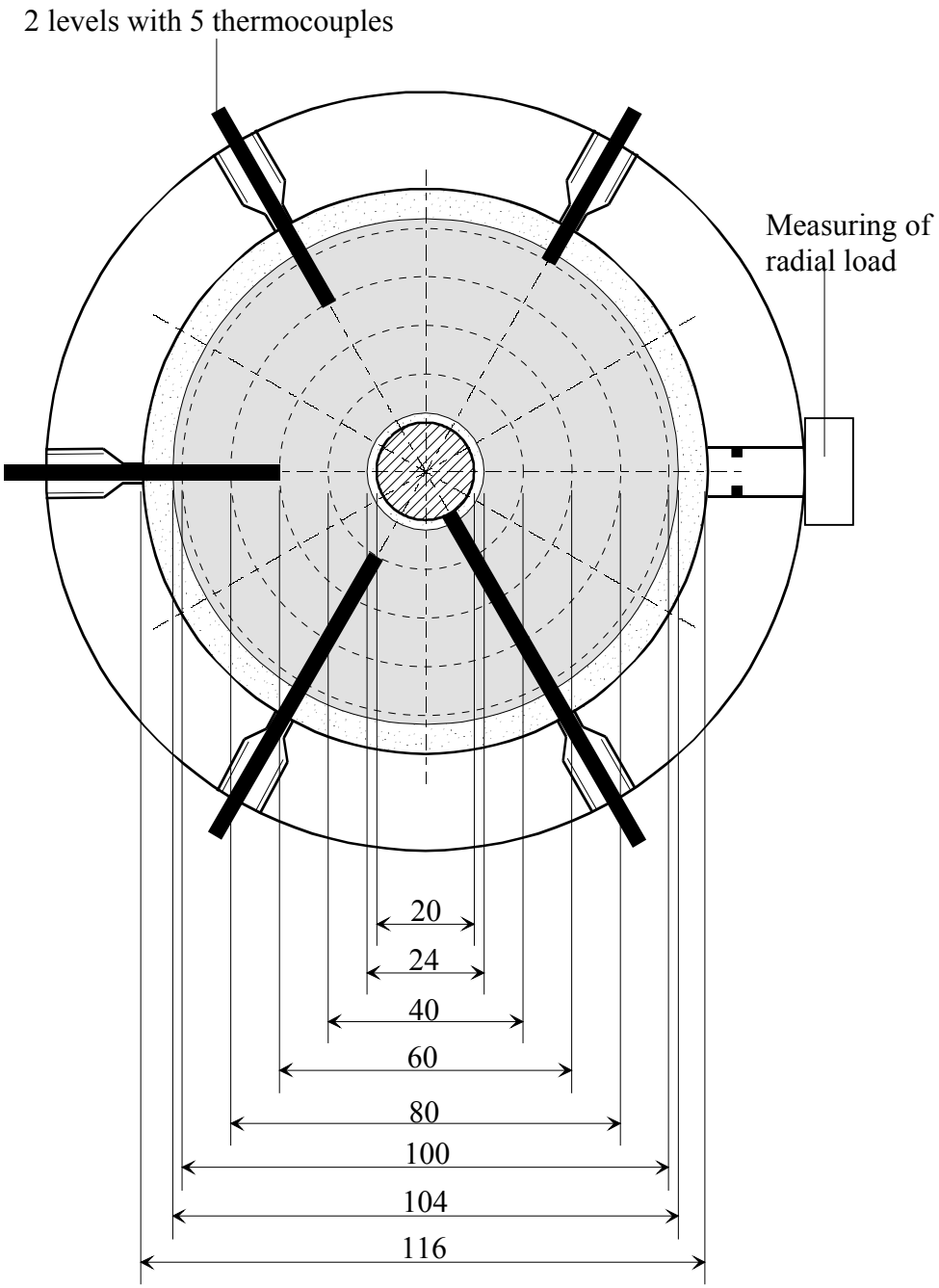

Figure 3-3. *Schematic drawing of the test equipment showing a central cut. The thermocouples had the same radial position on both levels.*

3.1.3 Preparation

The preparation was made as follows:

1. One of the PEEK lids was attached to the steel ring and the copper tube was put in position.

2. The sample was weighed and placed in position.

3. In order to get the thermocouples in the right positions, holes were drilled into the bentonite. The distance to the steel ring was locked by use of spacers. The holes were drilled using the inlets in the steel ring as guides. In order to obtain the correct hole depth marks were made on the drill. After drilling, the cuttings were removed and the thermocouples installed. The pressure transducer was mounted on the radial piston.

4. The spacers were removed and the slots, both the inner and the outer, were filled up with water. The weight of the water poured was determined.

5. The upper PEEK lid was mounted and the copper ends with heat wires (prepared earlier) were mounted.

6. The registration of data was started and the temperature applied.

3.2 Results

3.2.1 General

In both tests the temperature and swelling pressure were stabilised within 2 weeks. They were, however, running for about 6 weeks so that steady state conditions certainly were reached.

The clay samples and the added water was weighed during test preparation. Using these values, the known water ratio of the clay and the volume of the sample holder, the average density, water ratio and degree of saturation could be calculated (Table 3-1).

Table 3-1 The average values (including the water-filled slots) of dry density, void ratio, water ratio and degree of saturation

	ρ_d g/cm³	e	w %	Sr %
Test 1	1.45	0.922	25.6	78.0
Test 2	1.41	0.982	31.2	89.4

3.2.2 Temperature distribution

The accuracy when positioning the thermocouples is of importance when evaluating measured data. The positioning in radial direction should have an accuracy of ± 1mm. The innermost thermocouples were intended to touch the copper tube. A remaining slot between bentonite and copper will also strongly influence the measured value.

Figs 3-4 and 3-5 show the measured temperature and swelling pressure as a function of time. The temperature is quite stable during the entire test since the heating is temperature controlled. The large temperature drop between the two inner transducers, especially for level 1 at Test 1, indicates that there is a slot, which was also found after the test. However, the scatter in temperature of the inner transducers also indicates that probably only the transducer on level 1 at Test 1 is in direct contact with the copper tube. It is a little surprising to see that the temperature drop between the transducer and the other ones does not change during the test, which should have been the case if the water filled slot at first was sealed and then opened during the drying.

The swelling pressure increases with time and stabilises after about 2 weeks.

Fig 3-6 shows the temperature at steady state as a function of the distance from the copper tube. The existence of a slot is obvious in Test 1 but not in Test 2. The influence may be concealed by poor contact between the copper tube and the transducers.

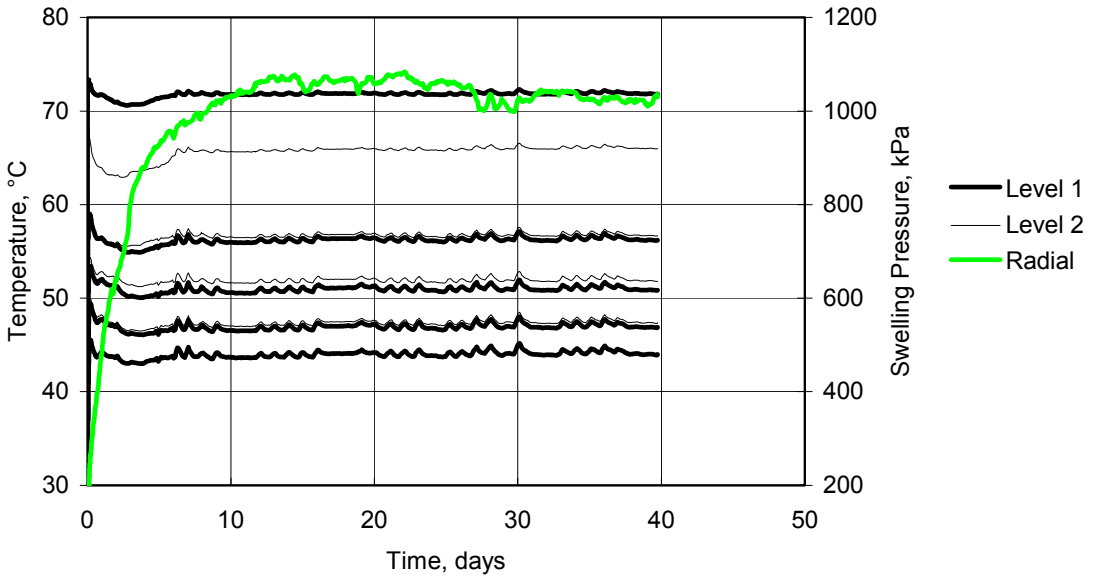

Figure 3-3. *Temperature (black lines) and swelling pressure (grey line) plotted as function of time for Test 1. The five bold lines (Level 1) and the five thinner lines (Level 2) represents the five radial positions with the highest temperature closest to the copper tube. Registered temperature in the steel ring was 43°C and in the PEEK lid 36°C.*

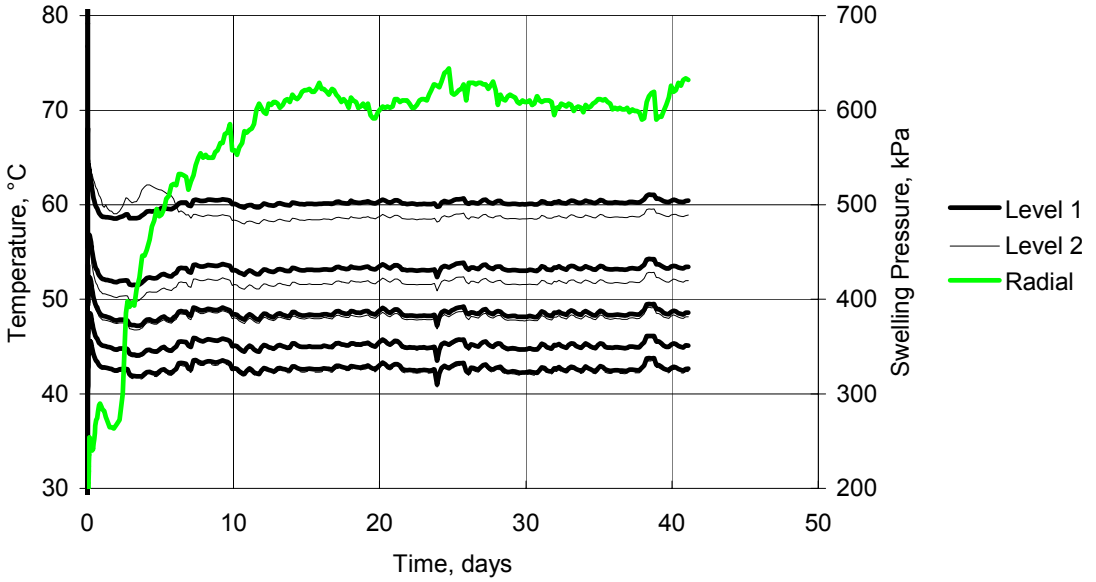

Figure 3-4. *Temperature (black lines) and swelling pressure (grey line) plotted as function of time for Test. The five bold lines (Level 1) and the five thinner lines (Level 2) represent the five radial positions with the highest temperature nearest the copper tube. Registered temperature in the steel ring was 42°C and in the PEEK lid 35°C.*

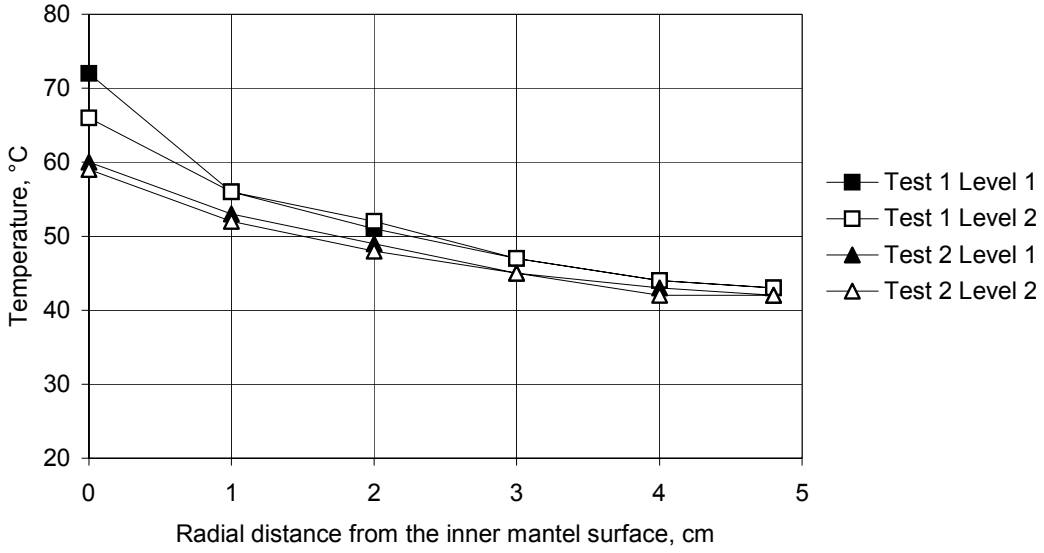

Figure 3-5*. Temperature distribution at steady state for Test 1 and Test 2. The outermost point is situated in the steel ring.*

3.2.3 Swelling Pressure

The swelling pressure is plotted against time in Figs 3-4 and 3-5. The measured swelling pressures at steady state, 1050 kPa in Test 1 and 600 kPa in Test 2, correspond well to the expected swelling pressure (at void ratios extrapolated to the periphery) as shown in Table 3-2.

Table 3-2. Properties at the periphery

	Water ratio at periphery	Void ratio (S_r = 100%)	Swelling pressure
Test 1	0.37	1.03	1 400
Test 2	0.44	1.27	600

3.2.4 Appearance and slot widths at termination

At termination both test samples were photographed and the former slots were inspected (Figs 3-7 to 3-9). In both samples an obvious gradient from light grey to dark grey depending on the water distribution could be seen. Especially in the sample from Test 1, it was evident that a large amount of water was located at the periphery, almost as a shell (Fig 3-7).

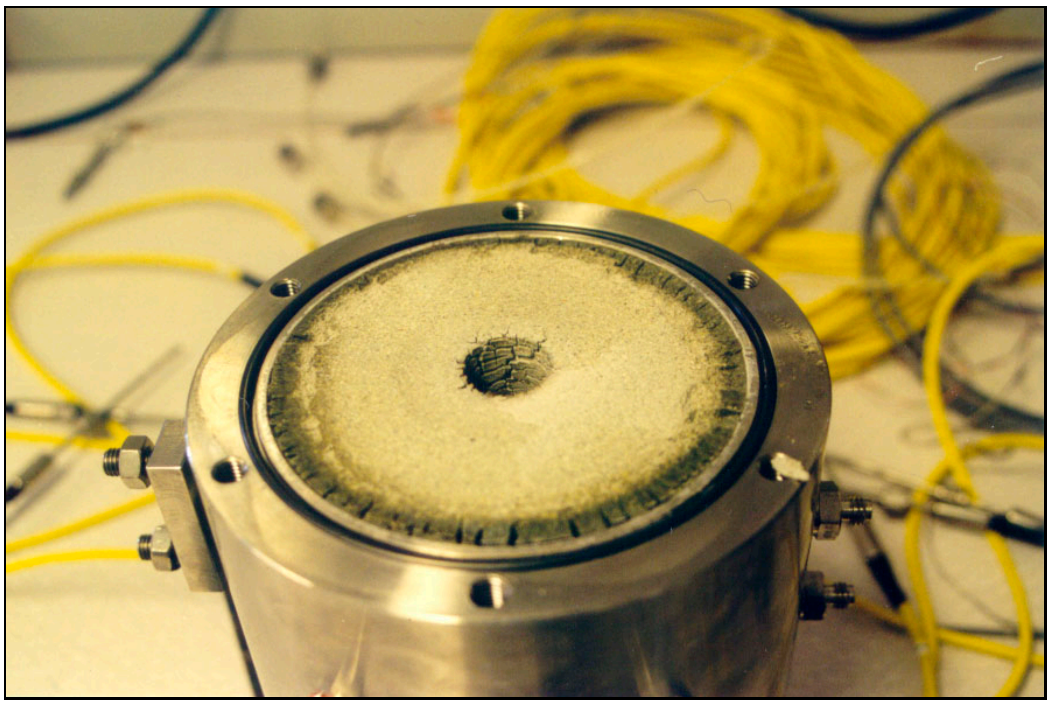

Figure 3-7*. Photo from Test 1 showing the appearance at termination*

The outer slot for both samples was completely sealed. That was not surprising, since a swelling pressure had been registered during the test period.

The inner slot was, however, for both tests still present. The slot width at start was 2mm. The remaining slot width after the test period was measured to be about 1mm. The surface on the inner slot was for both samples very fractured (Fig 3-9).

Figure 3-8 *Photo from Test 2 showing the appearance at termination. Note the inner slot, which still exists*

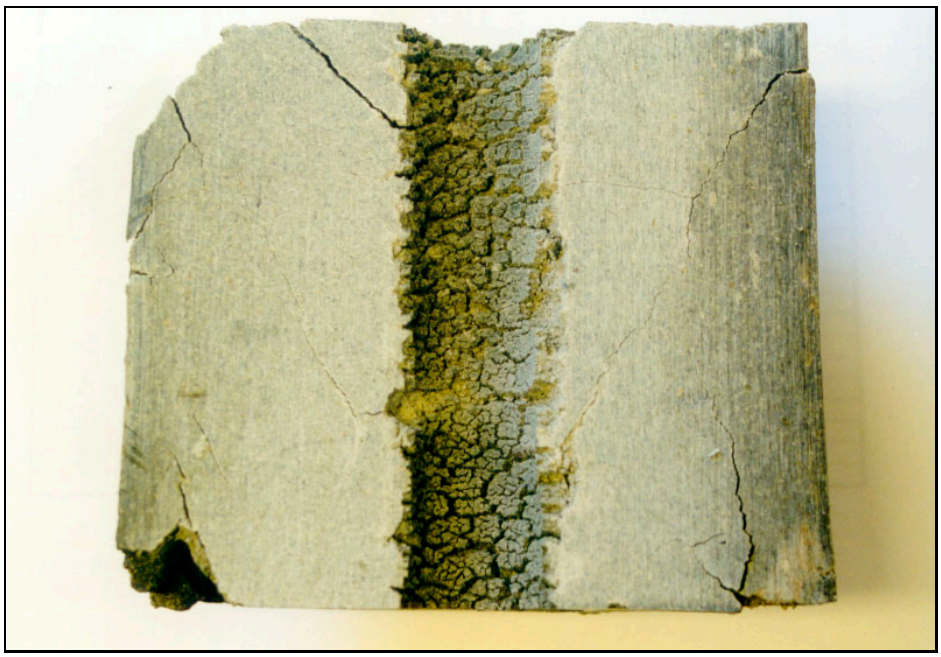

Figure 3-9. *Photo from Test 2, after cutting up the sample, showing the surface of the inner slot*

3.2.5 Sampling after test

General

After termination the test samples were investigated with respect to water content and density. The sampling was done according to Fig 3-10. Water ratios were determined by drying during 24h at 105°C. The densities were measured by submerging the samples in paraffine oil. Tables 3-3 and 3-4 show measured and calculated results from the laboratory tests. The samples were photographed and the slot widths were measured.

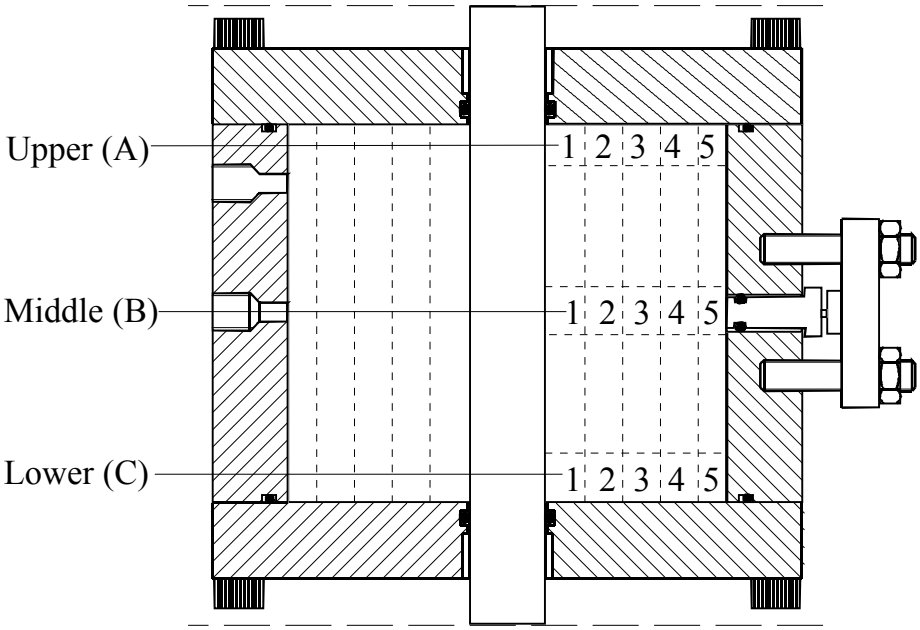

Figure 3-10*. Figure showing the sampling areas and the sampling nomenclature.*

Table 3-3 Results from laboratory tests on samples from Test 1

Sample	ρ	w	Sr	e	ρ_m	ρ_d
	g/cm³	%	%		g/cm³	g/cm³
A1	1.96	16.3	70.3	0.646	2.08	1.69
A2-A3	1.93	20.6	77.3	0.739	2.02	1.60
A4	1.83	33.3	90.5	1.023	1.88	1.37
B1	1.89	17.2	65.7	0.726	2.03	1.61
B2-B3	1.89	22.1	77.5	0.791	1.99	1.55
B4	1.82	34.9	91.3	1.062	1.86	1.35
C1	1.96	17.6	73.0	0.670	2.07	1.66
C2-C3	1.88	22.6	77.8	0.809	1.98	1.54
C4	1.82	33.5	89.8	1.037	1.87	1.36

Table 3-4 Results from laboratory tests on samples from Test 2

Sample	ρ	w	Sr	e	ρ_m	ρ_d
	g/cm³	%	%		g/cm³	g/cm³
A1	1.97	22.9	86.5	0.736	2.03	1.60
A3	1.90	24.3	82.2	0.824	1.98	1.52
A5	1.82	39.8	97.0	1.141	1.83	1.30
B1	1.97	20.8	82.4	0.703	2.05	1.63
B3	1.92	26.0	87.6	0.827	1.97	1.52
B5	1.83	41.4	100.8	1.143	1.83	1.30
C1	1.94	21.5	80.9	0.740	2.02	1.60
C3	1.89	26.3	85.4	0.854	1.96	1.50
C5	1.81	38.9	95.0	1.138	1.83	1.30

Water ratio distribution

The water ratio distribution in both samples is shown in Fig 3-11. There is an obvious gradient in both samples. The water added in the slots has been redistributed due to the temperature gradient (~ 5°C/cm).

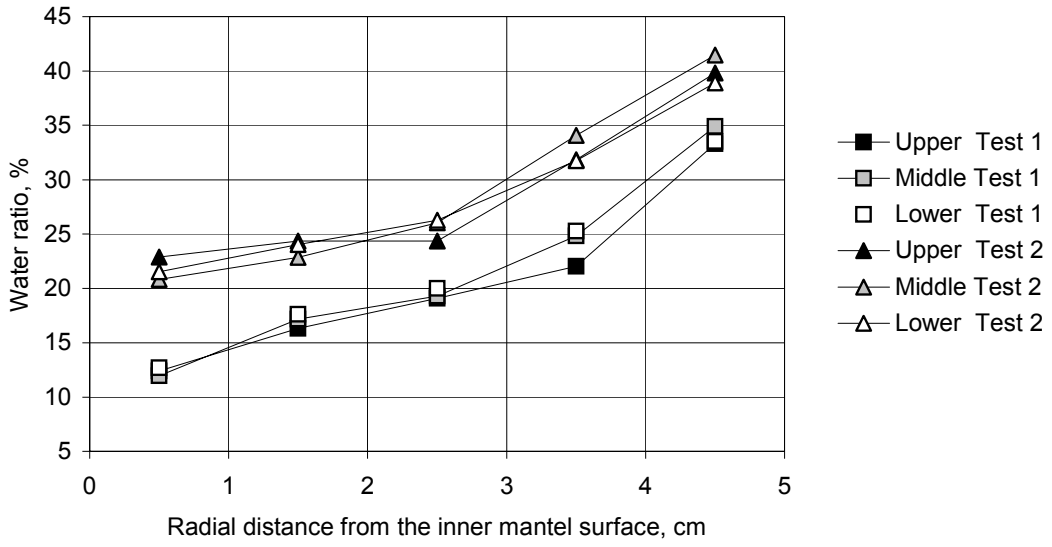

Figure 3-11. *Diagram showing the water ratio distribution after the test*

Density and void ratio

The density was not determined in as many positions as the water ratio, due to difficulties to trim proper samples. As shown in Fig 3-4, it is, however, obvious that there is also a density gradient in radial direction in both samples.

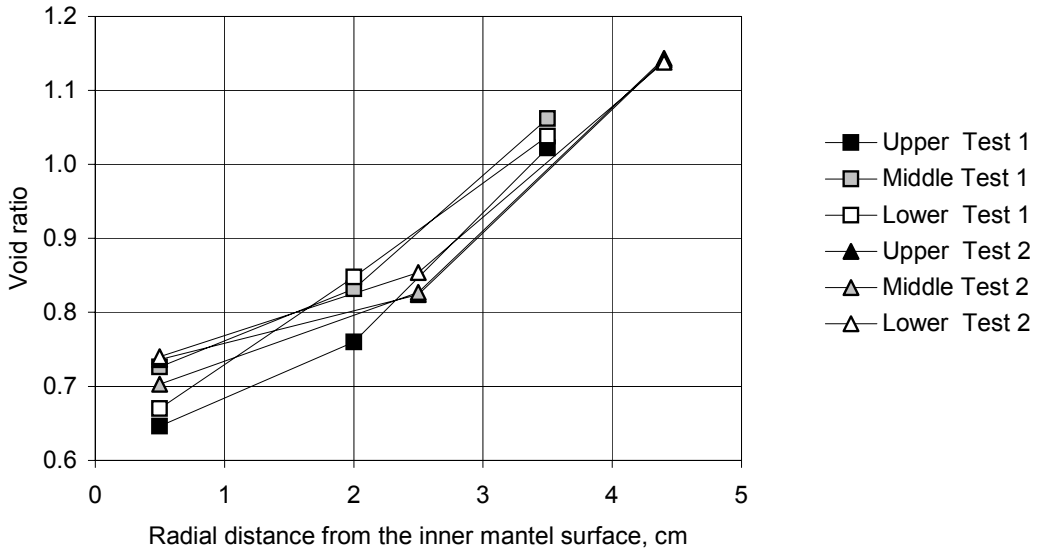

Figure 3-12. *Diagram showing the void ratio distribution after the test*

Degree of saturation

The degree of saturation varied a lot in the sample. The outermost samples showed a rather high degree, 90-100%, while the sample closest to the copper had a degree of saturation of approx. 70% for Test 1 and approx. 85% for Test 2.

Water mass balance

Since the bentonite was heated during 40 days in both tests, there is a risk that there may have been a loss of water. In order to check the water mass balance, the average water ratio before and after the test has been calculated, which yielded the following results:

Test 1:

Water ratio before heating: $w = 25.6\%$

Water ratio after heating: $w = 24.2\%$

Test 2:

Water ratio before heating: $w = 31.2\%$

Water ratio after heating: $w = 31.3\%$

The water ratio before heating was calculated from the sum of the initial water in the bentonite and the water added in order to fill the slots. The water ratio after heating was calculated from the measured water ratio in each radial section. It is concluded that no or very little water was lost during the heating.

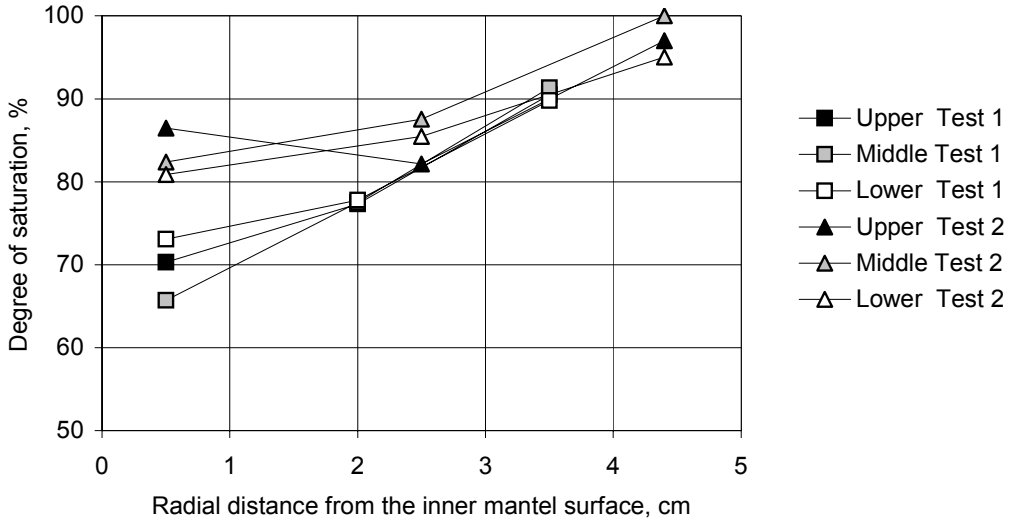

Figure 3-13. *Diagram showing the degree of saturation as a function of the distance from the inner mantel surface*

3.3 Conclusions

The two tests yielded similar results, in spite of that the initial water ratio was different. The bentonite rings in test 1 correspond to blocks compacted with 100 MPa at the natural water ratio of the bentonite MX-80 (10%), while the bentonite rings in test 2 correspond to blocks compacted with the same pressure but at an increased water ratio (16%). The following observations and conclusions can be made:

- A high radial water gradient and a high void ratio gradient were observed after the tests.

- The outer slots were sealed and the degree of saturation close to 100% at the periphery.

- The inner slots were re-opened and the degree of saturation close to the heater was about 70% for the dry bentonite and about 85% for the wetted bentonite.

- The surface of the inner slots was cracked in a square shaped net, which is typical for a dried clay surface.

It is notable that the final water ratios close to the heaters were increased compared to the initial water ratios. The drying cracks seem to be caused by the drying that took place after the initial wetting caused by the water added to the slot. It is thus likely that there will not be the same type of cracks if the inner slots are not filled with water, but this conclusion needs to be confirmed by additional tests.

4 Additional water uptake tests

Some additional water uptake tests have been made in order to check the water uptake rate at a different void ratio and to check the influence of temperature. The tests were made with the technique described in chapter 2.5.

Two tests were made at different temperatures (23 °C and 80 °C) and left for 310 hours before they were dismantled and sliced. Figs 4-1 and 4-2 show the results.

The initial conditions were the following:

$\rho_d = 1.55$

$w = 17\%$

which yield (ρ_s=2.78 g/cm^3; ρ_w=1.00 g/cm^3)

$e_0 = 0.79$

$S_r = 0.59$

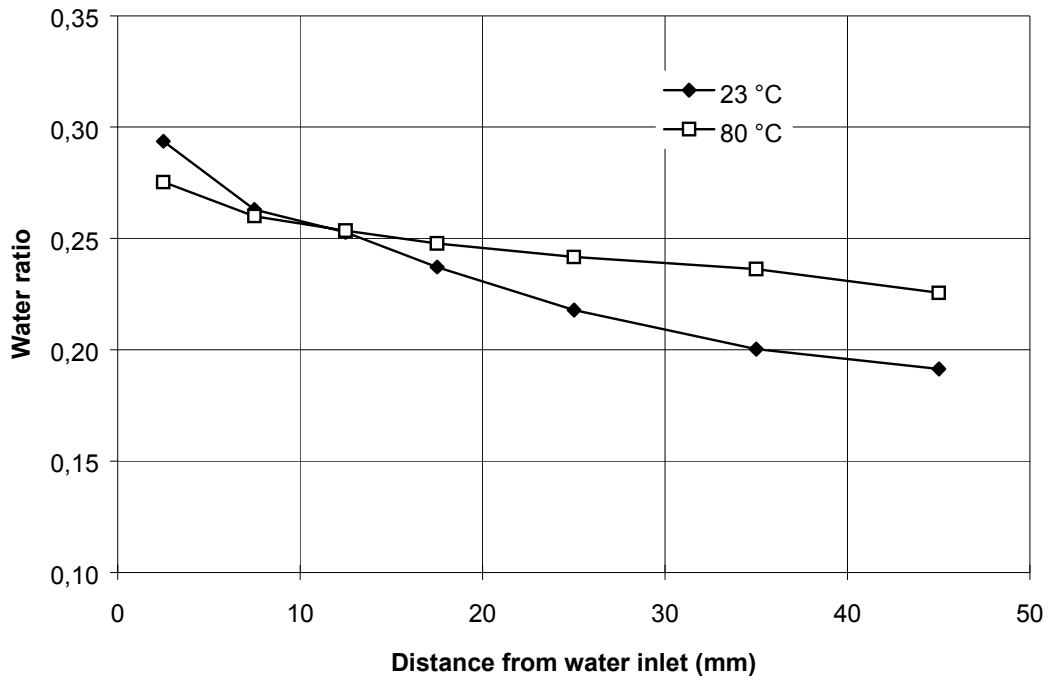

Figure 4-1. *Results of two water uptake tests left for 310 hours at different temperatures.*

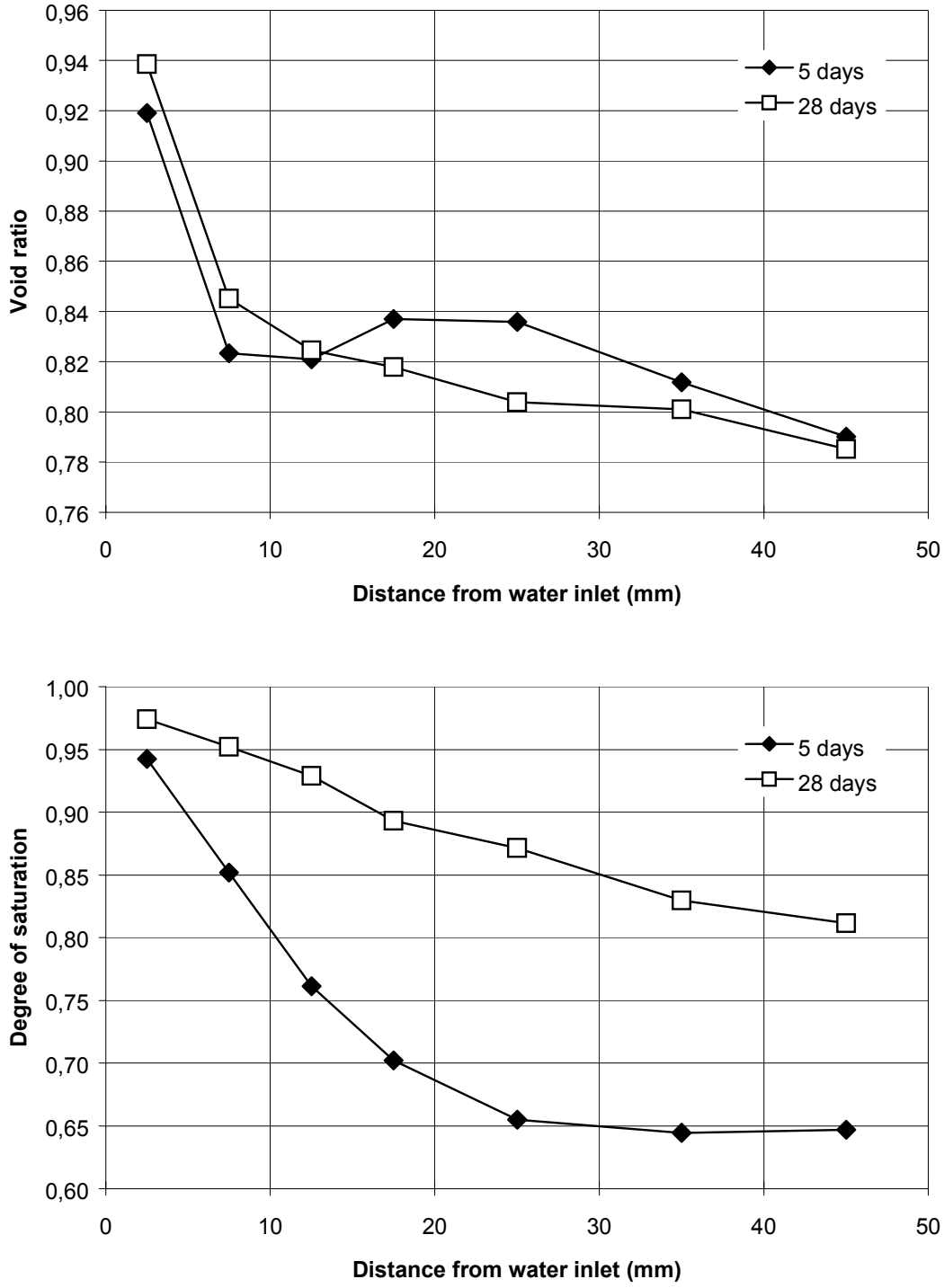

Figure 4-2. *Results of two water uptake tests left for 310 hours at different temperatures.*

Two other tests were made at the temperature 23 °C and dismantled after 5 days and 28 days. Figs 4-3 and 4-4 show the results.

The initial conditions were the following:

$\rho_d = 1.57$

$w = 17.3\%$

which yield

$e_0 = 0.77$

$S_r = 0.63$

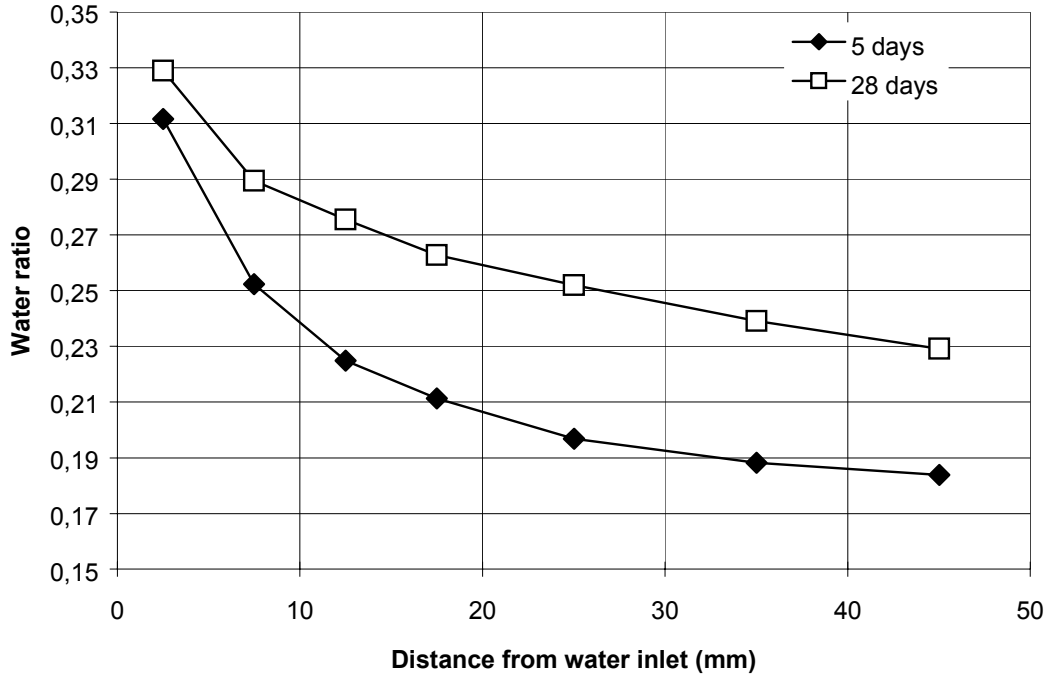

Figure 4-3. *Results of two water uptake tests dismantled after different times*

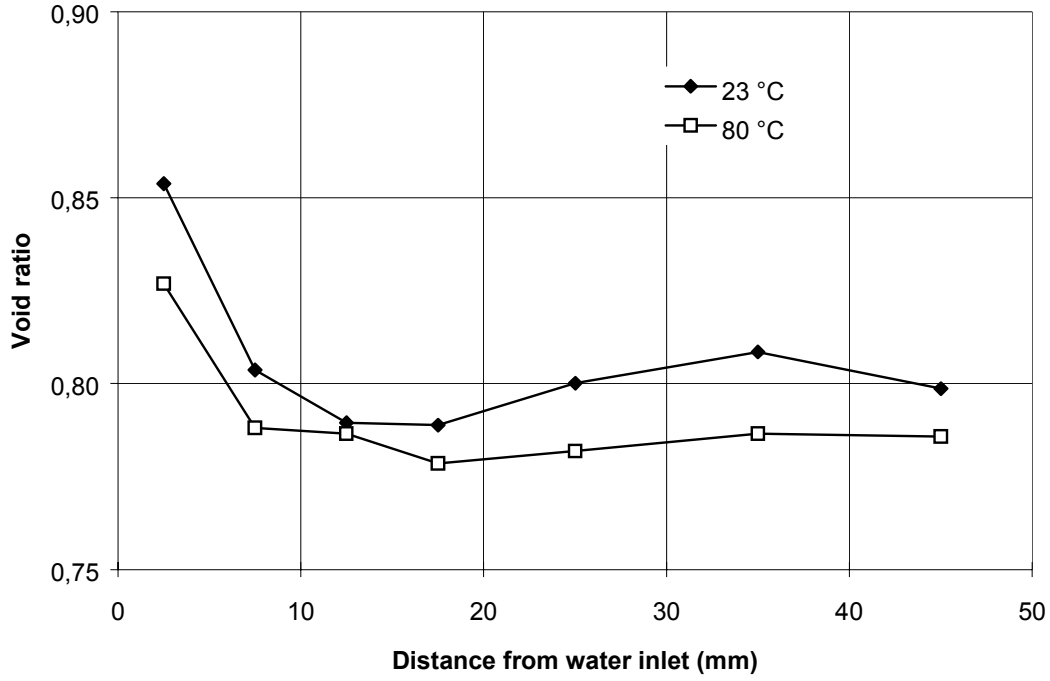

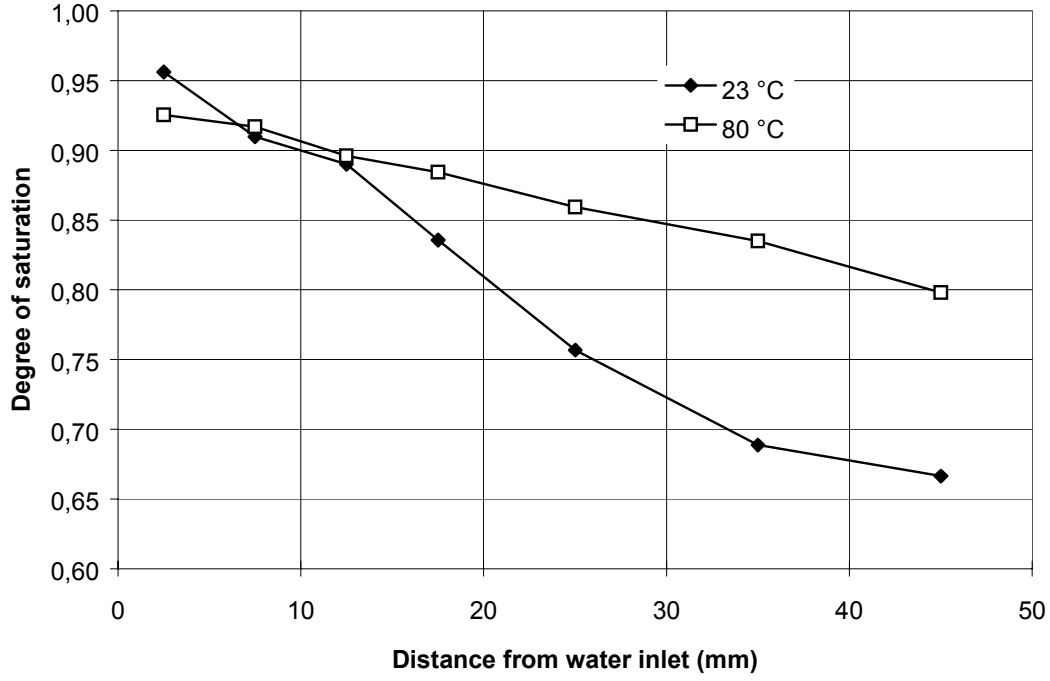

Figure 4-4. *Results of two water uptake tests dismantled after different times*

5 Water uptake tests with different slot filling materials and different simulated rock properties

5.1 Introduction

The bentonite blocks cannot be placed in the deposition holes unless the diameter of the hole is larger than the diameter of the blocks. In the Prototype Repository the difference is more than 10 cm implying a slot of more than 5 cm. Since the density of the buffer after swelling will be too low the slot must be filled with additional bentonite, either as powder or pellets. Pellets will be used in the Prototype Repository. In a real repository the slot might be decreased so much that no filling is required. Tests that simulate these three possible fillings have been made.

The wetting process is also depending on how the rock distributes the water to the buffer. In order to study the influence of the rock the tests have been made with either a filter or a small slit that provides the bentonite with water,

5.2 Test description

In order to study the influence of the slot filling material and the rock properties on the wetting process the following 6 laboratory tests have been made:

- 3 tests with a filter simulating a rock with very permeable rock matrix and either pellets, powder or no slot filling
- 3 tests with a 0.1 mm slit in a steel plate simulating the rock with a discrete fracture and either pellets, powder or no slot filling

The tests were made in an oedometer with the diameter 50 mm and the height 50-60 mm (see Fig 5-1). The steel plate with the slot was 11 mm thick and the slot was 0.1 mm wide and 30 mm long.

MX-80 bentonite with the water ratio 10% was compacted to a bulk density $\rho = 2.05$ g/cm^3, which corresponds to the void ratio e = 0.49. The height of the samples was 40-50 mm and adapted to the density of the slot filling so that the average void ratio including the slot would be 0.76. The bulk density of the powder and the pellets filling (including the space between the pellets) was about $\rho = 1.1$ g/cm^3, which with the water ratio 10% corresponds to the void ratio e = 1.8.

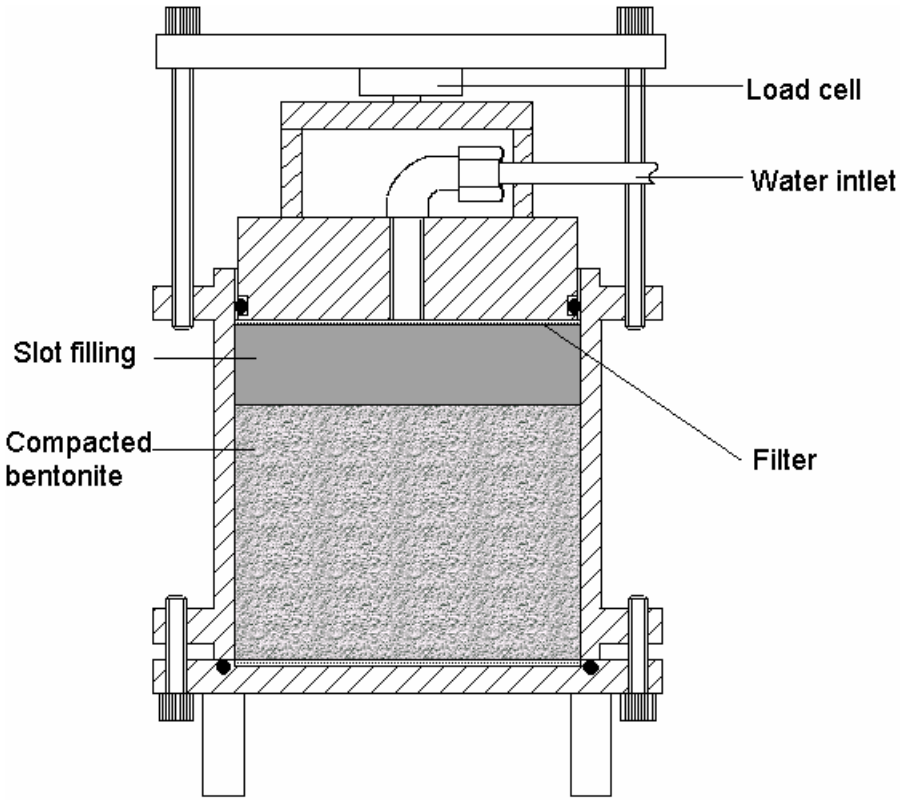

Figure 5-1. *Test equipment for the slot filling tests. For 3 of the tests the filter was replaced by a plate with a 0.1 mm wide fracture.*

The volume of the oedometer was kept constant with a piston above the slot and the swelling pressure measured with a load cell via the piston. At commencement of the test the slot was filled with water after application of vacuum in the filter, in order to remove the air in the system. The water inflow was also measured during the tests.

The tests were run for 400 hours and then cut in 8 slices. Water ratio and (if possible) density were determined on each slice.

5.3 Results

Fig 5-2 shows the results of the 3 tests with water supply through a filter. The results show that the difference between the tests is very small and thus that the influence of slot filling does not seem to be large, if the water is supplied through a filter. The results also show that the sample is far from water saturated and that there is a large difference and gradient in both void ratio and degree of saturation.

Fig 5-3 shows the results of the 3 tests with water supply through a fracture. The density could not be measured so only the water ratio distribution is shown. The results show

that the test with pellets in the slot has reached a higher water ratio than the other tests. A comparison between the results with filter and fracture in the case of pellets is shown in Fig 5-4. Although the wetting was faster with pellets than with the other fillings in the case of a fracture, the comparison shows that the filter is more effective in providing the bentonite with water.

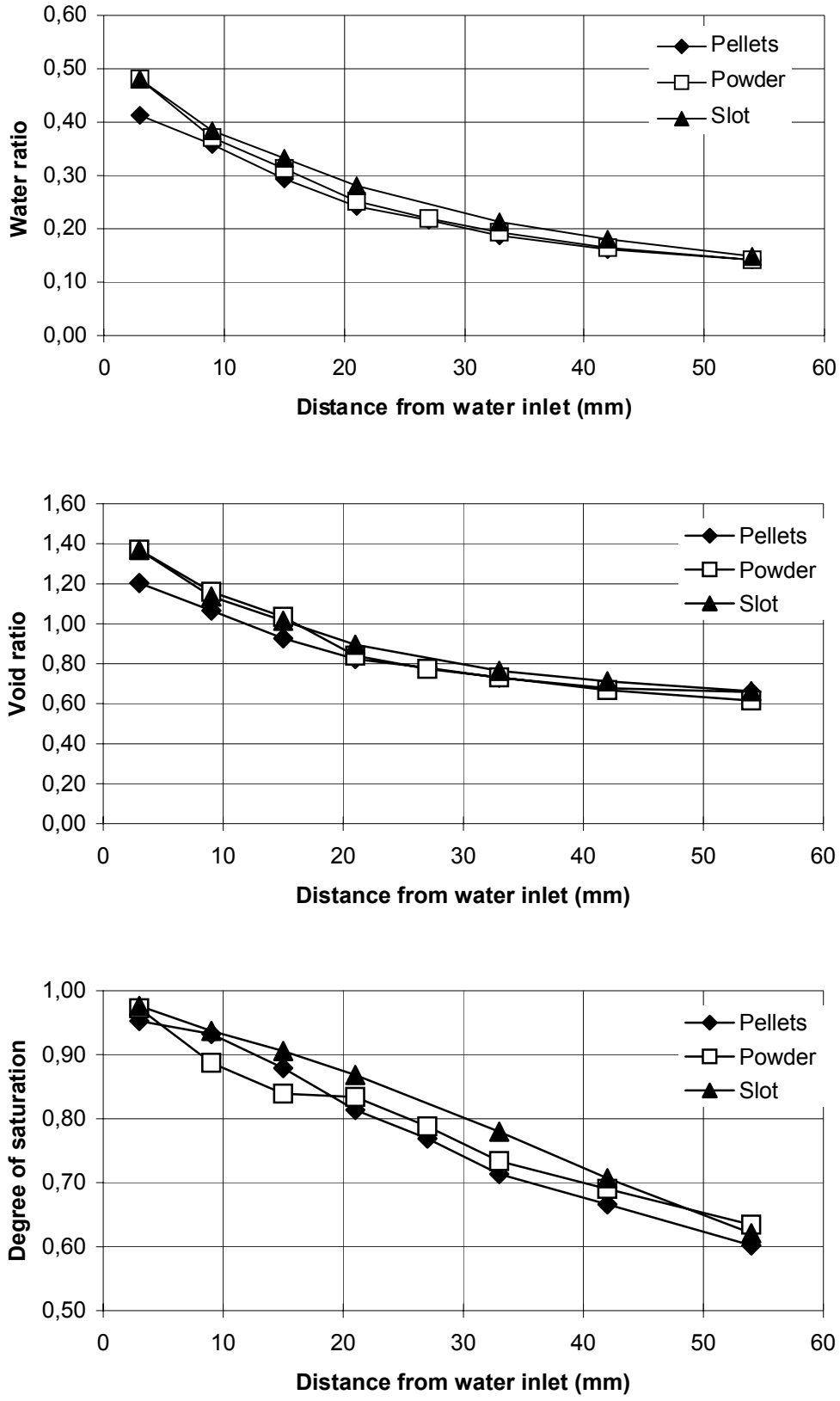

Figure 5-2. *Results from water uptake tests with different slot fillings and water supplied by a filter.*

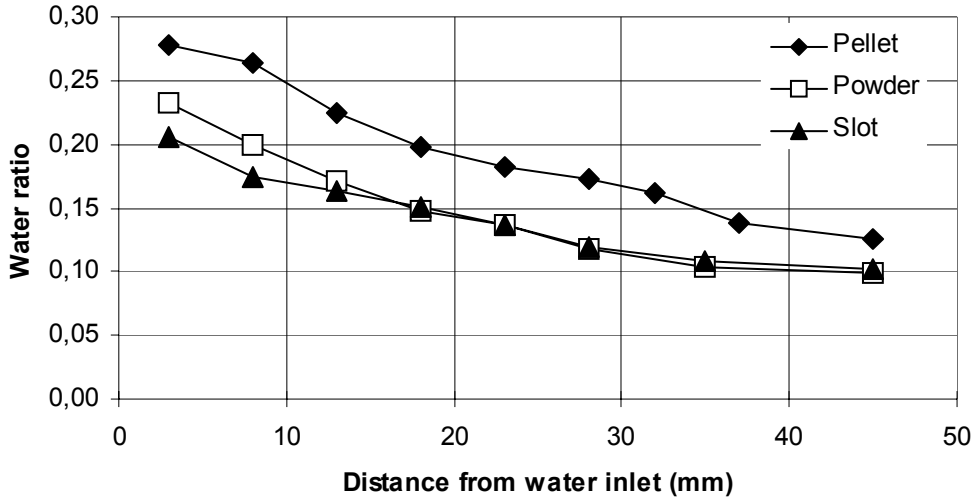

Figure 5-3. *Results from water uptake tests with different slot fillings and water supplied by a fracture.*

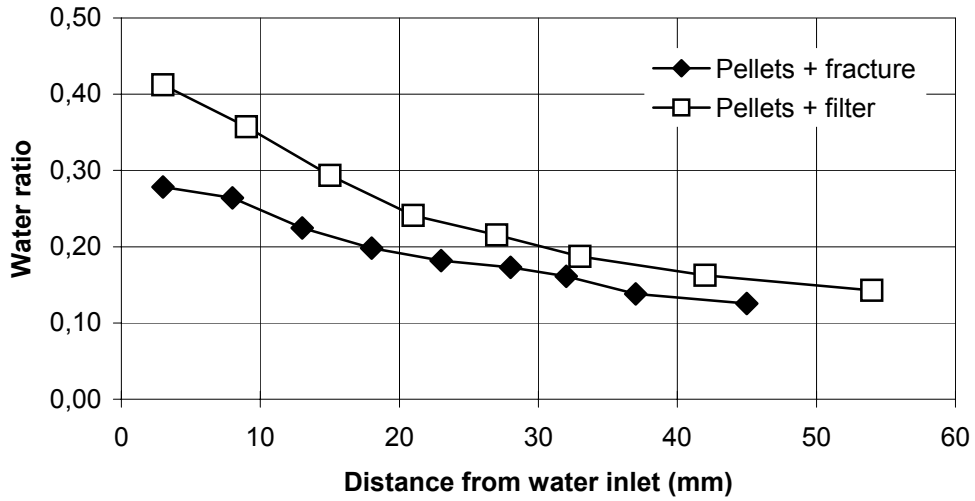

Figure 5-4. *Comparison between tests made with water supplied by a filter and by a fracture. Pellets in the slot*

6 Backfill material properties

6.1 Introduction

This chapter is based on work conducted in 1996.

6.2 Tested backfill materials

The material for backfilling in a repository is proposed to be composed of a mixture of 0-30% bentonite and 70-100% ballast material. Originally quartz sand was proposed for ballast material but recent investigations have pointed out the possibility to use crushed rock originating from the excavation. The ballast material in all laboratory tests described in this chapter is taken from the rest product of the TBM boring (TBM muck).

Crushed TBM muck was used in most of the tests. The grain size distribution of the natural TBM muck is shown in Fig 6-1. The maximum grain size of the natural TBM muck at sieving was 60 mm and the amount of particles with clay and silt size (<0.06 mm) was about 8 %. The grain size distribution of the crushed TBM muck is also shown in Fig 6-1. There are two curves in the figure showing the grain size for the crushed material, one for the material used in the lab tests (Crushed twice) and one for the material used in the field tests. The maximum grain size of the crushed TBM muck was 20 mm and the amount of particles with clay and silt size was still about 8%.

MX-80 sodium bentonite was used in the tests. The granule size distribution of the bulk material with its natural content of water is shown in Fig 6-2. The granules are received after drying and grinding the natural clay. They are composed of a large number of clay particles with the grain size distribution in dispersed form as shown in Fig 6-2. The liquid limit for the bentonite is about 500%.

The TBM muck and different amounts of bentonite were mixed in a mixer at different water ratios. The mixing was done with one of two different equipments, one paddle mixer with a capacity to mix 150 kg at each mixing sequence and one kitchen mixer (for mixing dough) with a capacity of about 2 kg. The crushed TBM muck was at first mixed with the air-dry bentonite and then the required amount of additional water to get a certain water ratio of the mixture was carefully poured into the mixer during stirring.

The following three different ”types” of water are present in these tests:

1. The natural water in air dry conditions
2. The water that is added during mixing
3. The water that flows into the backfill during the hydraulic conductivity tests

Generally, distilled water was added during mixing and flow testing but some tests were made with saline water with the following salt composition:

0.53 % NaCl
0.68 % CaCl

The total salinity was thus 1.2%. This water was added both during mixing and flow testing in some of the compression tests.

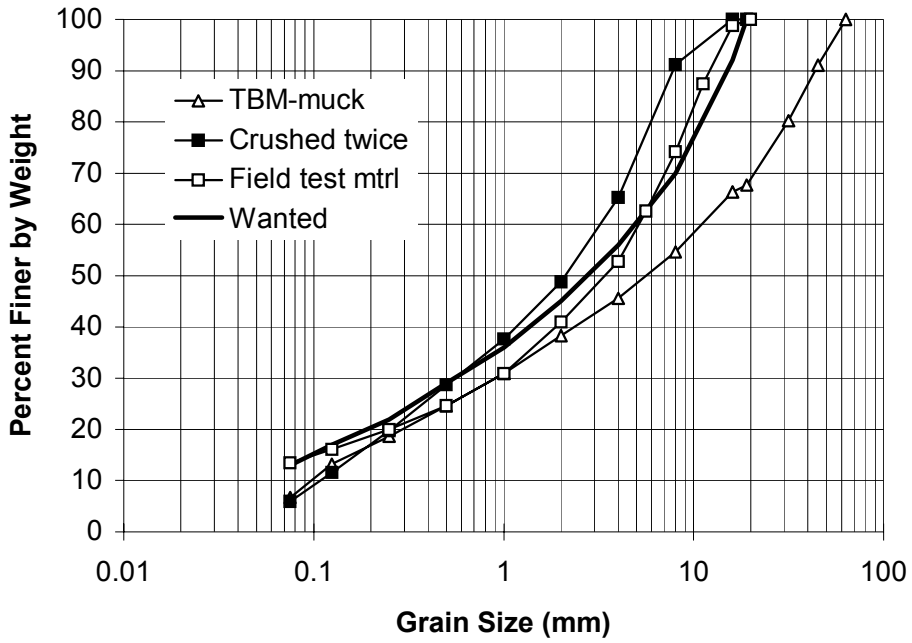

Figure 6-1. *Grain size distribution of the TBM muck, the material used in the lab tests (Crushed twice) and the field test material.*

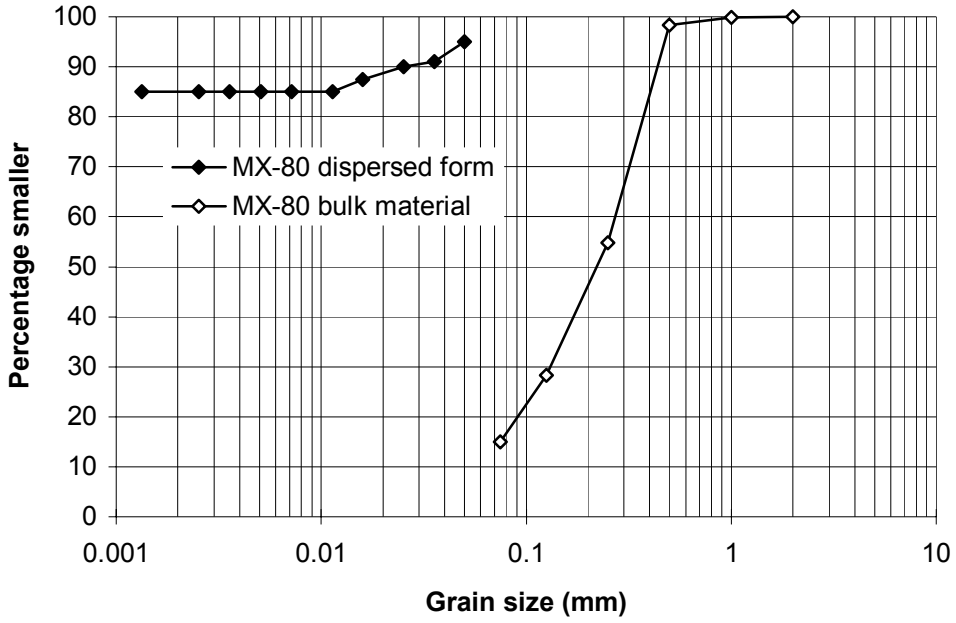

Figure 6-2. *Granule and grain size distributions of MX-80.*

6.3 Compaction tests

6.3.1 General

The compaction characteristics of a soil can be assessed by means of standard laboratory tests. Samples at different water ratios are compacted in the laboratory with different techniques and the density and water ratio are measured after compaction. The dry density can be calculated with the measured parameters. The results from a compaction test are normally accounted for as compaction curves with the dry density plotted versus the water content. Fig 6-3 shows schematic compaction curves for two different compaction efforts plotted. The maximum dry density curve is also plotted in the figure (saturation line). The curves show that for a particular compaction method there is a water content, known as the *optimum water content (w_{opt}),* at which a maximum value of dry density is obtained. The results of laboratory compaction tests are not directly applicable to field compaction because the compaction efforts are different and applied in different ways. However, the test usually gives an idea of the maximum density and the optimum water content for the materials at field compaction with standard compaction techniques.

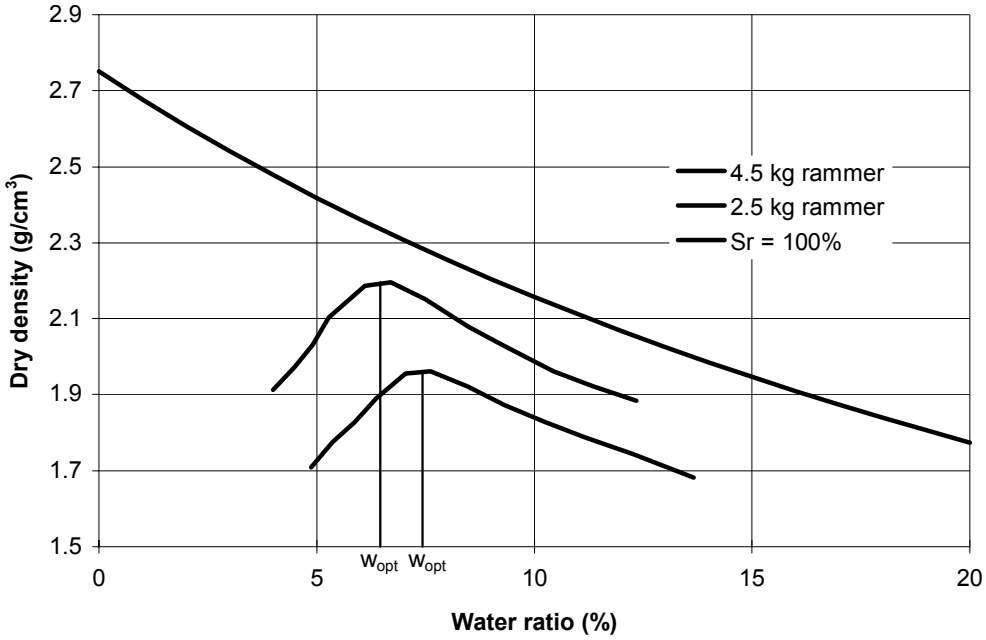

Figure 6-3. *Dry density - water ratio curves for different compaction effort (compaction curves).*

6.3.2 Test techniques

The following compaction tests were made:

- Modified Proctor Test
- Vibrating Plate Test
- MCV Test

The samples were compacted at a constant compaction effort in the Proctor and in the Vibrating Plate tests. The result from these tests is an optimum water ratio as shown in Fig 6-3. In the MCV-test the optimum compaction effort is measured. A sample at a certain water ratio is compacted to a stage when further compaction effort will not result in an increased density.

In a Modified Proctor test a soil sample is compacted in a mould with a volume of 944 cm^3. The sample is compacted by a rammer, with the mass 4.5 kg falling freely 45 cm. The soil is compacted in five equal layers; each layers receiving 25 blows with the ram. After the compaction the density and water ratio of samples are measured.

In the Vibrating Plate Test a soil sample is compacted in a mould with large diameter which in the present test was D=0.5 m. The compaction was made with a circular plate with ϕ 180 mm. A petrol engine vibrated the plate and the samples were compacted in

three layers with the thickness 15 cm for 4 minutes. The weight of the apparatus is 24 kg and the vibrating frequency 40 Hz. The advantage with this equipment is the large volume of the mould (100 times larger than the mould in the Proctor test), which means that particles larger than 200 mm could be included. After compaction the volume and weight of the sample was measured. Three small samples were taken from the material for measuring the water ratio.

In the MCV-test a mould with a diameter of 99 mm is used. MCV stands for Moisture Conditioning Value. The sample is compacted by a rammer with the same diameter as the mould. 1.5 kg of the soil with a maximum grain size of 20 mm is normally applied in the mould. A circular fibre disc is applied on the top of the sample and compacted with one blow of the rammer. The height of drop of the rammer is 250 mm and the compaction of the sample is read. The process is then repeated with readings of compaction after selected numbers of blows (see Table 6-1 and Fig 6-4). When the compaction between n and $4n$ blows is smaller than 5 mm, the sample is assumed to have reached its maximum density. The so-called MCV-value of the sample can also be calculated from the test. The MCV-value is defined according to Eqn 6-1 (see also Table 4-1 and Fig 6-4).

$$MCV = 10 \cdot \log(n) \tag{6-1}$$

where

n= number of blows for 5 mm change in penetration

The water ratio and density of the sample are measured after compaction. A high MCV value indicates that it is difficult to compact the sample to its optimum density.

Table 6-1. Typical results from a test with the MCV apparatus on a mixture of 10/90 bentonite/crushed TBM muck at the water ratio 9.4%.

Number of blows (n) of rammer	Penetration of rammer into mould (mm)	Change in penetration with additional 3n blows of rammer (mm)
1	73.5	11.5
2	79	11.5
3	82.5	12
4	85	10.5
6	88	10
8	90.5	9.5
12	194.5	7.5
16	95.5	7.5
24	98	7
32	100	6
48	102	5
64	103	
96	105	
128	106	
192	107	

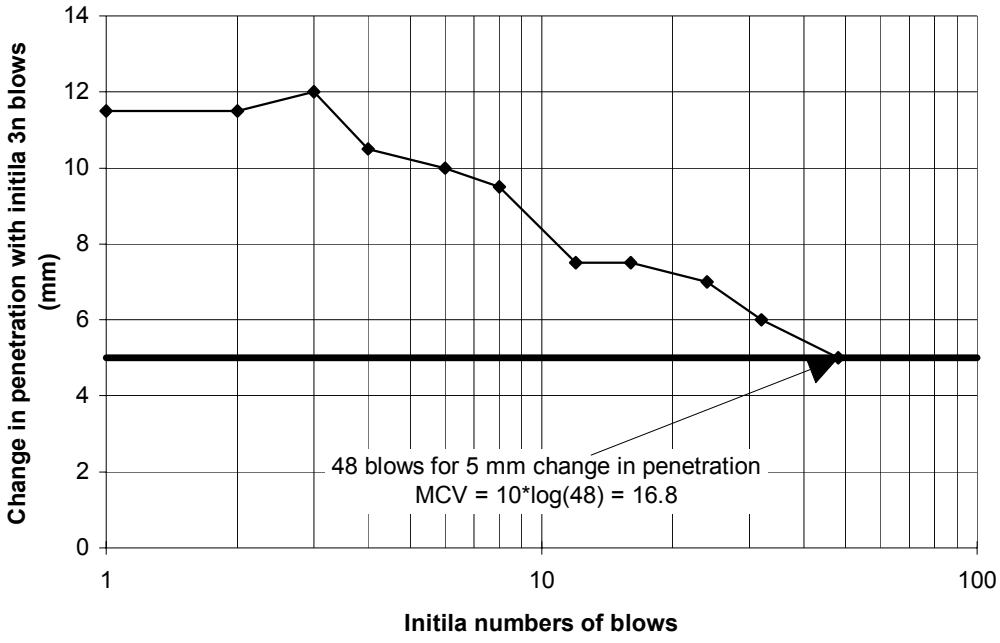

Figure 6-4. *Plot of the results in Table 6-1.*

6.3.3 Test results

General

The following five different backfill types have been tested regarding the compaction properties:

- Natural TBM-muck
- Crushed TBM-muck
- 10% bentonite and 90% crushed TBM-muck (10/90 bentonite/crushed TBM-muck)
- 20/80 bentonite/crushed TBM-muck
- 30/70 bentonite/crushed TBM-muck

The results will primarily be accounted for as compaction curves.

Natural TBM-muck

The results from the compaction tests on the natural TBM muck are shown in Fig 6-5. Because of the large grain size of the TBM muck the Vibro test was the only suitable laboratory test for this material. The figure shows that the maximum dry density was reached at a water ratio of 6%. The maximum dry density was 2.37 g/cm^3. It was not possible to compact TBM-muck with a higher water ratio than 6% since liquefaction occurred.

Crushed TBM-muck

The results from the compaction tests on crushed TBM muck is shown in Fig 6-6. The proctor and the MCV tests gave similar results while the Vibro tests gave somewhat lower density. The Proctor and MCV tests showed that the maximum density was reached at a water ratio of about 6.5%. The maximum dry density was 2.33 g/cm^3.

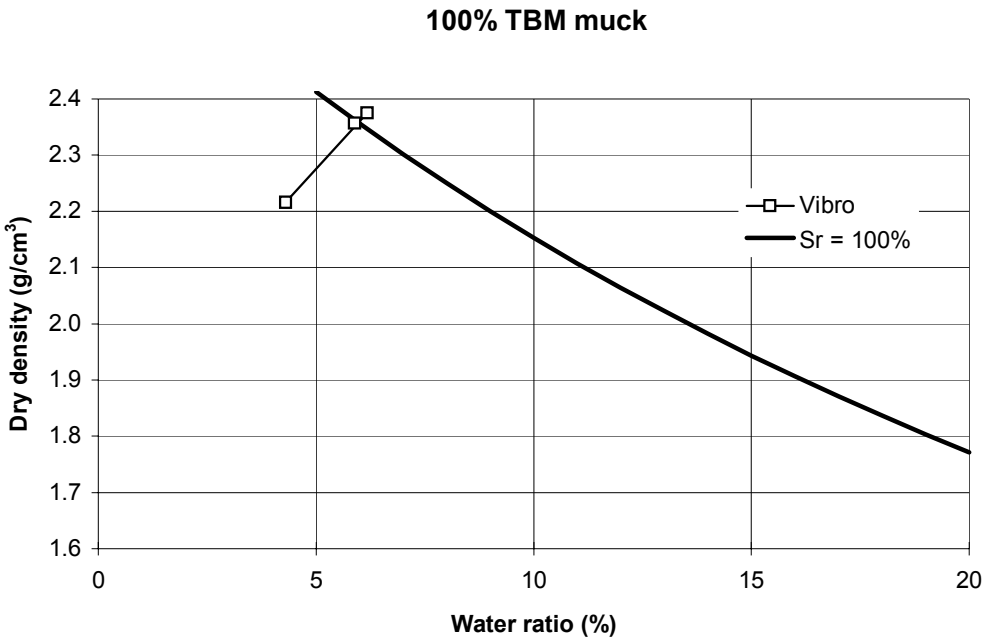

Figure 6-5. *Measured dry density of TBM muck plotted as a function of water ratio for the Vibrating Plate Test.*

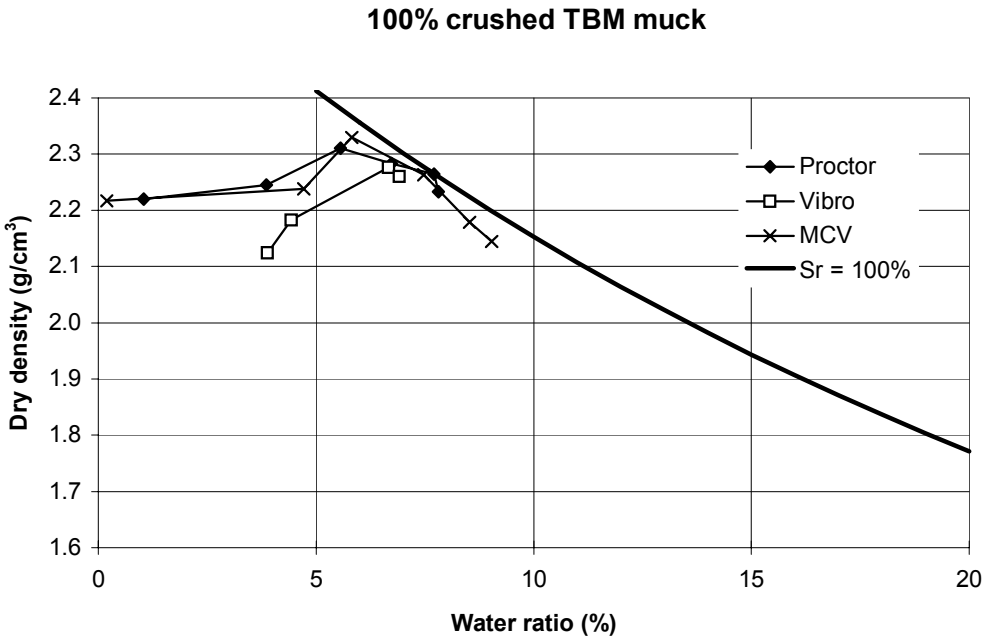

Figure 6-6. *Measured dry density of crushed TBM muck plotted as a function of water ratio for three different test techniques.*

10/90 bentonite/crushed TBM muck

The proctor and the MCV test on the mixture of 10% bentonite and 90% crushed TBM muck also gave similar results (see Fig 6-7) while the Vibro test gave significant lower densities. The maximum density in the MCV and proctor tests was reached at a water ratio of 6.5-7%. The maximum dry density was 2.21 g/cm^3.

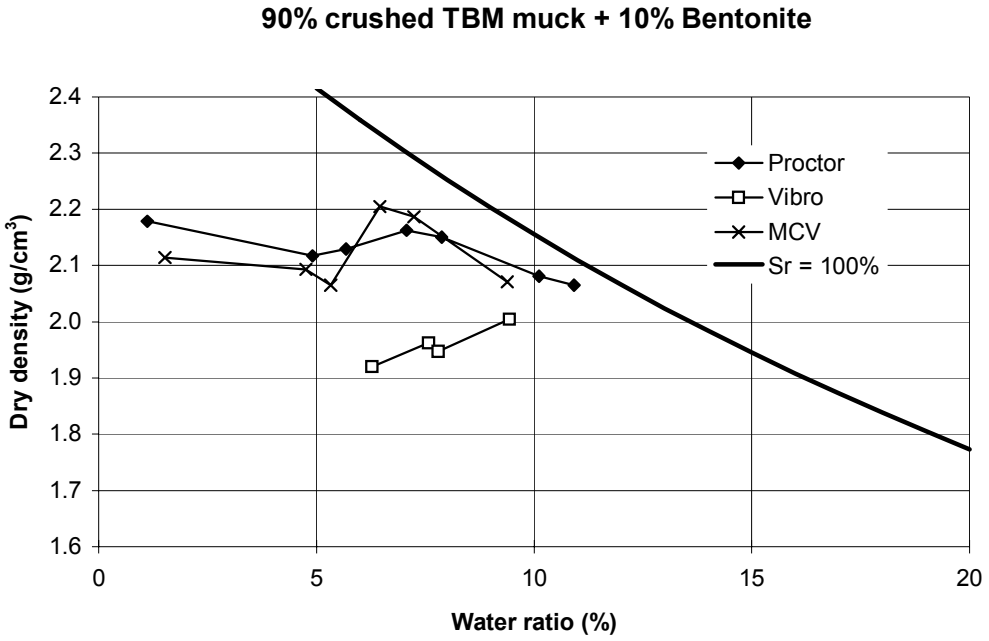

Figure 6-7. *Measured dry density of 10/90 bentonite/crushed TBM muck as a function of water ratio for three different test techniques.*

20/80 bentonite/crushed TBM muck

The results from the compaction tests on the mixture of 20% bentonite and 80% crushed TBM muck are shown in Fig 6-8. No significant maximum in dry density was obtained in the test. The Vibro tests gave also for this material lower densities than the other two compaction methods.

Another test series with the vibrating plate was performed with different compaction times but with the same compaction force. These tests were performed at a water ratio of 10%. The results are shown in Fig 6-9. The figure shows, as expected, that density increased with increasing compaction time (increasing compaction effort). The densities of the samples were also higher when a smaller square-shaped plate was used.

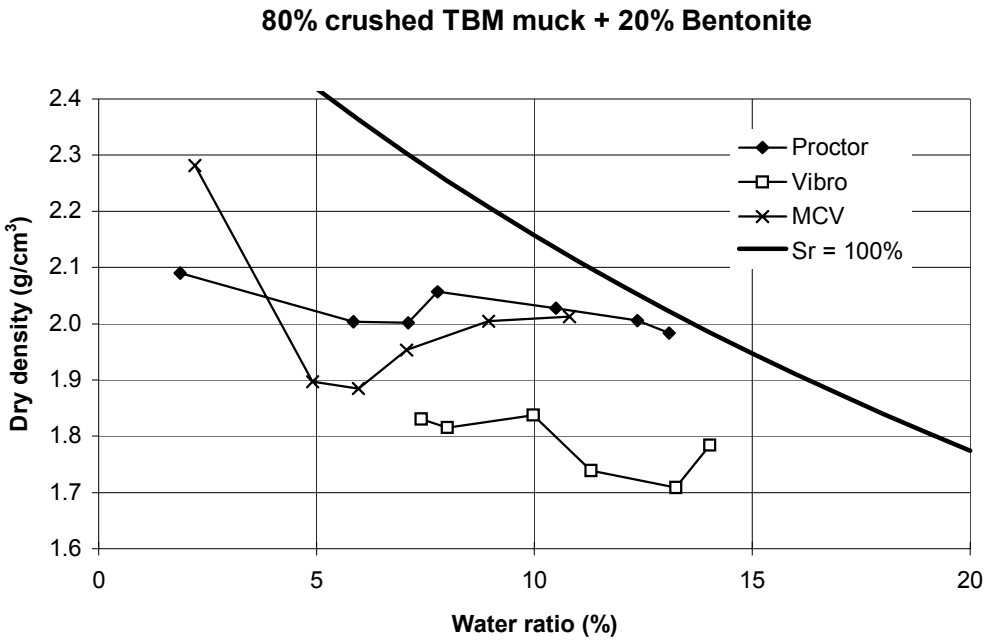

Figure 6-8. *Measured dry density of 20/80 bentonite/crushed TBM muck as a function of water ratio for three different test techniques.*

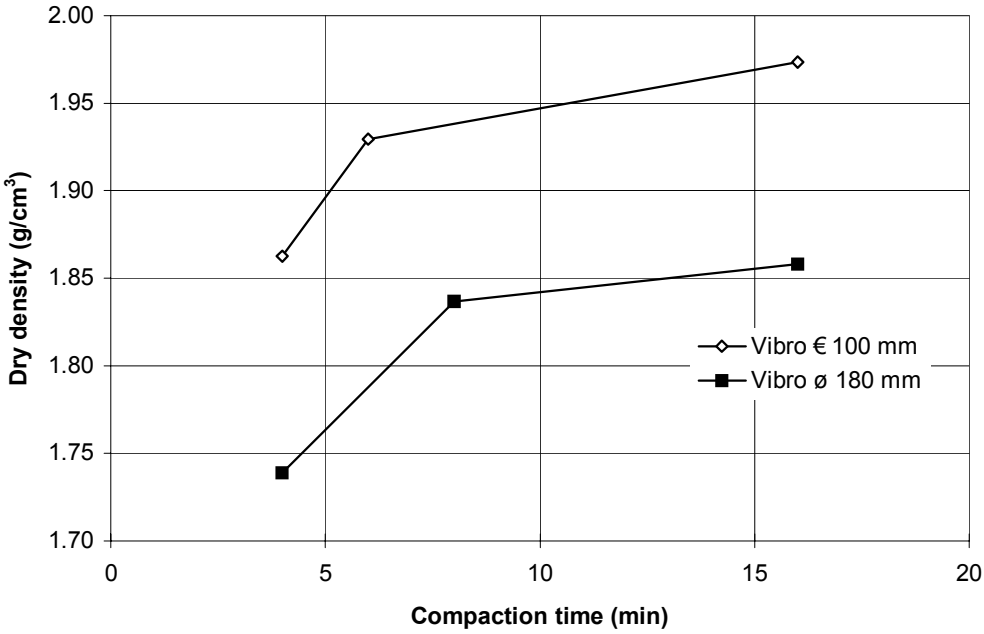

Figure 6-9. *Measured dry density of 20/80 bentonite/crushed TBM muck as a function of compaction time. The samples were compacted with the vibrating plate method. Two different plates were used (□ 100 mm and ϕ 180 mm). The water ratio of the samples was 10%.*

30/70 bentonite/crushed TBM muck

Fig 6-10 shows the results from compaction tests on 30/70 bentonite/crushed TBM muck. The figure shows that the compaction curves are almost parallel to the x-axis, meaning that the dry density was independent of the water ratio. The maximum density was 1.95 g/cm^3. Also for this material the vibrating plate gave considerably lower densities.

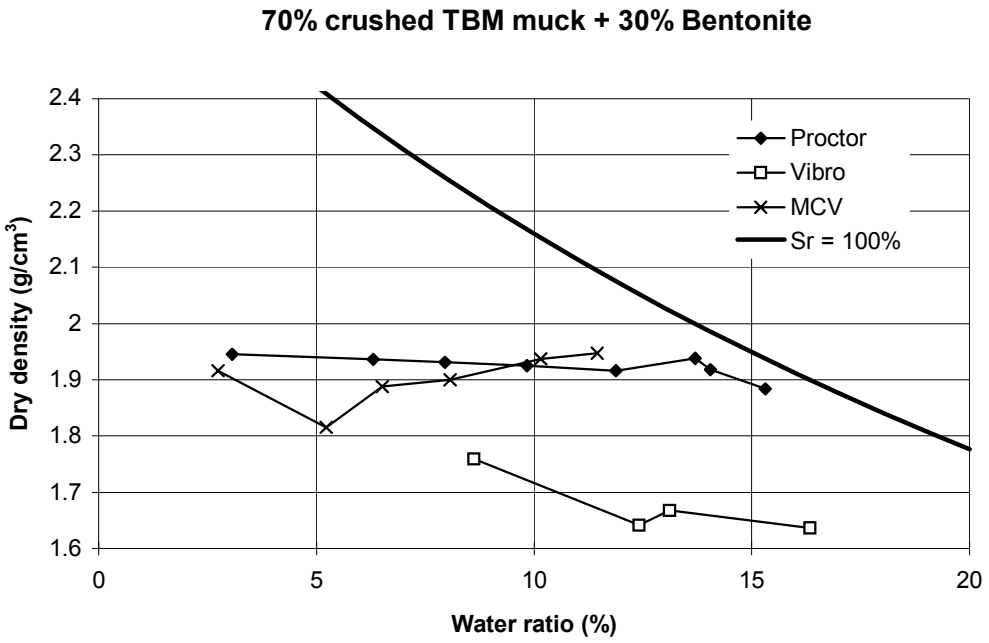

Figure 6-10. *Measured dry density of 30/70 bentonite/crushed TBM muck as a function of water ratio for three different test techniques.*

6.3.4 Evaluation and conclusions

The following general observations were made:

- The maximum dry density decreased with increasing bentonite content
- The vibrating plate tests gave significant lower densities than the other test techniques for the backfill materials with bentonite
- The peak of the compaction curves was less pronounced with increasing bentonite content and became almost independent of water ratio at 30 % bentonite content

The peak values of the dry density and the corresponding clay dry density at the Proctor compaction tests (100% Proctor) are plotted as functions of the bentonite content in Fig 6-11. These diagrams show that the dry density strongly decreases with increased bentonite content while the clay dry density increases.

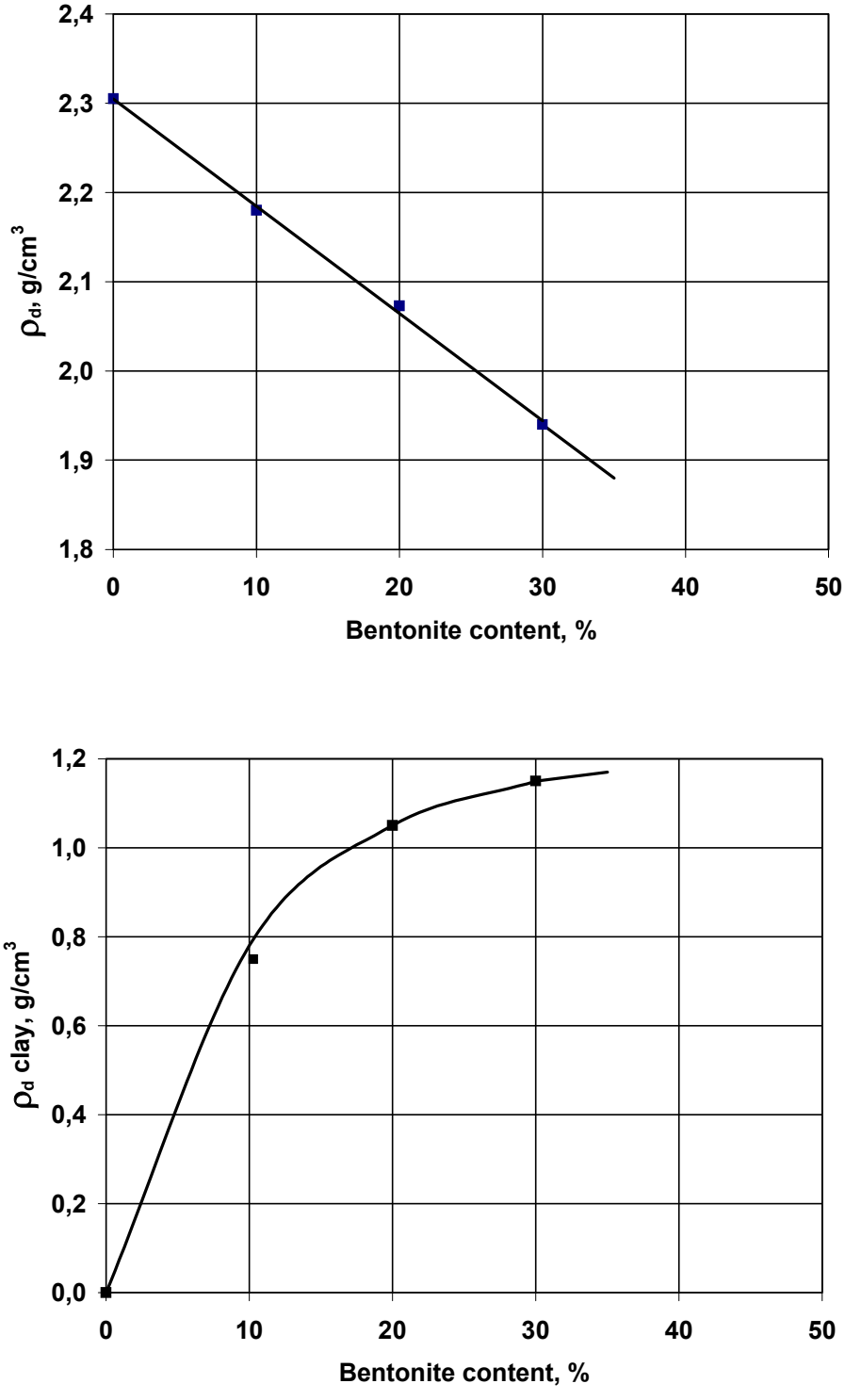

Figure 6-11. *Dry density ρ_d (upper) and clay dry density ρ_{dc} as function of the bentonite content*

Fig 6-12 shows the calculated MCV values for the different mixtures. The MCV value gives an idea of the compaction effort needed for reaching the maximum density at a certain water ratio.

The relation for crushed TBM-muck shows that the MCV value is relatively constant for water ratios lower than 6%. At higher water ratio the MCV value decreases with increasing water ratio. The reason for this is that the samples becomes nearly fully saturated during the compaction and at higher water ratios the samples reaches saturation with a lower compaction effort.

For 10/90 mixture there is a maximum MCV value corresponding to the water ratio for the peak dry density.

The maximum MCV value for 20/80 and 30/70 mixtures seems to appear at a water ratio higher than 10%. The reason is probably that their maximum densities are lower and that they thus need more water to become saturated.

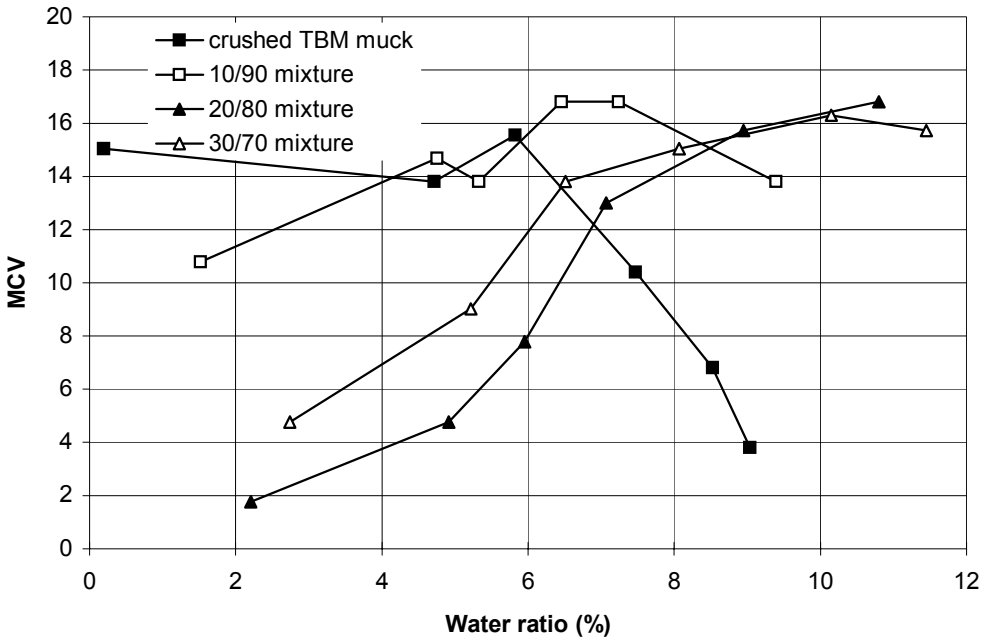

Figure 6-12. *MCV value as function of the water ratio for different backfill types*

6.4 Compression tests

6.4.1 General

The characteristics of a soil during one-dimensional compression or swelling can be determined by means of the oedometer test. The test sample is confined in a rigid ring and filter stones are mounted on the top and bottom of the sample. The *compression properties* are determined by stepwise increasing the vertical effective stress and measuring the deformation while the horizontal radial deformation of the sample is prevented by the ring. This is assumed to correspond to the conditions in a soil mass with a vertical load on the surface or if the water table is lowered permanently in a soil stratum. From the oedometer test also the *coefficient of consolidation* can be determined by measuring how the deformation of the sample is progressing with time. A momentary increase of the total load of the sample will result in an increase of the pore pressure in the sample and pore water will seep out from the sample through the filter stones on the top and bottom of the sample. The pore pressure will decrease with the time and there will be a settlement of the sample.

A typical displacement plot of a load step is shown in Fig 6-13 The total deformation of the sample is divided in to three types:

- Initial compression
- Primary compression
- Secondary compression

The initial compression is a time independent compression of the sample. The two other types of compression are time dependent and they are associated with a water seepage from the sample. The *primary compression* is the part of compression that is delayed due to the low permeability of the sample. The *secondary compression* or creep is developing so slowly that the permeability is not affecting the compression.

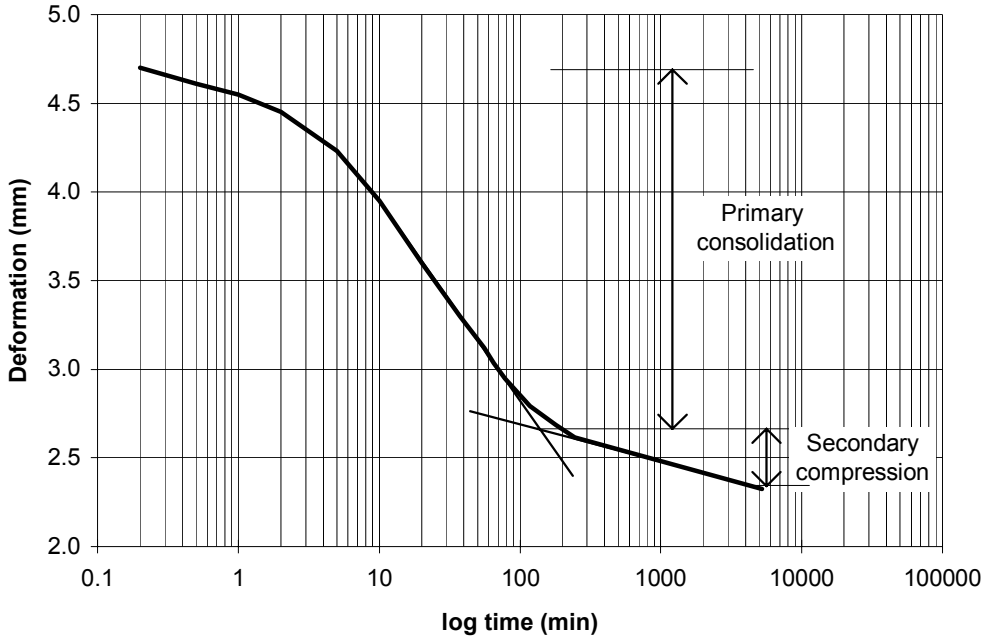

Figure 6-13. *Illustration of the deformation vs. time relation at one load step in an oedometer and how primary consolidation is separated from secondary consolidation.*

6.4.2 Test technique

Rowe oedometers were used for these tests. The backfill was compacted into the sample holder by hand in 5 layers to a desired density. The sample in these Rowe oedometers, are 80 mm high and 250 mm in diameter and confined by a filter in both ends. After finalising the preparation a diaphragm between one of the filters and the lid was pressurised with water to a pressure equal to the estimated swelling pressure of the backfill sample at water saturation.

The samples were de-aired with a vacuum pump and then supplied with water from both ends. During water saturation the deformation was measured and recorded. A load was then applied by increasing the water pressure in the diaphragm. When the sample had reached a new equilibrium a new load-step was applied. The load was increased in increments and the vertical displacement was measured continuously. The load was usually doubled for each step.

After completed testing the density and the water ratio were determined. The measured values were used to calculate the dry density (ρ_d), the void ratio (e) and the degree of saturation (S_r). The initial density and the density after each load step were calculated from these measurements and the measured deformation.

As mentioned the initially applied load was adapted to the expected swelling pressure of the different backfill types and densities. Usually this load resulted in a very small

swelling or compression. The initial load for the non-swelling bentonite free crushed TBM-muck was 100 kPa.

After equilibrium the samples were loaded in steps and the deformation measured for each step. After completed primary consolidation, the load was increased in the next step.

The results are also shown with the strain plotted as a function of the vertical pressure after completed consolidation at each load step. From these curves the compression properties can be evaluated as a secant module in the following way:

$$M = \frac{\Delta\sigma'_v}{\Delta\varepsilon_v} \qquad (6\text{-}1)$$

where

M = compression module
$\Delta\sigma'_v$ = vertical stress increment
$\Delta\varepsilon_v$ = vertical strain increment

6.4.3 Test results

Fig 6-14 shows an example of a plot with displacement vs. time. The difference between primary and secondary consolidation is clearly seen for this load step (30/70 at an increase in load from 600 kPa to 1200 kPa). For lower bentonite contents the end of the primary consolidation is often more difficult to evaluate. The other displacement vs. time results are not shown in this report.

Figs 6-15 to 6-18 show measured strain as a function of applied pressure for all tests. The basic data and evaluated compression modules *M* are shown in Table 6-2. *M* has been evaluated for the entire test, that is from ε_v=0 to the last load step. p_i is the initial vertical stress.

Table 6-2. Basic data and evaluated modules for the compression tests.

Mtrl	Proctor (%)	Water	ρ_d (g/cm^3)	e	M (MPa)	p_i kPa
crushed TBM	85	distilled	2.03	0.343	26.5	100
crushed TBM	89	distilled	2.11	0.290	25.1	100
crushed TBM	87	distilled	2.31	0.329	41.4	100
crushed TBM	94	salt	2.25	0.219	91.5	90
10/90	91	distilled	1.91	0.423	24.9	100
10/90	96	distilled	2.11	0.286	46.8	200
10/90	93	salt	2.02	0.347	68.5	175
20/80	84	distilled	1.74	0.579	17.9	150
20/80	90	distilled	1.91	0.435	40.4	400
20/80	88	salt	1.91	0.432	38.9	300
30/70	84	distilled	1.71	0.619	26.5	300
30/70	89	distilled	1.81	0.516	16.4	600
30/70	90	salt	1.83	0.492	55.3	500

Fig 6-15 shows the measured stress-strain relations for 30/70 bentonite/crushed rock. The initial stresses varied between 300 and 600 kPa. The figure shows that the relations deviate very little from straight lines. The inclination of the lines increases with decreasing density (or % Proctor). This corresponds to an increase in compression modulus with increasing density, which is logical.

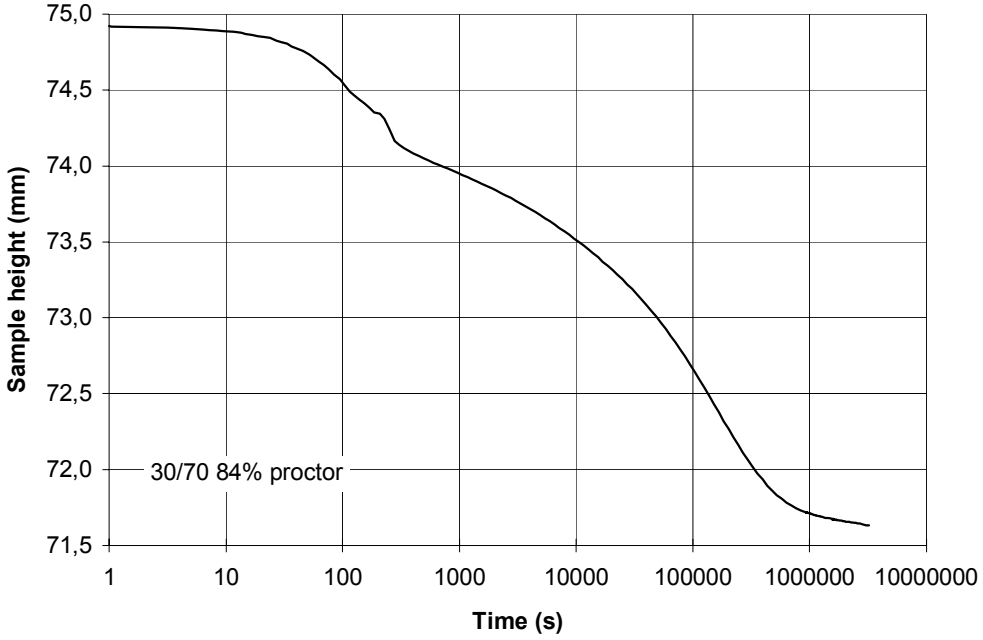

Figure 6-14. *Displacement as a function of time for load step 3 (increase in vertical stress from 600 kPa to 1200 kPa). 30/70 bentonite/crushed rock; 84% Proctor.*

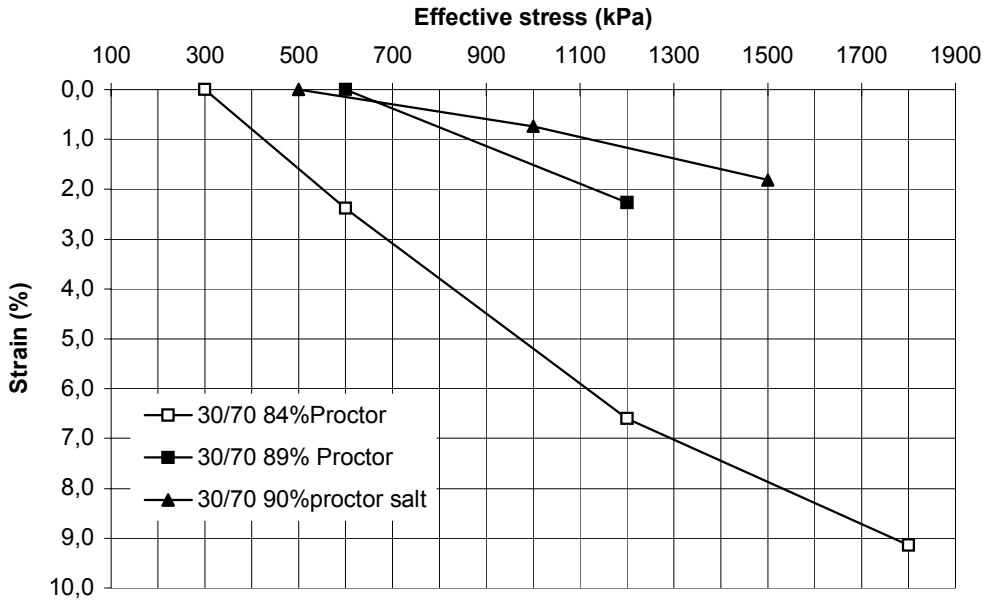

Figure 6-15. *Strain as a function of applied vertical stress for the compression tests on 30/70 bentonite/crushed TBM muck.*

Fig 6-16 shows the measured stress-strain relations for 20/80 bentonite/crushed rock. The initial stresses varied between 150 and 400 kPa. These results are very similar to the results of 30/70 with straight stress-strain relations and increasing compression modulus with increasing density.

Fig 6-17 shows the measured stress-strain relations for 10/90 bentonite/crushed rock. The initial stresses varied between 100 and 200 kPa. Also these results remind of the results from the tests on the 30/70 backfill.

Fig 6-18 shows the measured stress-strain relations bentonite free crushed rock. The initial stresses were 100 kPa. These stress-strain relations are not straight lines. The material behaves more like one can expect from a friction material.

The compression modulus mainly varies with bentonite content and density as shown in Table 6-2. The influence of salt pore water is small. It is interesting to study the difference in compression modules for the same compaction effort but different bentonite contents, like for the hydraulic conductivity. Fig 6-19 shows the compression module as a function of the compaction effort.

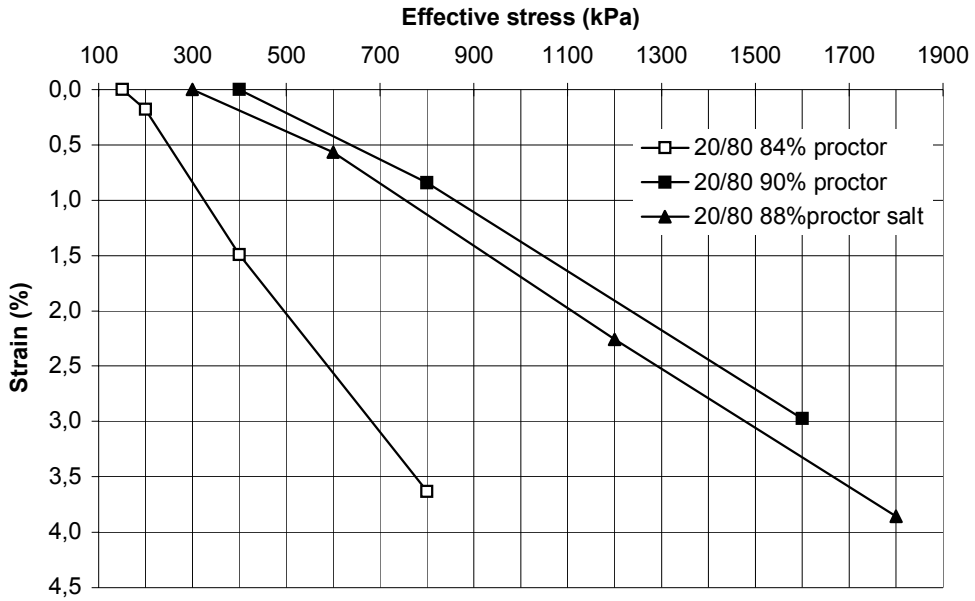

Figure 6-16. *Strain as a function of applied vertical stress for the compression tests on 20/80 bentonite/crushed TBM muck.*

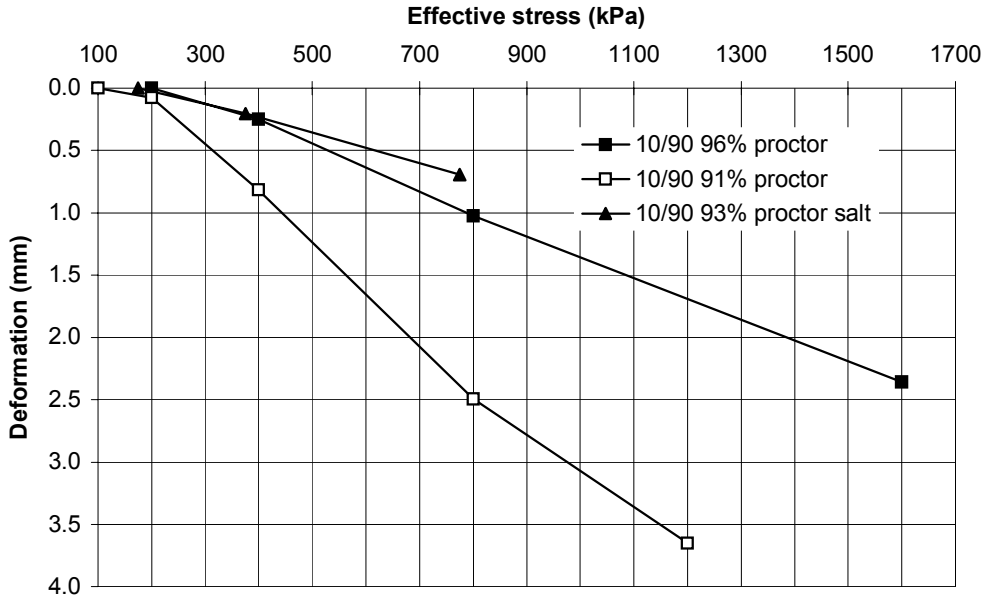

Figure 6-17. *Strain as a function of applied vertical stress for the compression tests on 10/90 bentonite/crushed TBM muck.*

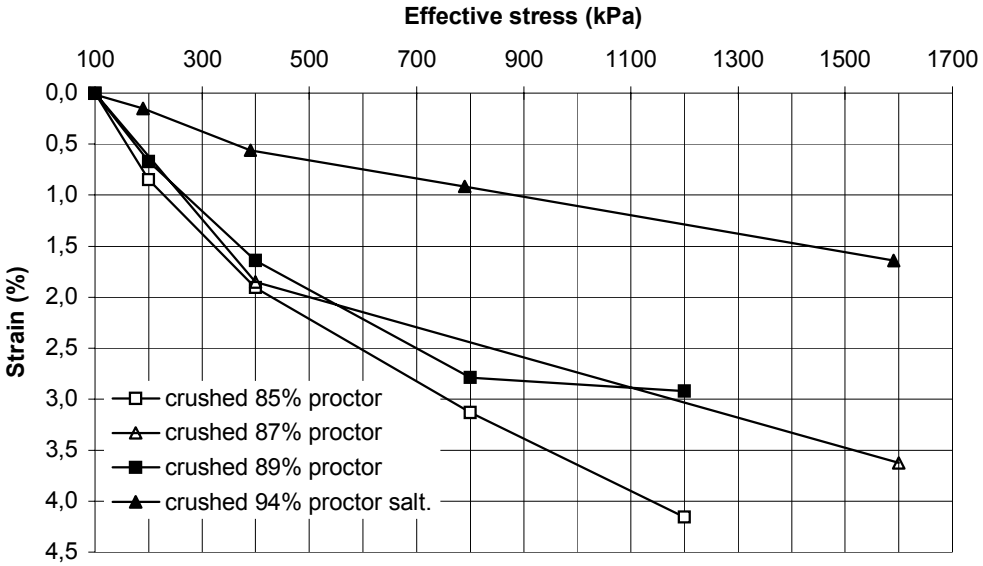

Figure 6-18. *Strain as a function of applied vertical stress for the compression tests on crushed TBM muck.*

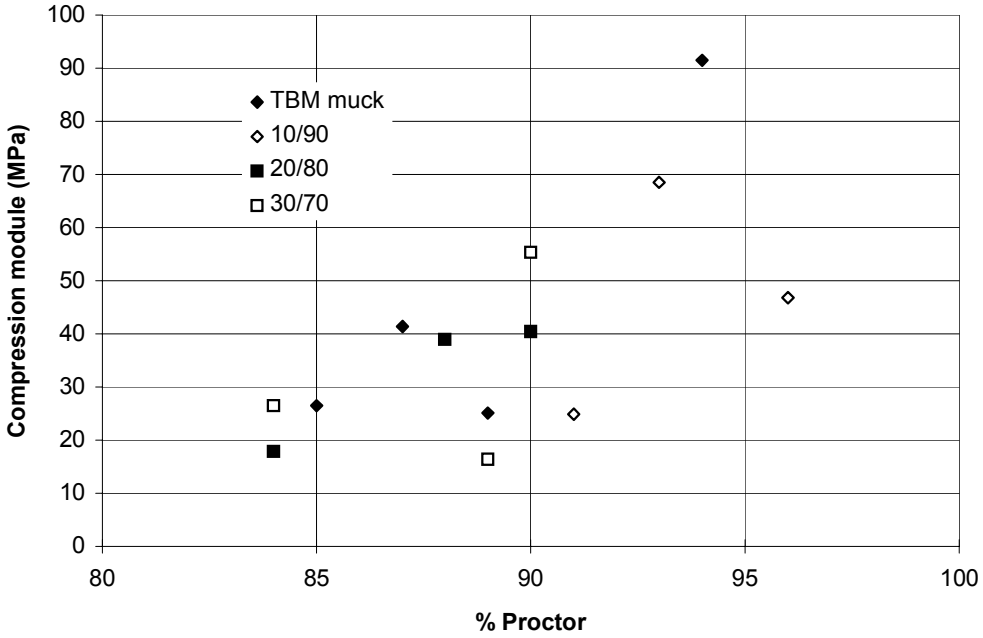

Figure 6-19. *Compression module as a function of the compaction effort (% Proctor) for all tests.*

6.5 Shear tests

6.5.1 General

The shear properties of backfill materials are not very important for the function in a repository, but are included in a mechanical model that is required for calculating the buffer/backfill interaction. A large shear apparatus is required for testing these properties since the backfill contains grains of crushed rock with a diameter of up to 20 mm. Due to the extensive work required for these tests only one shear test has been performed for each material.

6.5.2 Test technique

The shear behaviour was investigated by use of a direct shear apparatus shown in Fig 6-20. This apparatus was originally built to shear rock samples but has been rebuilt to fit soils as well. The upper cylinder ring is fixed to the apparatus but the lower one is mounted in a sleigh that can be moved. A motor drives the sleigh forwards. A rack connects the sleigh and the motor. The normal load is applied with a compression cylinder and controlled by regulation of air pressure in the cylinder.

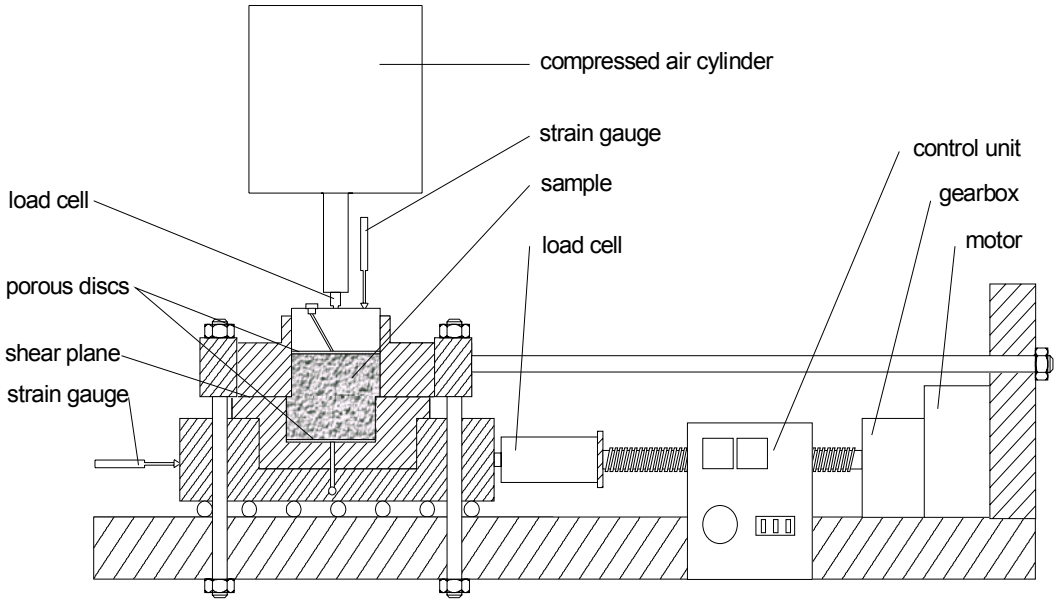

Figure 6-20. *Schematic drawing of the shear apparatus.*

The material was compacted into the sample holder by hand to a desired density. It was compacted in five layers (20, 10, 20, 10 and 20 mm of height) in order to get good

homogeneity and to get the shear plane in the middle of a layer. The material was compacted at its optimal water ratio to about 95% Proctor.

After preparation a constant normal load of 1000 kPa was applied. The sample, which is 160 mm in diameter and 80 mm high, is confined by filters in both ends. The sample, the filters and the connected tubes were de-aired by use of a vacuum pump and the sample supplied with water from both ends. The saturation, which was controlled by the water inflow, took 2-3 weeks. During saturation the vertical displacement of the sample was measured. The displacement after the instant elastic response was less than 0.1 mm.

After equilibrium the shearing was started and the horizontal and vertical displacement and the horizontal and vertical load were measured. Since the shearing had to be made under drained conditions, the shear velocity has to be slow. The apparatus is constructed for shearing rock so even when the velocity was adjusted to its lowest value the rate was much too high. To reduce the velocity the apparatus was equipped with an electronic timer. Every sixth hour, a shearing period of five minutes was applied. Because of this the shear curves were jagged. The average shear rate was 0.4-1 mm per day.

6.5.3 Test results

The basic data and results are summarised in Table 6-3.

Table 6-3. Results from the direct shear tests

Material	σ_N kPa	ρ_d g/cm^3	τ_f kPa	ϕ degrees
Crushed TBM muck	1000	2.21	1425	54.9
10/90 bentonite/crushed TBM muck	1000	2.16	625	32.0
20/90 bentonite/crushed TBM muck	1000	1.97	450	24.2
30/70 bentonite/crushed TBM muck	1000	1.85	320	17.7

σ_N = normal stress
ρ_d = dry density
τ_f = shear stress at failure
ϕ = friction angle

The results are shown in Figs 6-21 to 6-24 with two curves. One curve shows the measured shear stress as a function of the applied shear displacement δ_h while the other curve shows the volume change ε_v (calculated from the measured vertical displacement) as a function of the applied shear displacement δ_h.

The shapes of the curves are very similar and typical for direct shear tests. No peak value of the shear stress occurs but the increase is very small after 4-10 mm shear displacement. The volume change during shearing is very small. The volume decreased about 0.2 % at all tests except for at the test on 30/70 bentonite/crushed TBM muck, which was disturbed by a sudden decrease in vertical stress after problems with the air pressure.

Since only one test was made on each material only the friction angle, evaluated with the secant method by assuming no cohesion, can be calculated, as shown in Table 6-3. Fig 6-25 shows the shear strength as a function of the applied normal stress for comparison.

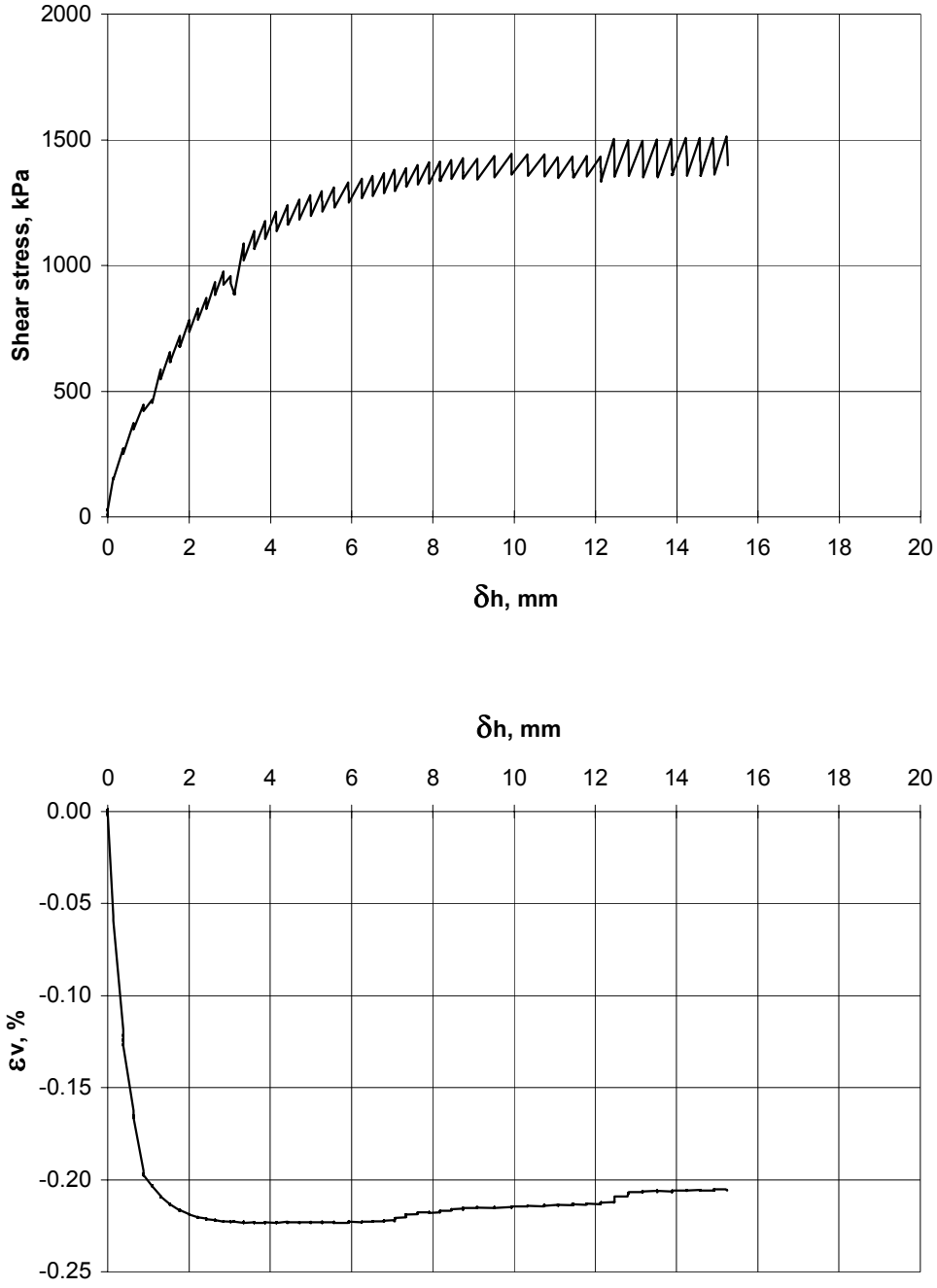

Figure 6-21. *Shear stress (upper) and volume change as a function of the shear displacement at the normal stress 1000 kPa for crushed TBM muck.*

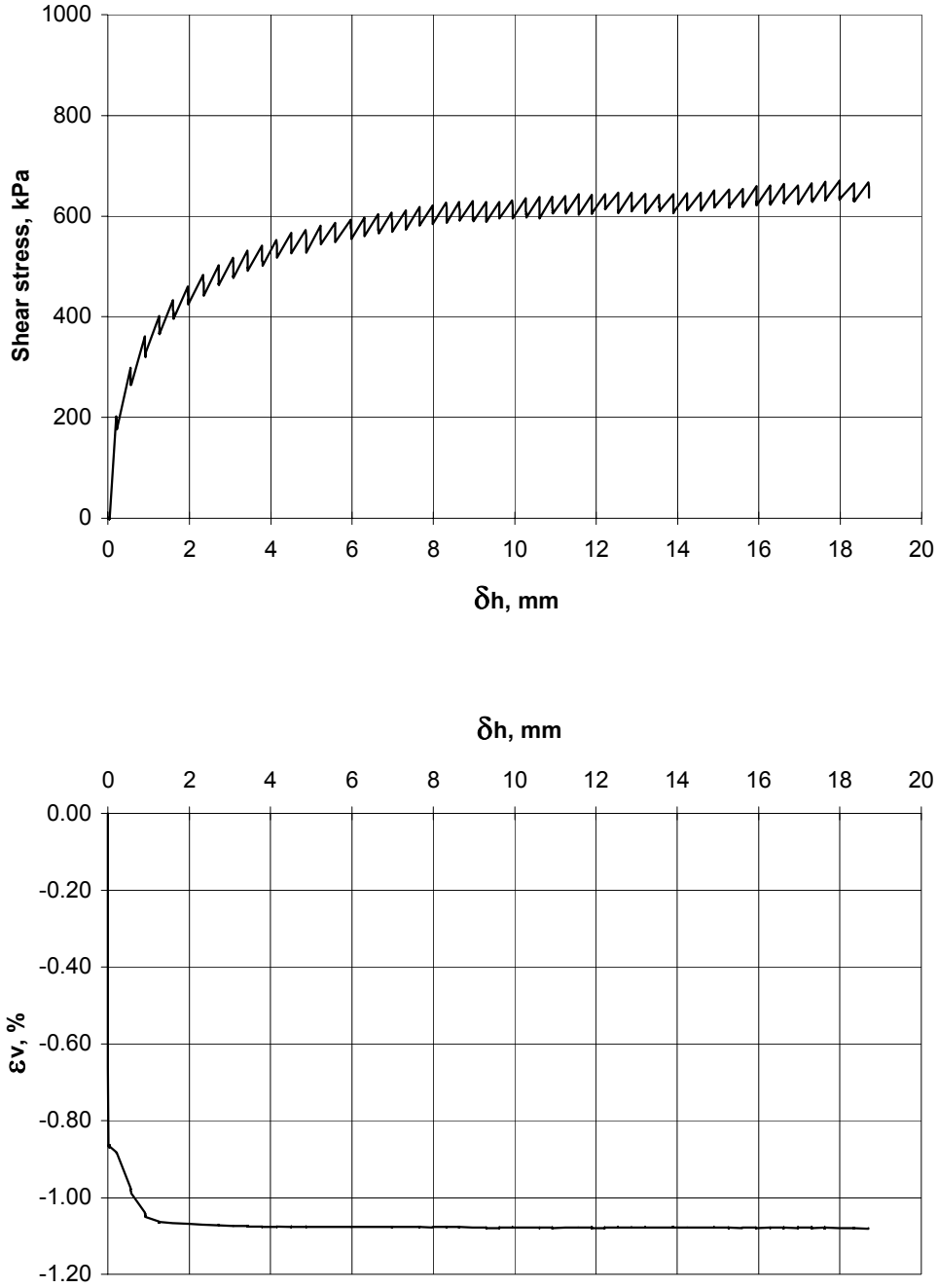

Figure 6-22. *Shear stress (upper) and volume change as a function of the shear displacement at the normal stress 1000 kPa for 10/90 bentonite/crushed TBM muck.*

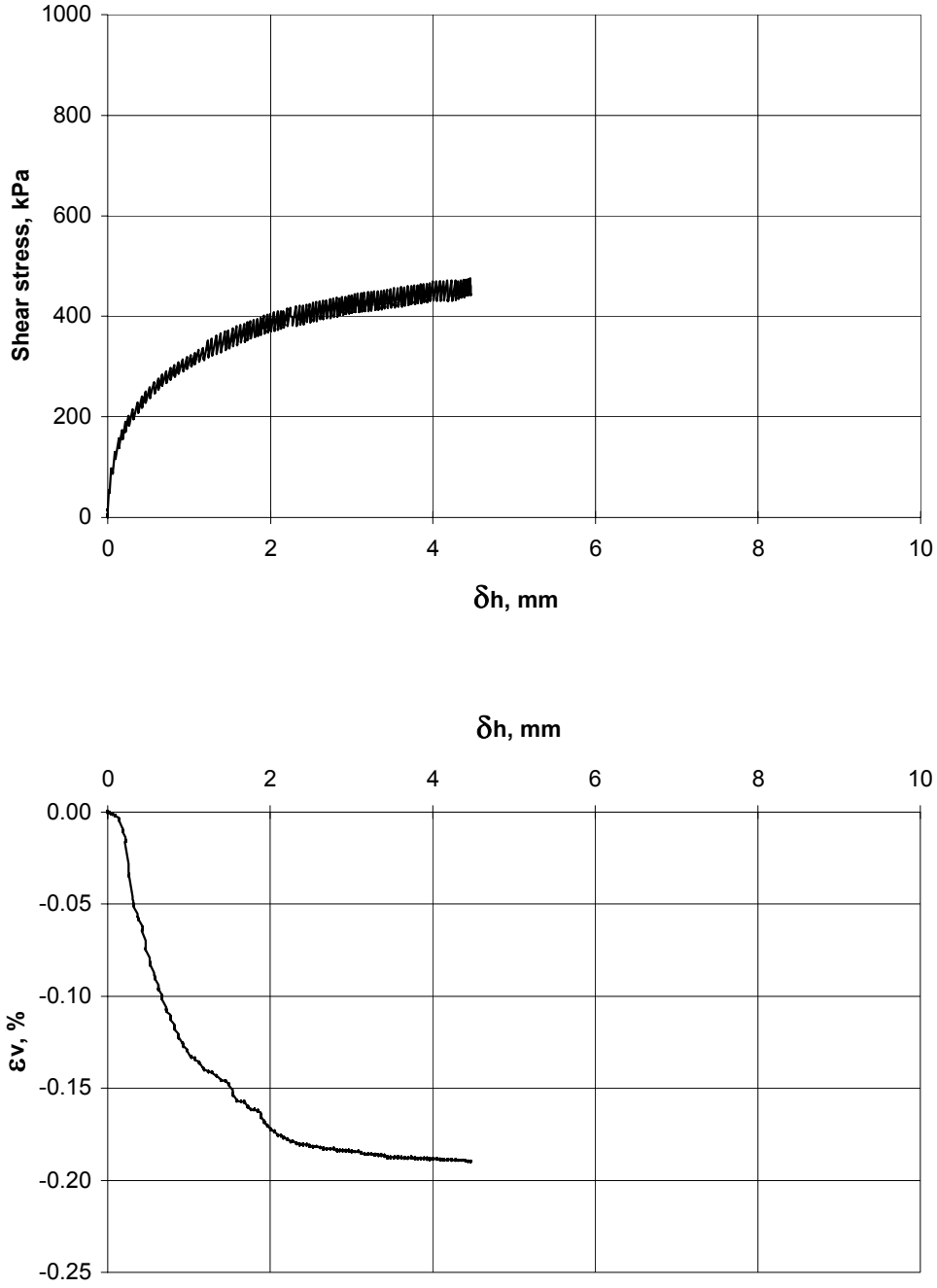

Figure 6-23. *Shear stress (upper) and volume change as a function of shear displacement at the normal stress 1000 kPa for 20/80 bentonite/crushed TBM muck.*

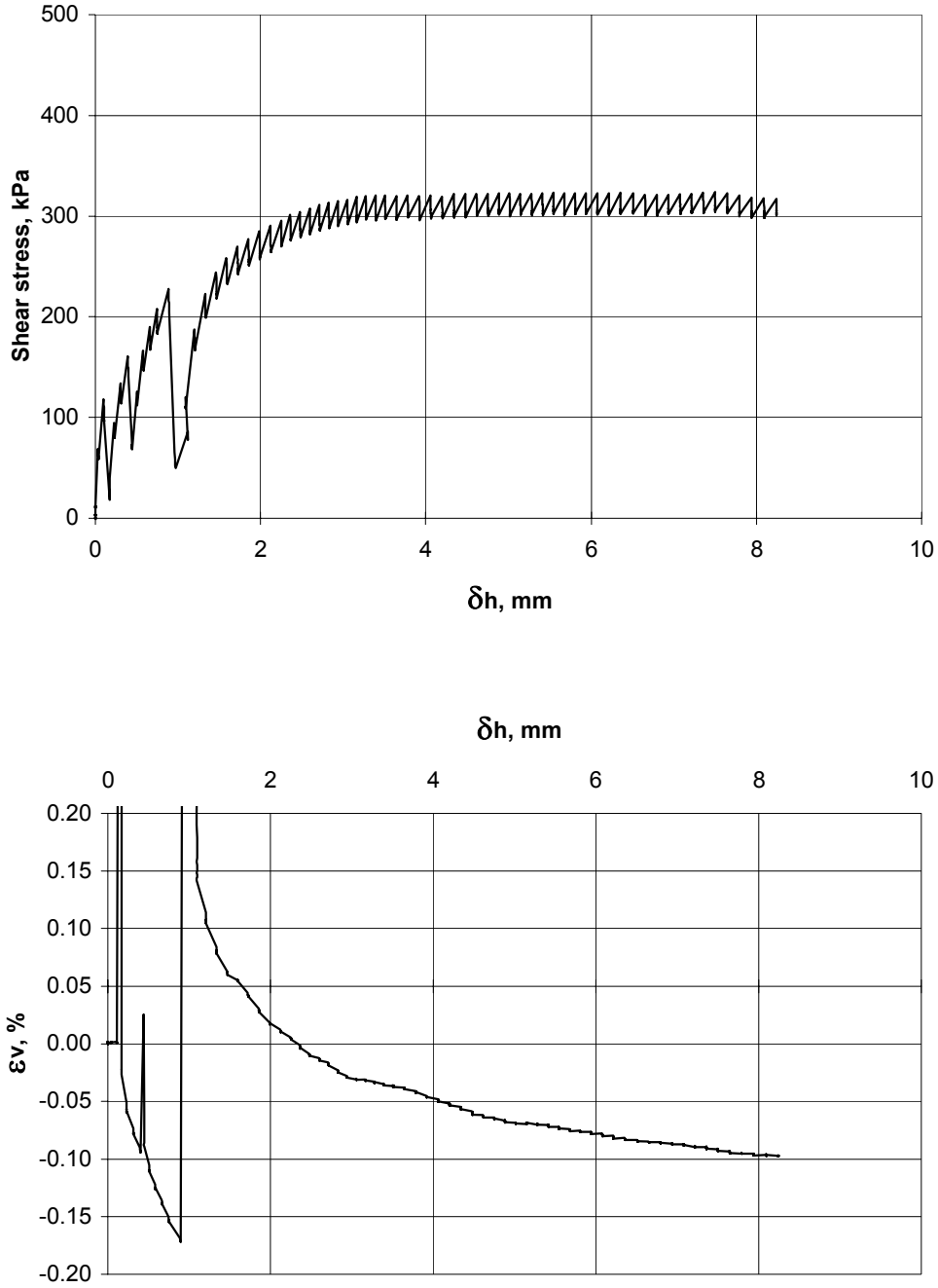

Figure 6-24. *Shear stress (upper) and volume change as a function of shear displacement at the normal stress 1000 kPa for 30/70 bentonite/crushed TBM muck.*

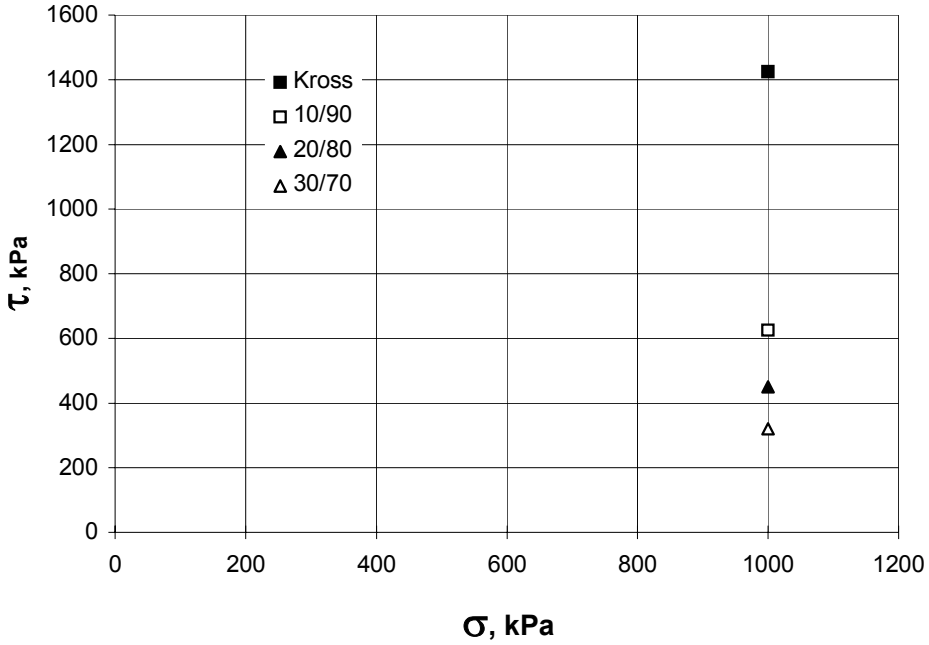

Figure 6-25. *The values of shear stress at failure as a function of the corresponding values of normal stress.*